

**Expression and function of the *let-7* microRNA during stem cell  
specification and development of the CNS**

**Dissertation**

zur Erlangung des akademischen Grades des  
Doktors der Naturwissenschaften (Dr. rer. nat.)

eingereicht im Fachbereich Biologie, Chemie, Pharmazie  
der Freien Universität Berlin

vorgelegt von

**Agnieszka Rybak**

Kolbuszowa, Poland

Berlin 2009

1. Gutachter: Prof. Dr. Robert Nitsch
2. Gutachter: Prof. Dr. Volker Haucke

Disputation am: 07.09.2009

*I wish to thank....*

*... my supervisor Dr F. Gregory Wulczyn for being an excellent mentor and teacher, for his invaluable guidance and assistance in making this research possible... for his patience, advice, encouragement but also criticism, which allowed me to keep this research on track and....for the daily question: 'what's new?', which indubitable made this work go faster....*

*...Professor Rober Nitsch for giving me the opportunity to join the Centrum for Anatomy, for his generous support during my stay, and for critical review of my work.*

*... Professor Volker Haucke for being a coreferee of this thesis*

*... Professor Uwe Heinemann and Professor Dietmar Kuhl for their guidance as a member of GRK College 123 Learning and Memory*

*... all my colleagues from the Center for Anatomy for scientific and non scientific discussion, support and for making everyday work more enjoyable, particularly Lena Smirnova, Elisa Cuevas, Vincenzo Catanzariti , Monika Dulinski, Nicola Brandt, Kristin Franke, Sascha Jonannes, Wolfgang Otto and Jens Baron*

*...Brita Scholte and Anja Gräfe for their skillful technical assistance*

*...Dr Thomas Neumann for the help with electron microscopy*

*... all the great scientists and teachers who influenced my scientific career, Professor Ryszard Zemla for introducing me to the field of biology, Prof Anna Skorupska and Dr Jaroslaw Krol , Prof Eric Haas Stapleton for their constant scientific support.*

*...my 'Berliner' friends Patapia Zafiriou, Anna Soriguera and Lorenza Magno for all the fun we had together. Girls, I really enjoy spending time with you!!*

*...my Polish friends Magda Materniak, Agnieszka Skalska for their support and long lasting friendship*

*...My parents, my brother and sister for their support and encouragement and love.*

*Last but not least Heiko Fuchs for being a wonderful partner at work and in my life, for sharing good and bad moments with me,...I can not even explain how thankful I am to you that you are!... thank you for being...*

## List

Acknowledgment	3
List	4
Abbreviations	8
Summary	10
Zusammenfassung	12
<b>1. Introduction</b>	<b>14</b>
1.1. From evolutionary freaks to important regulators of proteome, a short history of miRNA.	14
1.2. miRNA genes and their genomic distribution	15
1.3. miRNA expression	16
1.3.1. miRNA profiling methods	16
1.3.1.A. Sequencing and cloning	16
1.3.1.B. Hybridization	17
1.3.2. miRNA expression profiles	17
1.4. Biogenesis of miRNA	18
1.4.1. The Microprocessor complex	19
1.4.2. The exportin-5 complex	21
1.4.3. The pre-miRNA processing complex	21
1.4.4. The miRNA- containing ribonucleoprotein (miRNP) complex	23
1.4.5. P-bodies	24
1.5. How do miRNAs regulate gene expression?	25
1.5.1. Evidence that miRNAs inhibit translation at some stage after initiation	26
1.5.2. Evidence that miRNAs inhibit translation initiation	27
1.5.3. Evidence that miRNAs can promote target mRNA degradation	28
1.6. miRNAs targets	30
1.6.1. Prediction and validation of miRNA targets	30
1.6.2. Validation of miRNA targets	31
1.7. miRNA function	31
1.7.1. miRNAs in the nervous system	32

1.7.2.	miRNAs and synaptic plasticity	33
1.7.3.	miRNAs and cancer	34
1.7.4.	miRNAs and stem cell function	34
1.8.	Aim of this thesis	36
2.	<b>Materials and Methods</b>	37
2.1.	Materials	37
2.1.1.	Chemicals	37
2.1.2.	Equipment	38
2.1.3.	Software	38
2.1.4.	PCR Primers	39
2.1.5.	LNA oligonucleotides	42
2.1.5.A.	LNA modified anti-miRNA oligonucleotides	42
2.1.5.B.	miRNA precursors used for cells transfection and EMSA	42
2.1.5.C.	siRNA sequences used for cells transfection	43
2.1.6.	Vectors	43
2.1.7.	Constructs	43
2.1.8.	Bacterial strains	43
2.1.9.	Primary cells, cell lines and mouse strains	44
2.1.10.	Buffers and Solutions	44
2.1.11.	Media	46
2.1.12.	Antibodies	46
2.2.	Methods	48
2.2.1.	P19 (EC), HEK293 and HeLa cell culture methods	48
2.2.2.	Cell transfection with plasmid DNA and siRNA	48
2.2.3.	Molecular biology methods	49
2.2.3.A.	Total RNA isolation	49
2.2.3.B.	cDNA synthesis from total RNA	50
2.2.3.C.	Polymerase Chain Reaction (PCR)	50
2.2.3.C.1.	Semi-quantitative PCR	50
2.2.3.C.2.	Real-Time PCR	52
2.2.4.	Histo- and cytological methods	52
2.2.4.A.	Immunohistochemistry	52

2.2.4.B.	Preparation of brain and testis tissue sections and immunostaining	53
2.2.4.C.	Immunofluorescence staining for early stage mouse embryos	53
2.2.4.D.	Immunohistochemistry with floating brain sections for electron microscope	54
2.2.4.E.	Immunostaining with paraffin embedded tissue	54
2.2.4.F.	Preparation of mouse skin cryostat sections	55
2.2.5.	Fluorescent and confocal microscopy	55
2.2.6.	<i>in situ</i> hybridization	56
2.2.6.A.	<i>in situ</i> hybridization on mouse testis/brain slides	56
2.2.6.B.	Cells <i>in situ</i> hybridization	56
2.2.6.C.	Whole mount <i>in situ</i> hybridization	57
2.2.7.	DNA cloning methods	58
2.2.8.	Plasmid constructs cloned for this work	59
2.2.9.	In vitro pre-miRNA transcription	59
2.2.10.	RNA labeling for microarray	60
2.2.11.	Biochemical methods	61
2.2.11.A.	Protein electrophoresis and Western blots	61
2.2.11.B.	Immunoprecipitation	62
2.2.11.C.	Protein overexpression for anti-Lin41 antibody generation	62
2.2.11.D.	<i>In vitro</i> miRNA processing assay	64
2.2.11.E.	<i>In vitro</i> ubiquitination assay	65
2.2.11.F.	<i>In vivo</i> ubiquitination assay	65
2.2.11.G.	EMSA	66
<b>3.</b>	<b>Results</b>	67
3.1.	Characterization of <i>let-7</i> expression using <i>in situ</i> hybridization methods	67
3.2.	Identification of <i>let-7</i> target genes in pluripotent cells	72
3.3.	Characterization of the mouse <i>let-7</i> target gene- mlin-41 expression patterns and function	77
3.3.1.	mLin-41 is expressed in undifferentiated stem cells and in the mouse epiblast	78
3.3.2.A.	mLin-41 expression during embryonic development	81
3.3.2.B.	mLin-41 expression in the postnatal mouse brain	85
3.3.2.C.	Expression of mlin-41 in male germ cells and the reproductive tract	88
3.3.3.	mLin-41 co-localization to P-bodies	92

3.3.4.	The mLin-41 function	95
3.4.	Mechanisms regulating <i>let-7</i> expression	101
3.4.1.	<i>let-7</i> binding complexes	102
3.4.2.	<i>Pre-let-7</i> binding protein	108
3.4.3.	Lin-28 as a <i>pre-let-7</i> binding protein in undifferentiated cells	109
3.4.4.	Lin-28 as a <i>let-7</i> target gene	111
3.4.5.	Lin28/ <i>pre-let-7</i> interaction study	112
3.4.6.	Lin-28 interferes with Dicer activity	114
3.4.7.	Cytoplasmic action of Lin-28	115
4.	<b>Discussion</b>	117
4.1.	<i>let-7</i> miRNA expression	117
4.2.	<i>let-7</i> miRNA targets	118
4.3.	Characterization of the mouse lin-41 homolog- mLin-41	119
4.4.	Mechanism regulating <i>let-7</i> expression during neural stem cell commitment	123
5.	<b>Reference List</b>	125
6.	<b>Appendix</b>	143
6.1.	Statement	143
6.2.	Publications	144
6.3.	Oral presentations	144
6.4.	Poster presentations	144
6.5.	Workshops attended	145
6.6.	Curriculum Vitae	146

## Abbreviations

3'UTR	3' untranslated region
$\alpha$ MEM	$\alpha$ modified form of Eagle's minimal essential medium
$\mu$ g	Microgram
$\mu$ M	Micromolar
Ago1/2	Argonaute proteins 1 or 2
APS	Ammonium phosphate sulfate
BSA	Bovine serum albumin
Ci	Curie
cm	Centimeter
CMV	Cytomegalovirus
CNS	Central nervous system
CTP	Cytosin-5'-triphosphat
DMEM	Dulbecco's modified Eagle's medium
DMSO	Dimethyl sulfoxide
dNTP	Deoxynucleotidetriphosphat
dsRBD	Double-stranded RNA binding domain
DTT	1,4-dithiothreitol
DRG	Dorsal root ganglion
EDTA	Ethylenediamine-tetraaceticacid
EC cells	Embryonal carcinoma cells
eIF4E	Eukaryotic translation initiation factor 4E
EMSA	Electrophoretic mobility shift assay
ES cells	Embryonic stem cells
EST	Expressed sequence tag
et al.	Et alter
FACS	Fluorescence-Activated Cell Sorter
FBS	Fetal bovine serum
FMRP	Fragile X mental retardation protein
GAPDH	Glyceraldehyde-3-phosphate dehydrogenase
GFAP	Glial fibrillary acidic protein
GFP	Green fluorescent protein
h	Hours
HEK293	Human embryonic kidney cell line 293
HRP	Horseradish Peroxidase
ISH	In situ hybridization
IHC	Immunohistochemistry
L	Liter
mAb	Monoclonal antibody
min	Minutes
miRNA	microRNA
ml	Milliliter
mM	Millimolar
mm	Millimeter
ng	Nanogramm
nt	Nucleotide

ORF	Open reading frame
P19GM	P19 growth medium
PACT	PKR activating protein
PAGE	Polyacrylamide gel electrophoresis
PBS	Phosphate buffered saline
PCR	Polymerase chain reaction
PFA	Paraformaldehyde
Pol II/ pol III	Polymerase II or III
RIIID	RNAse III domain
RA	Retinoic acid
RISC	RNA induced silencing complex
RT	Room temperature
RT-PCR	Reverse transcription polymerase chain reaction
SAP	Shrimp Alkaline Phosphatase
SDS	Sodium dodecyl sulfate
s	Seconds
snRNA	Small nuclear RNA
SSC	Solution of sodium chloride and sodium citrate
TBE Buffer	Tris-borate-EDTA buffer
TCA	Trichloroacetic acid
TEMED	N,N,N',N'-Tetramethylethylenediamine
RNP	Ribonucleoprotein
TRBP	The human immunodeficiency virus transactivating response RNA binding protein
Tris	Tris(hydroxymethyl)aminomethane
Tween20	Polyoxyethylensorbitanmonolaurat
U	Units
UTP	Uracil-5'-triphosphate
V	Volt

## Summary

Contemporary biology has undergone a small revolution with the discovery of microRNAs (miRNAs), a class of 22 nucleotide regulatory RNAs. miRNAs are endogenously expressed, non-coding RNAs that inhibit the translation of target mRNAs by binding to cognate sites of imperfect complementarities found in 3' untranslated regions. In the past eight years, a rapidly expanding literature has begun to document the importance of this new mechanism in the regulation of eukaryotic gene expression.

To date, thousand of miRNA genes have been identified by a combination of cloning, direct sequencing and bioinformatic techniques. Computational analysis suggests that the total number of miRNA genes may be more than 1% of total protein coding genes. Experimental data and computational algorithms suggest that each miRNA may potentially target many different (ten to hundreds) mRNAs, taken collectively this indicates that over 30% of all genes may be regulated by miRNAs. By targeting the mRNA of protein-coding genes miRNAs play a critical role in a variety of biological processes like development, cell growth, proliferation, lineage determination and metabolism. miRNAs have also been implicated in the etiology of a variety of complex diseases like Fragile X syndrome, Tourette's syndrome, Alzheimer's disease, neurodegenerative diseases and a large number of cancers with different origins.

miRNAs are also crucial components of the gene regulation machinery that controls nervous system development and neural stem cell differentiation. The nervous system is a rich source of miRNA expression. Over 70% of experimentally detected miRNAs are expressed in the brain. Unfortunately, to date too little is known about the role of individual miRNAs in neural development and nervous system function.

In this context, the principal goal of this work was to investigate the expression and function of the *let-7* miRNA family during development of the CNS as well as during neural stem cell differentiation. The study focussed on the analysis of *let-7* expression, the identification of novel *let-7* target genes and their functional analysis.

Using *in situ* hybridization (ISH) in E9.5 mouse embryos, early induction of *let-7* in the developing central nervous system was demonstrated. The expression pattern of three *let-7* family members closely resembled that of the brain-enriched miRNAs *mir-124*, *mir-125* and *mir-128*, and was most prominent in the neuroepithelium of the brain and spinal cord, and in the cranial and dorsal root ganglia.

To identify genes regulated by *let-7*, microarray profiling of mRNA after ectopic expression of *let-7* in EC cells was performed. A majority of the most highly downregulated genes corresponded to direct *let-7* targets, as predicted by miRNA binding sites algorithms: TargetScan and PicTar. GO annotations suggest a statistically significant clustering of transcription factors and translational regulators. Three novel stemness genes (*hic2*, *arid3b* and *mlin-41*) were identified as candidate targets for *let-7* during embryonic development.

Detailed analysis of mLin-41 and *let-7* expression patterns revealed a reciprocal relationship in several pluripotent or multipotent cell environments: embryonic stem cells, the embryonic epiblast, the male and female germlines and skin. Functional analysis revealed that mLin-41 is a novel component of cytoplasmic P-bodies and that has E3 ubiquitin ligase activity.

Moreover, the mechanisms regulating *let-7* miRNA expression during stem cell commitment were characterized. It was shown that a pluripotent factor, Lin-28, directly interacts with the pre-*let-7* miRNA and blocks cytoplasmic *let-7* miRNA processing in undifferentiated stem cells. Lin-28 itself is a regulatory target of the *let-7* and *mir-125* microRNAs, which indicate both *let-7* and Lin-28 act in an autoregulatory pathway to control miRNA processing during neural stem cell differentiation.

## Zusammenfassung

Die Entdeckung der microRNA(miRNAs), eine Gruppe von ca. 22 Nukleotid langen regulatorischen RNAs, hat zu einer kleinen Revolution in der Biologie geführt. miRNAs sind endogen exprimierte, nicht kodierende RNAs, welche an bestimmte RNA-Sequenzabschnitte in der 3'UTR von mRNAs binden und deren Translation inhibieren. In den letzten acht Jahren sind zahlreiche Publikationen erschienen, die die Bedeutung dieses neuen eukaryotischen posttranskriptionellen Regulationsmechanismus dokumentieren. Unter Zuhilfenahme neuester Klonierungsmethoden, direct sequencing und der Bioinformatik konnten tausende miRNA-Gene identifiziert werden.

Durch experimentelle Daten und bioinformatische Algorithmen kann angenommen werden, dass jede miRNA zehn bis hunderte verschiedene mRNAs inhibieren kann und die Expression von 30% aller proteinkodierenden Gene durch miRNAs moduliert werden. Durch die Inhibierung verschiedenster mRNAs spielen miRNA eine kritische Rolle in diversen biologischen Prozessen, wie Entwicklung, Zellwachstum, Proliferation, Differenzierung von Zell- oder Gewebetypen und Stoffwechselprozessen. Dysfunktionen von miRNAs können auch verschiedene Krankheiten zur Folge haben wie zum Beispiel Martin-Bell-Syndrom, Touret Syndrom, Alzheimer, Neurodegeneration sowie Karzinome unterschiedliche Ursprungs.

Während der Neuronalen Stammzellendifferenzierung und der Entwicklung des Nervensystems spielen miRNA eine wichtige Rolle bei der Genregulation. Der Hauptteil der miRNAs wird im Nervensystem expremiert. Über 70% der bis dato experimentell entdeckten miRNAs werden im Gehirn expremiert. Bis jetzt ist allerdings wenig über deren Rolle für die neuronale Entwicklung und Funktion bekannt.

In diesem Zusammenhang lag das Hauptziel der hier vorliegenden Arbeit darin, die Expression und Funktion der *let-7* mikroRNA Familie während der neuronalen Stammzellendifferenzierung und der Entwicklung des Nervensystems eingehender zu untersuchen. Dabei wurde neben der *let-7* Expression Zielgene und deren Funktion analysiert.

Mittels whole mount in situ Hybridisierung an E9.5 Embryonen von Mäusen konnte eine frühe Induktion von *let-7* im entwickelnden ZNS gezeigt werden. Das Expressionsmuster von drei der *let-7* Familie zugehörigen miRNAs ähnelte dabei stark den im Gehirn angereicherten miRNAs *mir-124*, *mir-125* und *mir-128*. Es konnte eine starke Expression im Neuroepithelium des Gehirns, im Rückenmark sowie im Somatischen Ganglien gezeigt werden.

Um Gene identifizieren zu können, welche von *let-7* reguliert werden, wurde mRNA aus embryonalen Karzinom Zellen vor und nach ektopischer Expression isoliert und eine Microarray Analyse durchgeführt. Ein Großteil der am stärksten herunterregulierten Gene waren von TargetScan und PicTar vorhergesagte *let-7* Zielgene. GO Annotationen zeigten, dass es sich bei den meisten Zielgenen um Transkriptionsfaktoren und Translationsregulatoren handelt. Dabei konnten u.a. *hic2*, *arid3b* und *mlin-41* als potentielle Zielgene welche von *let-7* während der Embryonalentwicklung reguliert werden, identifiziert werden.

Eine detaillierte Analyse von mLin-41 und dem *let-7*-Expressionmuster wies eine reziproke Verteilung in verschiedenen pluripotenten und multipotenten Zelltypen wie embryonalen Stammzellen, embryonalem Epiblasten, der Haut sowie der männlichen und weiblichen Keimbahn auf. Funktionelle Analysen konnten mLin-41 als eine neue Komponente der zytoplasmatischen P-Bodies identifizieren. Darüber hinaus zeigt mLin-41 eine E3 Ubiquitin Ligase Aktivität.

In dieser Arbeit konnte darüberhinaus ein Mechanismus, welcher postranskriptionel die Expression von *let-7* steuert aufgedeckt werden: Lin-28 interagiert direkt mit der *pre-let-7* miRNA und verhindert so die *let-7* Prozessierung in undifferenzierten Stammzellen. Lin-28 konnte wiederum als *let-7* Zielgen identifiziert werden. Somit wird die *let-7* Prozessierung durch einen autoregulatorischem feed-back Mechanismus von Lin-28 und *let-7* während der neuronalen Stammzellendifferenzierung gesteuert.

## 1. Introduction

### 1.1. *From evolutionary freaks to important regulators of the proteome: a short history of miRNA*

The first miRNAs, *lin-4* and *let-7*, were identified from the genetic analysis of developmental timing in *C.elegans*. *let-7* or *lin-4* mutant worms fail to execute certain developmental switches, resulting in the abnormal repetition of specific larval stages. The initial cloning of *lin-4* and later *let-7* revealed these two genes to be particularly deviant—unusually small (>100 bp), encoding no protein products, and producing short (~22 nt) RNAs from characteristic hairpin RNA precursors. Moreover, it was demonstrated that these small RNAs are translational repressors of mRNAs that encode proteins of the developmental timing (heterochronic) pathway of the worm (Lee et al., 1993; Moss et al., 1997; Slack et al., 2000). For example, the *lin-4* RNA is complementary to sequences in the 3' untranslated region (UTR) of the *lin-14* and *lin-28* mRNAs. The synthesis of Lin-14 and Lin-28 proteins is repressed by *lin-4* during the early larval stages of *C. elegans* development to trigger a chain of stage-specific developmental events. When first described, *lin-4* was considered to be a kind of oddity in worm genetics. However, two remarkable discoveries refuted these considerations and gave a new insight on miRNAs as regulatory genes. The first of these was that *let-7* RNA is phylogenetically conserved—in size and nucleotide sequence in all bilaterally symmetric animals (Pasquinelli et al., 2000). Moreover, *let-7* has a similar developmental profile in diverse taxa. For example, homologs of the worm *let-7* target, *lin-41*, can be found in insects and vertebrates with their *let-7* complementary sites intact. A second discovery that supported the relative ubiquity of tiny RNAs like *lin-4* and *let-7* was the finding that small antisense RNAs of about 22 nt in length (called siRNAs) are central to RNA interference (RNAi) (Sharp, 2001). RNAi is an evolutionarily conserved genetic mechanism that can degrade a mRNA in response to the presence of double-stranded RNA corresponding to the targeted mRNA. *lin-4* and *let-7* are not siRNAs (they bind to mRNA targets with imperfect complementarity), but the ubiquity of the siRNA pathway suggested that small RNAs of the size of *lin-4* and *let-7* have been part of the eukaryotic milieu for a very long time. This was reinforced by the finding that the *lin-4* and *let-7* 22 nt RNAs are processed from their stem-loop precursor transcripts by Dicer, a key enzyme in the RNAi pathway (Grishok et al., 2001; Bernstein et al., 2001). Since Dicer is phylogenetically widespread, genes like *lin-4* and *let-7* could also be common. Indeed, recently hundreds more miRNAs have been discovered in

animals and plants and their importance as a novel players in proteome regulation has been demonstrated.

### **1.2. miRNA genes and their genomic distribution**

Bioinformatic algorithms predict over 1000 miRNAs may be encoded in the human genome, although fewer than 1000 miRNAs have been confirmed by physical means so far, (Ambros et al., 2003; Aravin et al., 2003; Dostie et al., 2003; Mourelatos et al., 2002). miRNAs genes are scattered in all chromosomes in humans except for the Y chromosome and they are non-randomly distributed. They can be grouped according to their location:

- **Intronic miRNAs in protein coding transcription units (~61%).** Many of miRNAs are co-expressed with their protein-coding host genes, implying that they generally derive from a common transcript (Lagos-Quintana et al., 2003; Rodriguez et al., 2004). The location of some of these intronic miRNAs is well conserved among diverse species (Baskerville and Bartel, 2005; Lagos-Quintana et al., 2003). For example, *mir-7* is found in the intron of heterogeneous nuclear ribonucleoprotein K (hnRNP K) in both insects and mammals (Arvin et al., 2003). Another example of such miRNAs are the *mir-186* and *mir-106b~25~93* family. *mir-186* is expressed in the human and mouse genomes and in both cases is located in intron 8 of the pre-mRNA of the zinc finger protein 265 (Lagos-Quintana et al., 2003). The *mir-106b~25~93* family was found in intron 13 of the minichromosome maintenance deficient 7 (MCM7) gene of both human and mouse (Kim and Nam, 2006).
- **Intronic miRNAs in non-coding transcription units (18%).** Examples of this class are the leukemia associated *mir-15* and *mir-16*. Both these miRNAs are located within the fourth intron of a transcribed region, DLEU2 on chromosome 13q14 (Calin et al., 2002).
- **Exonic miRNAs in non-coding transcription units (20%).** These miRNAs are transcribed from their own promoters as long primary transcripts, termed pri-miRNAs (Cai et al., 2004; Lee et al., 2004) *let-7*, *mir-23a*, *mir-27a*, *mir-24-2*, *mir-155*, *mir-21* are examples of such intergenic miRNAs.

‘Mixed’ miRNA genes can be assigned to one of the groups above depending on the given splicing pattern.

In many cases, miRNA genes are found in clusters and they are transcribed as polycistronic primary transcripts (Brennecke et al., 2003; Lagos-Quintana et al., 2001; Lau et al., 2001; Mourelatos et al., 2002). Examples of such clusters are the *mir-23a~27a~24-2* genes on human chromosome 19 and the *let-7a-1~let-7f-1* clusters on human chromosomes 9 and 17 and mouse chromosome 13 (Lagos-Quintana et al., 2001; Mourelatos et al., 2002). The miRNAs in cluster are often related to each other (the same miRNA family) and they may act together to regulate a set of target mRNAs (Baskerville and Bartel, 2005). An example of such a cluster, containing six closely related miRNAs genes, is the mouse *mir-290~mir-295* cluster or its human homolog the *mir-371~mir-373* cluster. They are expressed specifically in embryonic stem (ES) cells and downregulated upon differentiation (Houbaviv et al., 2003; Suh et al., 2004).

### **1.3. miRNA expression**

#### **1.3.1. miRNA profiling methods**

miRNA expression profiling presents significant technical challenges. Tiny length, low expression level, and high sequence similarity between miRNAs mean that traditional gene expression techniques are not suitable. Fortunately, the past several years brought significant progress in the development and improvement of several profiling methods, which in general can be divided in two different types: sequencing-cloning approaches and hybridization approaches.

##### **1.3.1.A. Sequencing and cloning approaches**

- random cloning and sequencing of size fractionated RNA (Lagos-Quintana et al., 2002)
- amplified partial sequencing, based on PCR amplification of adaptor ligated cDNA clones using primers with partial coverage of predicted miRNA sequence (Lim et al., 2003)
- sequence specific cloning, based on the sequence of predicted miRNAs; biotin-labelled oligonucleotides are designed and used to capture homologous miRNAs from a cDNA library enriched for small RNAs (Krichevsky, 2007)
- deep sequencing, a very sensitive method for detection and profiling of known and novel miRNAs, provides over 32 million sequencing reads in one run, with reading length limited to 32 bp (Friedländer et al., 2008).

### 1.3.1.B. Hybridization

- northern blot, used to validate predicted miRNAs
- membrane arrays, inexpensive radioactive detection method (Krichevsky et al., 2003)
- beads-based profiling; capture probes complementary to miRNAs of interest are coupled to microscopic polystyrene beads impregnated with a dye. The beads are used to capture the miRNA from an amplified library and the type and amount of miRNA are detected by flow cytometry (Barad et al., 2004).
- microarrays are the most common and powerful high-throughput tool capable of monitoring the expression of thousands of miRNAs at once. Several technical variants of miRNA arrays have been developed, and they differ in oligo probe design, probe immobilization, sample labelling and microarray chip signal detection methods (Liu et al., 2008).

### 1.3.2. miRNA expression profiles

Expression profiling studies indicate that most miRNAs are under the control of developmental or tissue specific signalling, but some of them are expressed ubiquitously (Aravin et al., 2003; Watanabe et al., 2005, Chen et al., 2005; Baskerville and Bartel, 2005; Krichevsky et al., 2003; Sempere et al., 2004; Sun et al., 2004). Table 1.1 presents some examples of different miRNA expression profiles in mice and human.

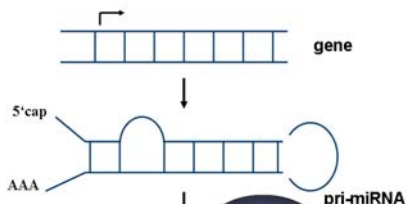
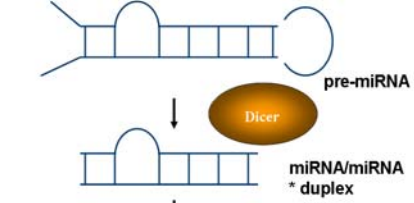
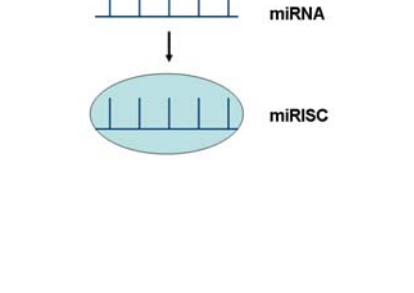
**Table 1.1 miRNA expression profiles.**

miRNA expression profile	example	reference
<b>ubiquitously expressed</b>	<i>mir-16, let-7a, let-7b, mir-26a, mir-30b, mir-30c, mir-92</i>	Sempere et al., 2004
<b>tissue specific</b>	liver: <i>mir-122a</i> ; spleen : <i>mir-189, mir-212</i> ; lung: <i>mir-18, mir-19a</i> ; heart: <i>mir-1, mir-208</i> ; brain: <i>mir-124, mir-9</i> ;	Lagos-Quintana et al., 2002; Sempere et al., 2004, Babak et al., 2004, Miska et al; 2004
<b>tissue enriched</b>	brain: <i>mir-125b, mir-128</i> ; heart: <i>mir-133, mir-206</i> ; liver: <i>mir-152, mir-215</i> ; spleen: <i>mir-99a</i>	Sempere et al., 2004; Sun et al., 2004
<b>regulated expression during development</b>	<i>let-7, mir-125b, mir-128, mir-266, mir-131, mir-196a</i>	Krichevsky et al., 2003 Smirnova et al., 2005
<b>lineage specific</b>	neuron: <i>mir-124, mir-12,</i> ; astrocyte: <i>mir-23</i> ; macrophage <i>mir-223</i> ; B-lymphoid cell: <i>mir-181</i> ; mouse ES cell <i>mir-293-297</i>	Calin et al., 2004, Chen et al., 2004; Houbaviy et al., 2003 ; Smirnova et al., 2005

### 1.4. Biogenesis of miRNAs

miRNA biogenesis is a complex process consisting of nuclear and cytoplasmic steps and involving several protein complexes (Table 1.2):

**Table 1. 2. miRNA biogenesis steps.**

<b>nucleus</b>	1. The Microprocessor complex	<ul style="list-style-type: none"> <li>- Transcription of the primary miRNA (pri-miRNA)</li> <li>- Processing of the transcript to the ~70 nt stem loop precursor miRNA (pre-miRNA)</li> </ul>	
<b>nucleus/ cytoplasm</b>	2. Exportin-5 complex	- Export of the pre-miRNA from the nucleus to cytoplasm	
<b>cytoplasm</b>	3. The pre-miRNA processing complex	Processing of the pre-miRNA to: <ul style="list-style-type: none"> <li>- ~22 bp miRNA duplex</li> <li>- release of the ~22 nt mature single-strand miRNA</li> </ul>	
	4. The miRNA-containing ribonucleoprotein (miRNP) complex and P- bodies	<ul style="list-style-type: none"> <li>- Assembly of the miRNA-induced silencing complex (miRISC)</li> <li>- miRNA binding to the 3'UTR of a target mRNA and inhibition of target gene translation</li> </ul>	

### 1.4.1. The Microprocessor complex

Most miRNA genes are transcribed by RNA polymerase II (Pol II) and the primary transcript contains a poly(A) tail and 7-methylguanosine cap, which is unique for Pol II transcripts. Pol II-dependent transcription was demonstrated by showing that miRNA transcription is sensitive to  $\alpha$ -amanitin, an inhibitor of Pol II activity. Moreover, Pol II is physically associated with miRNA promoters, as has been shown by chromatin immunoprecipitation (ChIP) assay (Lee et al., 2004). However, the possibility that some miRNAs genes might be transcribed by other RNA polymerases cannot be excluded. Examples are miRNAs lying within Alu – repetitive elements, which are transcribed by RNA polymerase III (Borchert et al., 2006).

The primary miRNA (pri-miRNA) transcript from intergenic clusters can be a several kilobases long and harbors one or more hairpin-loop structures corresponding to individual miRNAs. In the nucleus the primary miRNA transcript is recognized by the Microprocessor complex, which is composed of Drosha and the Pasha/DiGeorge syndrome critical region gene 8 (DGCR8) proteins (Figure 1.1).

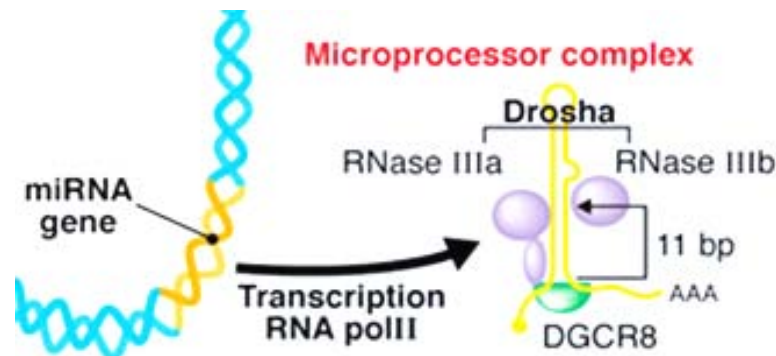
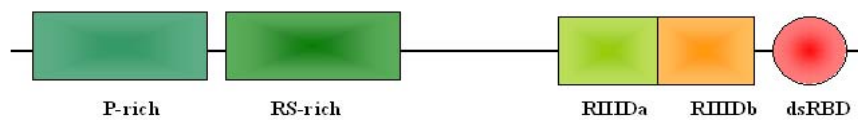


**Figure 1.1 Microprocessor complex.** The miRNA genes generate a non-translated RNA transcript known as the primary miRNA (pri-miRNA), which is recognized by the microprocessor complex composed of the ribonuclease III (RNase III) Drosha and the accessory DiGeorge syndrome critical region gene 8 (DGCR8) protein. DGCR8 binds to the dsRNA-ssRNA junction at the base of the pri-miRNA and acts as a molecular caliper that measures the distance of 11 bp, where the two RNase III domains of Drosha form an intramolecular structure with each domain cleaving one strand to produce the miRNA precursor (pre-miRNA). Adapted from Perron and Provost, 2008.

**Drosha** was characterized as a member of the class 2 RNase III proteins. The RNase III enzyme family includes endoribonucleases specific for dsRNA, which can be divided into 3 classes. Class 1 RNase IIIs are composed of a single RNase III domain and a C-terminal dsRNA binding domain (dsRBD, bacterial RNase III). Class 2, to which Drosha belongs, possesses two RNase III domains and a C-terminal dsRBD (Figure 1.2). Class 3 is represented by Dicer and contains two

RNase III domains, a C-terminal dsRBD and a putative N-terminal DexD/H-box helicase domain accompanied by domain of unknown function (DUF238) and central PIWI/Ago/Zwille (PAZ) domain.



### Human Drosha Protein structure

**Figure 1.2 Human Drosha protein structure:** Prolin-rich (P-rich) and serin-arginine-rich (RS-rich), the RNase III domains (RIIIDa and RIIIDb), the double strand RNA binding domain (dsRBD).

Drosha is a nuclease that executes the initiation step of miRNA processing. It binds to the pri-miRNA and excises the ~70-nt pre-miRNA. The current model of Drosha action proposes that Drosha functions as a monomer, with its RNase III domains forming an internal dimer structure able to recognize the substrate. Purified recombinant Drosha cannot cleave the pri-miRNA with precision, which suggests that the specificity of substrate recognition and the positioning of the catalytic center depend on Pasha/DGCR8 (Han et al., 2006).

**DiGeorge syndrome critical region gene 8 (DGCR8) protein** possesses two dsRBDs. Since Drosha lacks specificity in its absence, DGCR8 has been proposed to guide Drosha by functioning as a molecular anchor measuring the distance from the dsRNA-ssRNA junction in the pri-miRNA. Recently a new model for substrate recognition by the Drosha/DGCR8 complex was proposed (Han et al., 2006). They divided the structure of a pri-miRNA into four parts: the terminal loop, the upper stem and the two basal segments. By combining computational and biochemical approaches, they determined that the terminal loop is not essential for cleavage by the Microprocessor complex, while the flanking ssRNA segments appear to be critical. They have also observed that immunoprecipitated DGCR8, but not Drosha, interacts with pri-miRNAs both directly and specifically, and that flanking ssRNA segments are required for this binding to occur.

### 1.4.2. The exportin-5 complex

After production in the nucleus, the pre-miRNA is transported to the cytoplasm, by the transporter Exportin-5 (Exp-5) which was shown to specifically bind a typical pre-miRNA substrate in the presence of RanGTP (Figure 1.3). Exportin-5 is a member of the nuclear karyopherin  $\beta$  transporter family, which can mediate nuclear export of dsRNA binding proteins. The initial model suggests that Exp-5 and RanGTP associate with a dsRBD-containing protein in the nucleus and that this export complex translocates through the nuclear pore complex to the cytoplasm. Then, RanGTP hydrolysis in the cytoplasm releases the dsRBD-containing protein, allowing it to interact with regulatory elements within its mRNA target.

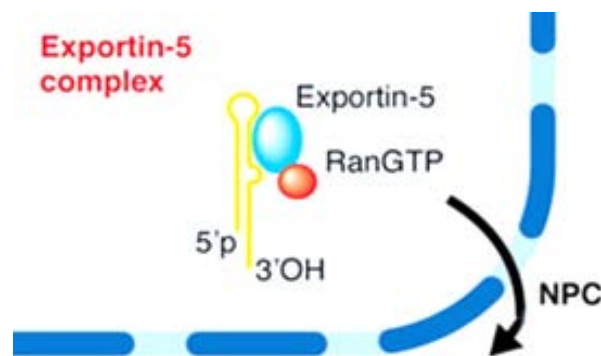


**Figure 1.3 The exportin-5 complex.** pre-miRNA is then exported into the cytoplasm through nuclear pore complex (NPC) by the Exportin-5 complex in a sequence of events involving RanGTP hydrolysis

### 1.4.3. The pre-miRNA processing complex

In the cytoplasm, Dicer is the key enzyme in the pre-miRNA processing complex, acting together with TAR RNA binding protein (TRBP). This pre-miRNA processing complex (Figure 1.4) accepts the 70 bp pre-miRNA product issued from the Microprocessor complex and cleaves it to form a miRNA duplex of ~ 21-23 bp.

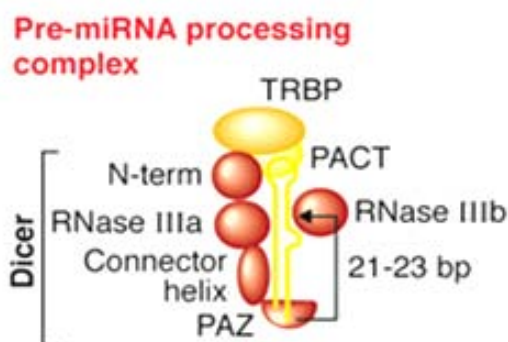
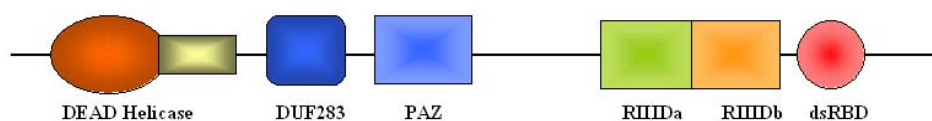


**Figure 1.4 The pre-miRNA processing complex**, composed of Dicer, TRBP and PACT, recognizes and processes the pre-miRNA substrate into a miRNA:miRNA\* duplex. The PAZ domain of Dicer has been proposed to act as an anchor for the 3'hydroxylated 2-nt overhang extremity. The connector helix is responsible of the measurement of the 21-23 bp length from the extremity and determines the positioning at the cleavage site of its two RNase III domains that form, as in Droscha, an intramolecular dimer with a unique catalytic site. Adapted from Perron and Provost et al., 2008)

**Dicer**, the core nuclease within the pre-miRNA processing complex, is responsible for the generation of miRNA duplexes with a 5' phosphate, a 3' hydroxylated end and a 2-nt overhang. Dicer has been reported to be localized in the cytoplasm where it is associated with the endoplasmic reticulum (ER). In mammals the presence of Dicer is essential, as Dicer-deficient mice die at the embryonic stage, suggesting its importance in mammalian development.

In the Zhang model of Dicer catalytic activity, Dicer may function by the intramolecular dimerization of its two RNase II domains, assisted by the PAZ and dsRBD domains (Zhang et al., 2004). The central PAZ domain specifically recognizes the 2-nt 3' overhang present in the pre-mirRNA. The PAZ and RNase IIIa domains may then act as a calliper in generating similarly – sized miRNA.



### Human Dicer protein structure

**Figure 1.5 Human Dicer protein structure**: the DEAD-box , the RNA-helicase, the DUF283 domain, the PAZ , the RIIID domains, the dsRBD.

**TAR RNA binding protein (TRBP)** was discovered as a cellular factor acting in synergy with the viral TAT protein in the transactivation of the long terminal repeats (LTR) of HIV-1. TRBP

possesses three dsRBDs and is present in two isoforms in the cell. TRBP was found by immunoprecipitation to interact with Dicer protein via the C-terminal dsRBP domain. Furthermore, the TRBP/Dicer complex interacts with Argonaute 2 (Ago2) (Chendrimada et al., 2005).

**PACT** (PKR activating protein) interacts directly with TARBP and this complex associates with Dicer to facilitate siRNAs production (Kok et al., 2007).

#### 1.4.4. The miRNA- containing ribonucleoprotein (miRNP) complex

Mature miRNAs are incorporated into the effector complex, which is known as the miRNP or miRISC (miRNA-containing RNA-induced silencing complex). During miRISC assembly the 22-nt duplex cleavage product is asymmetrically unwound with one strand degraded and the other retained for binding to partially complementary sequences within the 3'UTR of the target mRNA (Gregory et al., 2005; Maniataki and Mourelatos, 2005; Diederichs and Haber, 2007). miRISC-bound mRNA transcripts are subject to several alternative fates, including translational suppression, destabilization by deadenylation or degradation by Ago2 RNase activity (Doench et al., 2003; Petersen et al., 2006).

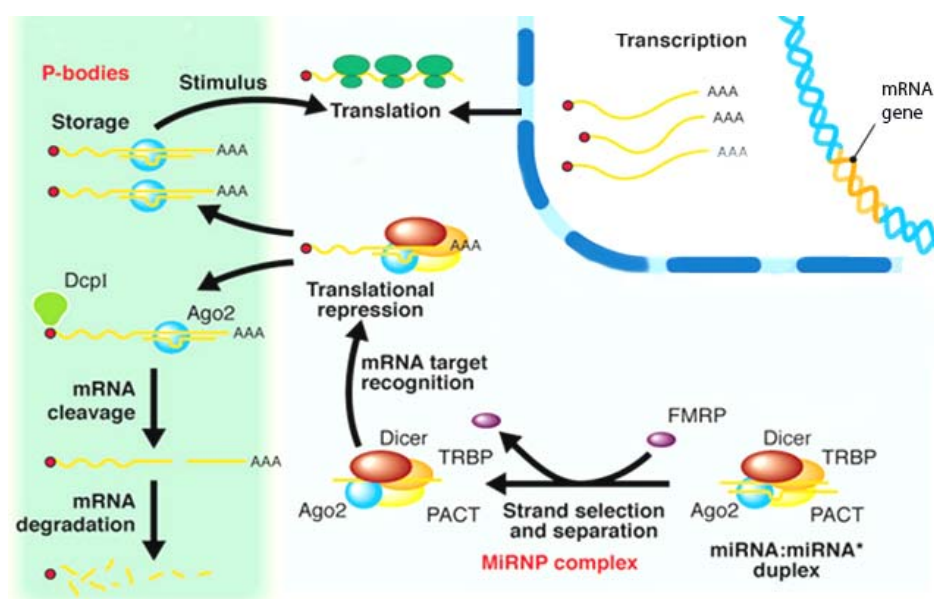


**Figure 1.6 The miRNA- containing ribonucleoprotein (miRNP) complex.** Separation and selection of the initial miRNA:miRNA\* duplex is accompanied by miRNP complex rearrangement and association with Ago2 to form the effector complex. The complementarity of the miRNA to its target loads the effector miRNP complex onto a specific mRNA to negatively regulate it, and ultimately direct it to P-bodies. These punctuate foci in the cell contain silenced mRNAs, which can be either released from their inhibition upon a cellular signal, or simply degraded. (Adapted from Perron and Provost et al., 2008).

The core components of the miRISC are Argonaute (Ago) family proteins. The human genome encodes four Ago proteins and four Ago-related proteins called Piwi (Sasaki et al., 2003). Furthermore, numerous Ago-associated proteins have been identified, including helicases, nucleases and RNA-binding proteins (Maurelato et al., 2002; Meister et al., 2005; Robb and Rana, 2007). However, the exact role for many Ago-associated proteins for miRISC function has not yet been established and the molecular composition of the miRISC is the subject of continuing investigation.

**Ago-2** (also known as eIF2C2) is the so-called Slicer RNase in the RNAi pathway, providing the cleavage activity to degrade target mRNAs that are complementary to the guiding siRNAs. In case of partial complementarity, the Ago-2 protein fails to cleave, but instead interferes with translation of the target mRNA via its translational repression activity (Liu et al., 2004; Meister et al., 2004). Ago-2 is the only human Ago protein with intrinsic endonuclease activity, which is encoded by a PIWI domain (DDE motif) with similarity to RNase H domain (Song et al., 2004). Ago-2 is essential for mouse development and cells lacking this protein are unable to perform siRNA mediated silencing (Liu et al., 2004). In addition to Ago-2, other mammalian Ago proteins are also part of miRNA effector complexes that mediate translational inhibition of target mRNAs (Liu et al., 2004; Meister et al., 2004).

**Fragile X mental retardation protein (FMRP)** has been identified in a miRNP complex containing Dicer and Ago2 proteins in mammalian cells *in vivo* (Jin et al., 2004). FMRP is a RNA-binding protein containing two K-homology (KH) domains and an RGG box known to be involved in the regulation of mRNA translation. Recently, it was demonstrated that human FMRP can act as a miRNA acceptor protein for Dicer and facilitates assembly of miRNAs on specific target RNA sequences (Plante et al., 2006).

#### **1.4.5. P-bodies**

P-bodies are large cytoplasmic aggregates of translationally repressed mRNAs associated with the translational repression and decay machinery (Hillebrand et al., 2007). P-bodies were initially thought to be primarily sites of mRNA decapping and 5' to 3' exonucleolytic degradation (Sheth and Parker, 2003). Recently, a link between these structures and the miRNA-guided RNA silencing pathway has been established. Ago proteins have been shown to localize to these complexes (Liu et al., 2005) and to directly interact with GW182 (Pauley et al., 2006). Core P-body protein components are conserved from yeast to mammals (Table 1.3) and include: (a) the

mRNA decay machinery, including the decapping enzymes Dcp1p/Dcp2p and the 5' to 3' exoribonuclease, Xrn1/Pcm; (b) the activators of decapping, Edc3p, RAP55/Scd6p, and the Lsm1p-7p complex; and (c) the enhancers of decapping and general translational repressors, Me31B/RCK/Dhh1p and Pat1p. P-bodies also contain components of RISC, including the Argonaute proteins (Ago1 and Ago2), indicating a role in miRNA/siRNA-mediated gene silencing (Behm-Ansmant et al., 2006; Ding et al., 2005). P-bodies are now thought to also be sites of translational regulation via miRNA, nonsense-mediated decay (NMD), and general repression pathways (Parker and Sheth, 2007). Several lines of evidence suggest that P-body proteins also have direct functions in general translational repression in higher eukaryotes (Eulalio et al., 2007).

**Table 1.3 P-bodies components**

COMPONENTS OF P-BODIES	PROTEIN CLASS
Xrn1p	5'to 3' RNA exonuclease
Edc3p, Pat1p	Enhancers of decapping
Lsm1	Sm-like involving in decapping
Dcp1p/Dcp2p	Decapping enzymes
PABP	Poly(A)-binding
Hed1, Ge-1	Decapping co-activator
Gemin5	Involved in assembly of U snRNPs
EDC3	Decapping co-activator
Ago1/Ago2	miRNA, siRNA machinery
Mov10	RNA helicase, translational repression
TNRC6B	Involved in translational repression

### ***1.5. How do miRNAs regulate gene expression?***

The mechanisms of gene regulation by miRNAs have been the subject of many studies. Initial publications and reviews proposed that miRNAs do not promote degradation of their targets, but down-regulate mRNA translation at either the initiation step or some stage after initiation. However, recent studies report larger miRNA dependent decreases in mRNA abundance and emphasize mRNA degradation as an important aspect of miRNA-mediated repression of gene expression (Lim et al., 2005). Moreover, miRNA might also silence their targets by sequestering mRNAs in P-bodies (described above), which exclude the translational machinery. There is supporting evidence for each of these different mechanisms of miRNA action.

### 1.5.1. Evidence that miRNAs inhibit translation at some stage after initiation

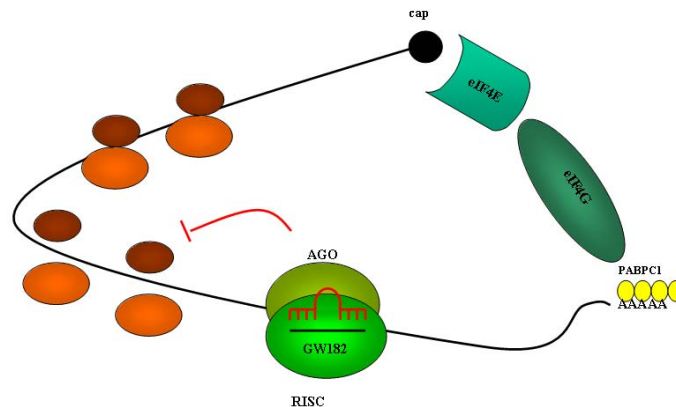


**Figure 1.7 Inhibition of translation elongation.** miRNAs (red) repress translation of target mRNAs (black) by blocking translation elongation or by promoting premature dissociation of ribosomes (ribosome drop off)

The hypothesis that miRNA-mediated repression of target genes due to inhibition of mRNA translation at a post-initiation step was based on studies of the *lin-4/lin-14* interaction in *C.elegans*. The *lin-14* mRNA was found to stably associate with polysomes, suggesting either an arrest of translational elongation (ribosomal stalling), or co-translational peptide degradation of the nascent protein chain as mechanisms (Olsen and Ambros, 1999). More recent publications (Moroney et al., 2006; Nottrott et al., 2006; Petersen et al., 2006) also present evidence that miRNAs repress protein synthesis after translation is initiated. Although these studies differ in details their final conclusion is that miRNAs and their target mRNAs are associated with actively translating polysomes as determined by sucrose sedimentation profiles. This observation that targets of miRNAs appear to be actively translated while the corresponding protein products remain undetectable prompted the proposal that the peptide chain may be degraded cotranslationally (Nottrott et al., 2006).

To investigate how miRNAs silence their targets Petersen et al (2006) designed a synthetic miRNA reporter containing a 3' UTR with six identical sites complementary to a transfected siRNA. When this reporter was transiently expressed it associated with polysomes, although its expression was repressed by the siRNA. If translation initiation was inhibited, these ribosomes dissociated more rapidly than those associated with control RNAs. That suggests that miRNAs cause premature ribosome dissociation or ribosome drop-off.

Additional evidence supporting miRNA-mediated translational inhibition after initiation is that silencing occurs even when reporter mRNA translation is initiated by a 5'UTR containing an internal ribosome entry site (IRES). Because IRES initiate translation of mRNAs independently of the mRNA cap structure, this result strongly indicates that miRNAs repress translation after the cap recognition step (Petersen et al., 2006).

### 1.5.2. Evidence that miRNAs inhibit translation initiation

In contrast, other groups have presented evidence that miRNAs and their targets are not in fact associated with polysomal fractions but rather with the free mRNP pool in mammalian cells. This indicates that targeted mRNAs are not actively translated (Pillai et al., 2005). Furthermore, in these studies miRNAs translated through cap-independent mechanisms were not sensitive to repression, which strongly supports inhibition of cap-dependent translation initiation by miRNAs (Humphreys et al., 2005; Mathonnet et al., 2007; Wakiyama et al., 2007).

Chendrimada et al. have proved that Ago2 associates with both eIF6 and large ribosomal subunits and inhibits an early initiation step (Chendrimada et al., 2007). In the normal situation eIF6 binds to the large ribosomal subunits and prevents premature joining of the small ribosomal subunit. If Ago2 recruits eIF6, the large and small ribosomal subunits are not able to associate and translation is repressed.

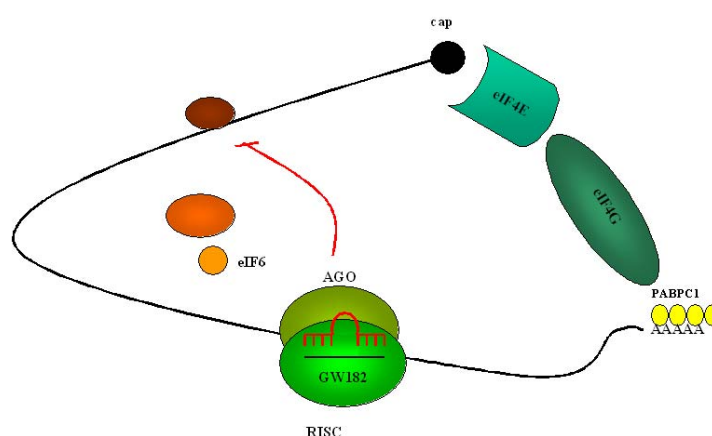


**Figure 1.8 Inhibition of ribosomal subunit joining.** Argonaute proteins recruit eIF6 which prevents the large ribosomal subunit from joining the small subunit.

Furthermore Kiriakidou et al.(2007) reported that Argonaute proteins exhibit similarities to the cytoplasmic cap-binding protein eIF4E (eukaryotic translation initiation factor 4E) which is essential for cap-dependent translation initiation. eIF4E binds the m7Gppp-cap structure of mRNAs by stacking the methylated base of the cap between two tryptophans. Argonaute proteins have phenylalanines at equivalent positions that could mediate similar interactions. To prove it, Kiriakidou performed a m7GTP sepharose binding experiment and indeed showed that Ago2 binds m7GTP and that there is competition for this binding by a methylated cap analog. Moreover, the substitution of phenylalanines in Ago2 with another amino acid abrogated silencing activity. These results support the idea that miRNAs inhibit translation at the cap-recognition step by displacing eIF4E from the cap structure.

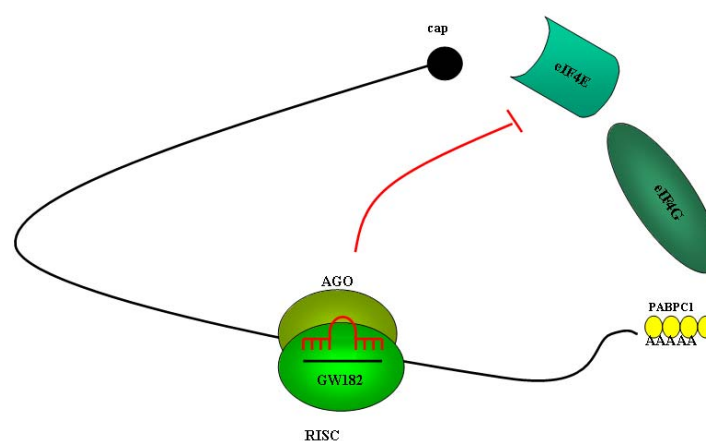


**Figure 1.9 Inhibition of initiation.** Argonaute proteins compete with eIF4E for binding to the cap structure.

### 1.5.3. Evidence that miRNAs can promote target mRNA degradation

Some recent publications reported large miRNA-dependent decreases in mRNA abundance, consistent with mRNA degradation as an important aspect of miRNA mediated repression of gene expression (Figure 1.10).

Microarray analyses of HeLa cell mRNAs showed that ectopic overexpression of the brain-specific *mir-124* or the muscle specific *mir-1* decreases the abundance of different subsets of mRNAs, specifically mRNAs that are of low abundance in brain or muscle, respectively (Lim et al., 2005).

Smutter and Wu demonstrated miRNAs-mediated acceleration of target mRNA degradation through the normal pathway of deadenylation, followed by decapping and subsequent degradation of the mRNA by 5'→3' exonuclease activity. The only difference from the normal

pathway is that a miRNP bound to its 3' UTR target sites can act as a barrier to the 5'→3' exonuclease, leading to accumulation of deadenylated decay intermediates with 3' sequences (Smutter et al., 2006; Wu et al., 2006).

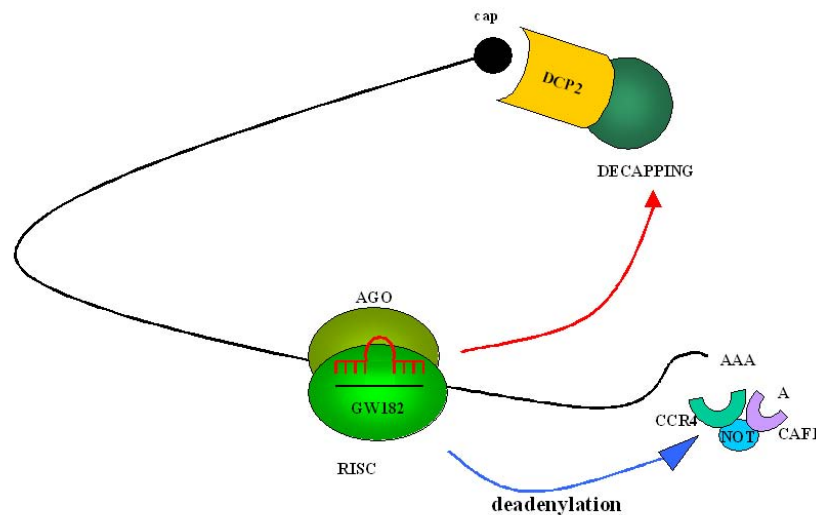


**Figure 1.10 Deadenylation and decapping.** miRNAs trigger deadenylation and subsequent decapping of the mRNA target.

As an example, in mammalian cells transfected with a reporter containing *mir-125* binding sites under control of the *c-fos* promoter (allowing transient transcription), deadenylation and accelerated decay was dependent on *mir-125* expression (Wu et al., 2006). Similarly, in zebrafish embryos the expression of the *mir-430* miRNA leads to deadenylation and subsequent degradation of several hundred maternal mRNAs. This serves to clear the maternal mRNAs from the embryo. In mutated embryos lacking *mir-430* the degradation of maternal transcripts was delayed and led to abnormalities in brain development (Giraldez et al., 2006).

Evidence of so many different models for miRNA regulation of gene expression can be explained in different ways. On the one hand, different modes might reflect different experimental approaches and their interpretations. On the other hand, miRNAs might indeed silence gene expression by multiple mechanisms depending on experimental or biological context. Another possibility is that miRNAs can silence gene expression by a common and unique mechanism and the multiple modes represent secondary effects of these primary events (Eulalio et al., 2008). Currently, we can not exclude any of these possibilities and the mechanisms of miRNA action still remain hotly debated.

## 1.6. miRNAs targets

### 1.6.1. Prediction of miRNA targets

The accurate prediction and validation of miRNA target genes is one of the major research challenges in the miRNA field. To date, several computational approaches have been developed and thus far have allowed the identification of numerous miRNA targets (Bentwich, 2005; John et al., 2006; Rajewsky, 2006).

Most of the prediction algorithms scan the 3' untranslated regions for potential target sequences for miRNAs based on homology and structural criteria. These criteria include sequence complementarity, thermal stability of the RNA-RNA duplexes, target site conservation across species and the presence of multiple target sites in the same gene (Bentwich, 2005). The most commonly used target prediction programs are summarized in Table 1.4.

**Table 1.4 miRNA targets prediction programs.**

<b>MiRNA prediction algorithm</b>	<b>Criteria of target miRNA recognition</b>	<b>False-positive rate</b>	<b>Reference</b>
<b>miRanda</b>	<ul style="list-style-type: none"> <li>-Sequence complementarity with higher weight to matches at 5' end of the mature miRNA</li> <li>-Free energy of RNA-RNA duplexes (RNAfold)</li> <li>-Extent of conservation of the target sequences in related genes across species</li> </ul>	24-39%	Enright et al., 2003 John et al., 2004 Bentwich, 2007
<b>PicTar</b>	<ul style="list-style-type: none"> <li>-Perfect matches between the mRNA and the 5' seed region of the miRNA</li> <li>-Required target conservation across several species</li> <li>-Biased toward perfect seed region complementarity</li> </ul>	~30%	Krek et al., 2005 Bentwich, 2007
<b>TargetScan</b>	<ul style="list-style-type: none"> <li>-Perfect matches between the mRNA and the 5' seed region of the miRNA with extension the matches as far as possible, allowing G:U wobble pairing</li> <li>-Optimize base pairing of the remaining portion using RNAfold to calculate the thermodynamic free energy of binding</li> <li>-Ranking of predicted targets based on position of binding sites in the 3'UTR</li> </ul>	22-31%	Lewis et al., 2003 Bentwich, 2007 Grimson et al., 2007

### 1.6.2. Validation of miRNA targets

Validation of predicted miRNA targets is much more challenging than prediction, mainly because there does not exist a simple method for biological validation. Recently used methods rely on a combination of informatics and biological validation strategies. The recent use of high-throughput mass spectrometry methods should allow rapid progress in the refinement of prediction algorithms (Grosshans and Filipowicz, 2008; Baek et al., 2008).

#### **Informatics validation:**

- Evaluate an algorithm's success in correctly identifying known miRNAs targets
- Compare the number of postulated binding sites that an algorithm finds for a real miRNA, with that found for a control group of artificially generated fictitious miRNAs (Baek et al., 2008)

#### **Biological validation:**

- Reporter-gene constructs (Lewis et al., 2003 ; Krek et al., 2005)
- Mutation studies (Klostermann et al., 2004)
- Gene silencing techniques (O'Donnell et al., 2005; Johnson et al., 2005)
- Rescue assays (Brennecke et al., 2003)
- Pulsed-SILAC (stable isotope labelling with amino acids in cell culture)

### 1.7. miRNA function

The discovery of large numbers of miRNAs has outstripped our ability to study their individual functions. Recent studies reveal that miRNAs are involved in a multitude of cellular processes. The mutational phenotype seen in case of the original miRNAs *lin-4* and *let-7* indicated a role in animal development. Other studies have pointed out their roles in specific cells or tissue types including the development and specification of myoblasts, adipocytes or hematopoietic and neuronal stem cells (Krichevsky et al., 2006; Chen et al., 2004; Naguibneva et al., 2006). More detailed examples are: *mir-1* with a function in cardiogenesis and muscle development (Sokol et al., 2008), *mir-155* with a function in B cell activation and the immune response (Rodriguez et al., 2007) or *mir-208* in cardiac stress response (van Rooij et al., 2007).

In the context of my study I would like to summarize miRNA function in the nervous system, stem cell biology and cancer in more detail.

### 1.7.1. miRNAs in the nervous system

The development and function of the nervous system requires precise spatial and temporal control of gene expression on both the transcriptional and translational levels. The nervous system is a rich source of miRNAs and they represent an additional level of control over protein expression. Around 70% of experimentally detectable miRNAs are expressed in the brain. During brain development the expression levels of some miRNAs change dynamically (Miska et al., 2004; Smirnova et al., 2005). miRNA expression profiles have also been examined in cell culture systems such as primary neurons (Kim et al., 2004) and EC (embryonic carcinoma) cells upon retinoic acid (RA) treatment. In either case scores of miRNAs are induced, including brain-specific, brain-enriched and ubiquitously expressed miRNAs (Sempere et al., 2004). However, some brain expressed miRNAs like *mir-128* or *mir-29* are not detected in neurons derived from RA-treated EC cells. In some cases these miRNAs are probably present in the brain in non-neuronal cell types like glia. Some miRNAs indeed show lineage-specific expression, as detected in primary cultures of neurons and astrocytes (Smirnova et al., 2005).

**Table 1.5 miRNA in the nervous system.**

Brain specific miRNAs	mir-9, mir-124, mir-128	Babak et al., 2004 ; Barad et al., 2004 ; Kim et al., 2004
Brain enriched miRNAs	mir-125	al., 2004 ; Kim et al., 2004
brain specific/enriched (?)	mir-7, -34, -127, -132, -135, -136,-138,-139,-149,-153,-154,-218,-219,-222,-323,-326,-329 etc.	Miska et al., 2004, Sempere et al., 2004
<b>neural related miRNA</b>		Kirchevsky et al., 2003
- increase continuously during embryonic development, gradually decline during postnatal period	mir-9, - 125b, - 181a	Miska et al., 2004 Smirnova et al., 2005
- increase continuously during embryonic development, plateau around birth	mir-124a,-130b	
- highest expression at E12, decrease to adult	mir-103,- 128	
- start to be expressed after postnatal day 14	mir-17,-18,-19,-20,-92,-199a mir-29	
<b>miRNA examined in primary neurons in culture:</b>		Kim et al., 2004
-expression level increases from day	mir-128,-191,-323,-324-5p,326,329,344	

1.5 to day 14 - remain relatively constant	mir-103, -124a,-335,-129,-151	Kim et al., 2004
<b>miRNA induced by retinoic acid treatment in EC cells:</b> - brain specific/enriched - not enriched in the brain	mir-9,-124,-125,-135,-218,-219 let-7, mir-23,-26,-30,-91,-98,-100,-103,-156	Sempere et al., 2004
<b>miRNAs with lineage specific expression:</b> -highly restricted to neurons -preferentially expressed in neurons -expressed in astrocytes	<i>mir-124, - 128</i> <i>mir-125</i> <i>mir-23</i>	Smirnova et al., 2005

### 1.7.2. miRNAs and synaptic plasticity

Four important observations point to a role for the miRNA pathway in synaptic plasticity and formation of long term memory (LTM).

First, it was demonstrated by Schratt et al. that in the hippocampus *mir-134* (one of the brain specific miRNAs) controls dendritic spine morphogenesis via regulation of the mRNA encoding LimK1, a protein kinase that has been implicated in spine development (Schratt et al., 2006). In mammals, dendritic spine development and morphogenesis correlates strongly with synaptic plasticity.

Second, the FMRP protein has been shown to be required for dendritic spine morphogenesis in humans and for synaptic plasticity in *Drosophila* (Michel et al., 2004; Pan et al., 2004). Mutations in the FMRP locus result in Fragile X Syndrome, the most common form of hereditary mental retardation in human (Ule and Dornell, 2006). FMRP has been shown to be a part of the miRNP complex (Siomi et al., 2004; Caudy and Hannon, 2004).

Third, in *Drosophila* a direct connection between the RISC machinery and synaptic plasticity has been demonstrated (Ashraf et al., 2006). In the olfactory system, the RISC component Armitage is required for formation of LTM. Moreover, Armitage and Dicer are involved in the regulation of synaptic translation of  $\alpha$ -calmodulin dependent protein kinase II ( $\alpha$ -CaMkII), a predicted target of mir-280 and mir-289. The neuronal RNA binding protein Staufen and kinesin heavy chain are also predicted targets of mir-280. Expression of both proteins is enhanced in Dicer as well as Armitage mutants (Kosik, 2006).

Finally, haploinsufficiency of the *Dgcr8* gene, which encodes a RNA-binding moiety of the Microprocessor complex, contributes to the behavioral and neuronal deficits, spine width and dendritic complexity associated with the 22q11.2 microdeletion (Stark et al., 2008).

### 1.7.3. miRNA and cancer

Examination of tumour specific miRNA expression profiles has revealed widespread deregulations of these molecules in diverse cancers (Kent and Mendell, 2006). Moreover, it has been reported that over 50% of miRNAs map to regions in the genome associated with chromosomal locations linked to cancer (Calin et al., 2004).

Some miRNAs appear to act as oncogenes. For example, *mir-21* is relatively overexpressed in glioblastoma multiform, cervical and breast cancer (Liu et al., 2007) and increased expression of *mir-21* appears to decrease apoptosis. Similarly, the locus containing seven miRNAs of the *mir-17-92* polycistronic cluster is amplified in a variety of B-cells lymphomas (Woods et al., 2007)

Conversely, some miRNAs can act as tumour suppressors, genes whose deletion promotes the process of tumorigenesis. An important example is the *let-7* miRNA and its target, the proto-oncogene Ras. Activating mutations in Ras, result in increased expression, causing cellular transformation. *let-7* family members are downregulated in human lung cancer, and it has been speculated that this leads to increased severity of the cancer due to misregulation of Ras (Takamizawa et al., 2004)

**Table 1. 6 miRNA in cancer.**

miRNA	role	cancer type	targets	reference
mir-15a	tumor suppressor	B-CLL, pituitary adenomas	BCL-2	Calin et al., 2005
mir-16-1		B-CLL, pituitary adenomas	BCL-2	Calin et al., 2005 Johnson et al., 2005
let-7		Breat, cervix, lung, ovaries	Ras	Yanaihara et al., 2006 Calin et al., 2004
mir-143		Colon, breast	?	
mir155	oncogene	B-lymphoma, breast, colon	AT1R	Volinia et al., 2006
mir-21		glioblastoma, colon, lung	apoptosis related genes LATS2	Volinia et al., 2006 Chan et al., 2005
mir-372		testical germ cell tumor		Voovhoeve et al., 2006

#### **1.7.4. miRNAs and stem cell function**

Stem cells are a group of remarkable cells with the properties of self-renewal and pluripotency. The mechanisms by which stem cells maintain these dual properties are still unclear. Recent studies indicate that the expression profile of miRNAs in stem cells are different from other tissues and suggest that miRNAs may play an essential role in stem cell self-renewal and differentiation.

Stem cell specific miRNAs have been identified in humans and mice. Six mouse ES cell-specific miRNAs (*mir-290*, *mir-291*, *mir-292*, *mir-293*, *mir-294*, *mir-295*) are organized as a gene cluster (Houbaviy et al., 2003). Similarly, in human two miRNA gene clusters were identified. The first contains eight miRNA genes (*mir-302b\**, *mir-302b*, *mir-302c*, *mir-302c\**, *mir-302a*, *mir-302a\**, *mir-302d*, *mir-367*) and the other four (*mir-371*, *mir-372*, *mir-373*, *mir-373\**) (Barroso-del et al., 2008).

Dicer mutants provided a new insight into miRNA function in stem cells. In ES cells, loss of Dicer activity results in defects in cell division and proliferation (Murchison et al., 2005). Mice deleted for Dicer are non-viable and do not survive beyond early stage embryonic development (E7.5) (Berstein et al., 2003).

An additional study indicates that miRNAs regulate stem cell division. Hatfield et al observed a significant decrease in cyst production in *Drosophila* germline stem cells lacking Dicer, due to the fact that Dicer mutants were delayed in the transition from G1 to S cell cycle phases ( Hatfield and Ruohola-Backer, 2008). This suggests that germ cell miRNAs make the cells insensitive to environmental signals and allow them to divide over a long period of time (Croce and Calin, 2005).

miRNAs are also involved in regulating stem cell differentiation, cell lineage specification and development (Kanellopoulou et al., 2005; Giraldez et al., 2005; Smirnova et al., 2005).

### 1.8. Aim of this thesis

The major aim of this thesis was to investigate the developmental expression and function of the *let-7* miRNA, as well as the mechanisms controlling its expression. Moreover, a part of the work was focused on characterizing one of the novel *let-7* target genes, mouse *lin-41*.

In pursuit of this goal the following questions were addressed and experimental approaches adopted:

1. Where is *let-7* expressed in the developing and adult nervous system?
  - different variations of *in situ* hybridization using DIG labelled LNA probes.
2. Which genes are regulated by *let-7*?
  - mRNA profiling after ectopic *let-7* overexpression
  - validation of predicted *let-7* target mRNAs by RT-PCR and qRT-PCR
3. What is the function of genes regulated by *let-7* (in particular focus of mLin-41 and Lin-28)?
  - detailed analysis of mLin-41 expression ( *in situ* hybridization, RT-PCR, antibody generation against mLin-41, western Blot, immunocytochemistry and immunohistochemistry)
  - functional studies of mLin-41 (intracellular colocalization studies, siRNA approaches, immunoprecipitation, *in vitro* ubiquitination assays)
4. What are the mechanisms responsible for the regulation of *let-7*?
  - characterization of *pre-let7* binding complexes (EMSA, siRNA knockdown, Western blot)
  - identification of *pre-let7* miRNA binding proteins and their effect on *let-7* biogenesis (EMSA, processing assay, *in situ* hybridization)

## **2. Materials and Methods**

### **2.1 Materials**

#### **2.1.1. Chemicals**

Chemicals for experiments were purchased from the following companies, unless indicated otherwise: Ambion, BD Clontech, Gibco, Sigma, Invitex, Invitrogen, Fermentas, Stratagene, Chemicon, BioLabs, Biochrom, Roth, Roche, Merck, Pierce, BioRad, Fluka, Serva, Promega. Anti-mLin-41 sera were generated by Pineda-Antikörper-Service.

#### **Enzymes, Kits and Transfection Reagents:**

- Advantage RT-for-PCR Kit (Clontech)
- BCA protein assay reagent kit (Pierce)
- CombiZyme DNA polymerase Mix (Invitex)
- DIG oligonucleotide 3'-end labeling kit 2<sup>nd</sup> generation (Roche)
- DIG oligonucleotide tailing kit 2<sup>nd</sup> generation (Roche)
- ECL chemiluminiscent reagents (Amersham Biosciences)
- Effectene transfection reagent (Qiagen)
- Fast red substrate- chromatogen system (Pierce)
- Fugene 6 transfection reagent (Roche)
- In-gel Tryptic Digestion Kit (Pierce)
- Lipofectamine 2000 transfection reagent (Invitrogen)
- Lipofectamine LTX reagent (Invitrogen)
- Lipofectamine RNAiMAX reagent (Invitrogen)
- NucleoBond PC 100/PC 500 (Macherey-Nagel)
- Phusion High-Fidelity DNA polymerase (Finnzymes)
- Plasmid-Mini Kit (SeqLab)
- QIAquick Gel Extraction Kit (Qiagen)
- QIAquick Nucleotide removal Kit (Qiagen)
- Restriction endonucleases (BioLabs)
- RNeasy Plus Mini Kit (Quiagen)

- Shrimp Alkaline Phosphatase (SAP) (Promega)
- T4 DNA Ligase (BioLabs)
- T4 Polynucleotide Kinase (Fermentas)
- T7 Transcription Kit (Fermentas)
- TaqMan 2x Universal PCR Master Mix No AmpErase UNG (Applied Biosystems)
- TaqMan Gene Expression Assay (Applied Biosystems)
- T7 TNT in vitro translation assay (Promega)
- Topo TA cloning Kit (Invitrogen)

### **2.1.2. Equipment**

- ABI PRISM TM7500 Sequence Detection Systems (Applied Biosystems)
- Cell incubator (Hereaus Instruments)
- Centrifuges: Rotina 35 R (Hettich); 5417R, 5804R (Eppendorf); Biofuge pico (Heraeus)
- Confocal equipment TCS SL (Leica Microsystems)
- Dounce homogenizer Sonopuls GM70 (Bandelin)
- Fluorescent microscope BX 51 (Olympus)
- Gel electrophoreses and blotting equipment (BioRad)
- Hybridization oven MWG (Biotech)
- PCR Block (MJ Research)
- pH Meter 537 (WTW)
- Photometer Ultrospec 2000 (Pharmacia Biotech)
- Plate reader ELX 800 (Biotech Instruments)
- Power pac 200/300 (BioRad)
- Scintillation counter LS 6500 (Beckmann)

### **2.1.3. Software**

- Adobe Acrobat Reader 5.0
- Adobe Photoshop CS3
- BLAST (<http://www.ncbi.nlm.nih.gov/BLAST/>)
- CLUSTALW (<http://align.genome.jp/>)
- CorelDRAW 10

- Ensembl genome browser (<http://www.ensembl.org/index.html>)
- ImageJ 1.34s
- JaMBW (<http://hometown.aol.com/lucatoldo/myhomepage/JaMBW/index.html?f=fs>)
- Leica Confocal Software v. 2.61 Build 1537
- Magnafire
- MFOLD program (<http://www.bioinfo.rpi.edu/applications/mfold/rna/form1.cgi>)
- Microsoft Office 2000
- Microsoft Windows 2000 Professional
- miRanda software (<http://www.microrna.org/>)
- miRNA database (<http://www.sanger.ac.uk/Software/Rfam/mirna/>)
- NCBI database (<http://www.ncbi.nlm.nih.gov/>)
- Primer3 program (<http://frodo.wi.mit.edu/>)
- PicTar ([http://pictar.bio.nyu.edu/cgi-bin/new\\_PicTar\\_mouse.cgi](http://pictar.bio.nyu.edu/cgi-bin/new_PicTar_mouse.cgi))
- RNA22 (<http://cbcsrv.watson.ibm.com/rna22.html>)
- SMART([http://smart.embl-heidelberg.de/smart/set\\_mode.cg](http://smart.embl-heidelberg.de/smart/set_mode.cg))
- Statistics software (<http://www.physics.csbsju.edu/stats/>)
- TaqMan 7500 Fast System Software
- TargetScan software (<http://genes.mit.edu/targetscan>)
- Volocity 3.0, Improvion

#### 2.1.4. PCR Primers

The primers were designed using Primer3 program, and analyzed in BLAST for specificity.

##### 2.1.4.A. Cloning primers used for plasmid constructions:

Name	Forward Primer (Sequence 5'-3')	Reverse Primer (Sequence 5'-3')	T <sub>a</sub> (°C)	bp
mLin-41	AAGGCGAAGGTGGTCCAGTCTG	GTGGTCGTAGCCCATGACAGTG	64	550
mLin-41	GCGGCCGCGAAATCTCAGGAAAAGTC	GCGGCCGCGGATCCCGCAGTGAAATTGCGA	65	505
mLin-41	GCGGCCGCGGACTTTGGCAACAATCGAATCCTC	CACAGTATTCTCAAGAACACAAATAC	62	553
Primers for mLin-41 constructs for antigen generation				
mLin-41	GTGGGATCCAAGGCGAAGGTGGTCCA	TTTGTCTGACTTAGAAGATGAGGATTC	65	1540
mLin-41(NHL domain)	CTGGGATCCGGCAGTGAAGGTGACGG	TTTGTCTGACTTAGAAGATGAGGATTC	65	840

mLin-41(Bbox domain)	GTGGGATCCAAGGCGAAGGTGGTCA	TTTGTCTGACTCAGCTGCGGCCCGACTTGAC	65	700
Primers for mlin-41 truncation constructs				
mLin41_1	TATAGTCGACATGGCTTCGTTCCCGGAG	TATAGGATCCATCCTGGAGGTAGGCGAA	59	900
mLin-41_2	TATAGTCGACATGGCTTCGTTCCCGGAG	TATAGGATCCTCAGGGGGCGTGAACATAAT	58	1340
mLin-41_3	TAT AGT CGA CAT GGC TTC GTT CC CG GAG	TAT AGG ATC CCT CCC CGT CAC CTT CAC T	57	1760
mLin-41_4	TATAGTCGACCCCTTCTCCATTCCTCGGT	TATAGGATCCGAAGATGAGGATTCGATGTGTTG	58	1800
mLin-41_5	TATAGTCGACTTCGCCTACCTCCAGGAT	TATAGGATCCGAAGATGAGGATTCGATGTGTTG	59	1650
mLin-41_6	TATAGTCGACATTATGTTACACGCCCCCTGA	TATAGGATCCGAAGATGAGGATTCGATGTGTTG	59	1200
mLin-41_7	TATAGTCGACAGTGAAGGTGACGGGGAG	TATAGGATCCGAAGATGAGGATTCGATGTGTTG	58	820
Primers for T7 template for <i>in vitro</i> transcription and translation (3 steps PCR)				
Kozak sequence whole	TATAGGGAGCCACCATGGCTTCGTTCCCGGAGACCGA	GTCGACTTAGAAGATGAGGATTCGAT	59	~2560
T7 promoter whole	TCTAATTTTATAAATACGACTCACTATAGGGAGCCACCATGGCTTCGTT	GTCGACTTAGAAGATGAGGATTCGAT	59	~2560
Upstream T7 Promoter whole	AATTAATTAATCTAATACGACTCACTATAGGGAGCCA	GTCGACTTAGAAGATGAGGATTCGAT	59	~2560
T7 RING fragment	TATAGGGAGCCACCATGGCTTCGTTCCCGGAGACCGA	GACTTACGAGAGTCTCTGCAGGGCATC	59	~980
	TCTAATTTTATAAATACGACTCACTATAGGGAGCCACCATGGCTTCGTT			
	AATTAATTAATCTAATACGACTCACTATAGGGAGCCA			
T7 RING/BBOX	TATAGGGAGCCACCATGGCTTCGTTCCCGGAGACCGA	GACTTAGGTCTTGAGCTCCTGCACCTGG	59	~1340
	TCTAATTTTATAAATACGACTCACTATAGGGAGCCACCATGGCTTCGTT			
	AATTAATTAATCTAATACGACTCACTATAGGGAGCCA			
T7 NHL fragment	AGCCACCATGCGGGCACTCACCATCCAGCT	GTCGACTTAGAAGATGAGGATTCGAT	59	~1650
	TAATACGACTCACTATAGGGAGCCACCATGCGGGCACTCAC			

## 2.1.4.B. Primer sequences used for cDNA amplification:

Name	Forward Primer (Sequence 5'-3')	Reverse Primer (Sequence 5'-3')	T <sub>a</sub> (°C)	bp
------	---------------------------------	---------------------------------	---------------------	----

Cct4	ACTGCCATTGGGTACTCTGG	TGGTCAATGTGAGCAACTGG	58	423
Dicer	CTTAGAATTCCTGGGAGATGGC A	GCATCATCGGATAGTACACCTGC	67	410
Dicer1	TTACCAGCGCTTAGAATTCCTG	AACTTGGCAGTTTCTGGTTCC	60	510
HMGA2	ACATCAGCCCAGGGACAA	TTCCTAGGTCTGCCTCTTGG	56	324
Isn1	CTCTACGAGTGCCACCACTG	CCCTGCAAGTACTGCCCGGC	58	540
mLin41	AAGGCGAAGGTGGTCCAGTCTG	GTGGTCGTAGCCCATGACAGTG	58	550
mlin-41 3'UTR	GGACTTTGGCAACAATCGAATC CTC	CACAGTATTCTCAAGAACAATAATC	62	553
MOV10	AGGCTGCTCACCTGGAGGTT	ACTCCAGACTCCGATCGTACAGCT	70	373
Nanog	GAGGAAGCATCGAATTCTGG	GCTTGCACCTCATCCTTGG	59	390
Phox2b	ATACCTCCAGCTTGGCTTCA	TCAGTGCTCTTGGCTCTTT	59	570
Slc35c2	TCATGTTTTCTGGCCTCTTC	GACGTTCTGGAGACCAGGAG	57	430
TARBP2	CTTCCAAAAGCTGGCAAAG	GGGCAGAAGGAGCAAGAAGT	60	461
TNRC6B	AACTCAAATTAAGCAGGACAC	TCACTTGATCCACCTCCTCG	62	395
TRBP2	CCTCCAAAAGCTGGCAAAG	GGTGGACAGTTCCACTAGGC	65	371
Wdr48	CATGCATCTTCAGGAGCAA	GAAACATGGCGACTGATGTG	56	470
Wnt5a	CTGGCAGGACTTTCTCAAGG	GCCGCGTATCATACTTCTC	58	520
$\beta$ -actin	CTAGGCACCAGGGTGTGATGG	CGTAGATGGGCACAGTGTGGG	65	387

2.1.4.C. Primer sequences used for *in vitro* RNA transcription:

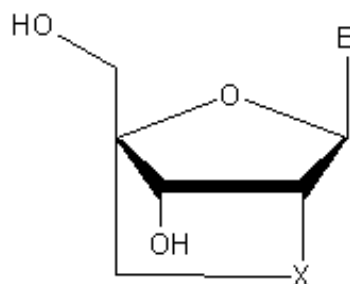
Name	Forward Primer (Sequence 5' - 3')	Reverse Primer (Sequence 5' - 3')	T <sub>a</sub> (°C)	bp
let-7a-T7 (precursor)	TAATACGACTCACTATAG GAGGTAGTAGGTTGTATAG	GGAAAGACAGTAGATTGTA	65	90
let-7e-T7	TAATACGACTCACTATAGGAG GTAGGAGGTTGTATAG	GGAAAGCTAGGAGCCGTA	62	84
mir-128b-T7	CGTAATACGACTCACTATAGGG GGCCGATGCACTGTA	GAAAGAGACCGGTTCACTG	62	79
mir-294-T7	TAATACGACTCACTATAGCTCA AAATGGAGGCCCTAT	ACACACAAAAGGGAAGCACT	62	76
mir-291-T7	TAATACGACTCACTATAGATCA AAGTGGAGGCC	ACAAACAAAATCCATGC	61	76
mir-125-T7	TAATACGACTCACTATAGCCCT GAGACCCTAACTTGTG	AGCTCCCAAGAGCCTAACCCG	63	350
pri-let-7a-T7	TAATACGACTCACTATAGGTCA TTACACAGGAAACCGGAAT	AAAACAAAAGGTCAGAATTCACC	62	420

## 2.1.4.D. Primers and FAM-probes used for Real-Time PCR:

Name	Forward Primer (Sequence 5' - 3')	Reverse Primer (Sequence 5' - 3')	FAM-Probe
muGAPDH	CTGCCACCCAGAAGACTGTG	CCGTTCACTCTGGGATGAC	6FAM-TGG CCC CXT CTG GAA AGC TGT GGC G--PH
18 S	CGGCTACCACATCCAAGGAA	GCTGGAATTACCGCGGCT	6FAM-CGC AAA TTA CCC ACT CCC GAC CC -BHQ1
mlin-41	The primers and FAM probe were designed by Applied Biosystems		

### 2.1.5. LNA oligonucleotides

LNA (Locked Nucleic Acid) contain a methylene bridge that connects the 2'-oxygen of ribose with the 4'-carbon. The bridge results in a locked 3'-endo conformation, conferring enhanced hybridization performance and exceptional biostability (Dwayne et al., 2001).



#### 2.1.5.A. LNA modified anti-miRNA oligonucleotides (Exiqon, Proligo)

Name	Sequence	T <sub>m</sub> (°C)
anti-let-7a	AACTATACAACCTACTACCTCA	71
anti-let-7e	ACTATACAACCTCCTACCTCA	71
anti-let-7c	AACCATACAACCTACTACTACCTCA	74
anti-let-7i	ACAGCACAAACTACTACCTCA	76
anti-mir-125b	TCACAAGTTAGGGTCTCAGGGA	79
anti-mir-128a	AAAAGAGACCGGTTCACTGTGA	77
anti-mir-140	CTACCATAGGGTAAAACCACTG	71
anti-mir-7	CAACAAAATCACTAGTCTTCCA	69
anti- mir-1	TACATACTTCTTTACATTCCA	64
anti-mir-34a	AACAACCAGCTAAGACACTGCCA	80
anti-mir-30a-3p	GCTGCAAAACATCCGACTGAAAG	74
m1in-41	ACCCTCCTTATCAACACTCACG	76
m1in-41 mismatch	ACCCTGGTTTTTCAACACTCACG	75
Trim-2	ATAAGTTGACCTCCAACCTCCATG	78
anti-pre-let-7a	GTGGTGGGTGTGACCCTAAA	
anti-pre-let-7g	CTGTACCGGGTGGTATCATAGA	
anti-let-7a mut	AACTATACAAACTACAACCTCA	70
anti-pre-let-7g mut	CTGTACCGGCTGGAATCATAGA	78
anti-pre-let-7a mut	GTGTTCGGTATGACCCTAAA	70

#### 2.1.5.B. miRNA precursors sequence (Ambion) used for cells transfection and EMSA

Name	Sequence
hsa-let-7e	UGAGGUAGGAGGUUGUAUAGUU
hsa-let-7a	UGAGGUAGUAGGUUGUAUAGUU
hsa-mir-128b	UCACAGUGAACCGGUCUCUUU
hsa-mir-125a	ACGGGUUAGGCUCUUGGGAGCU

#### 2.1.5.C. siRNA sequence used for cells transfection

Name	sequence
lin-41-1	CCCAAGAAGAUGACCGCAUUAUGUU
lin-41-106	CCUCGCCCUC AAGUCAUUGGCUUU
lin-28-1	ACGGGTTGTGATGACAGGCAA
lin-28-2	AGCGTGATGGTTGATAGCTAA
lin-28-3	AGGGTGGTACAGAGACATTAA
lin-28-4	AACGGGACAAATGCAATAGAA
lin-28b-1	CAGCCCATGATTGATACTAAA
lin-28b-2	CTCGACCATCATGCTAAAGAA
lin-28b-3	CCAGTGAAGTTTACATTTAAA
lin-28b-4	CAGGATGAGCACTCAGATCAA
Dicer-1	ATCGATCATATGTCCAGTCTA
Dicer-2	AACGGATCTTACAGCAATTAA
Dicer-3	CACCATATCCATCGAGCTGAA
Dicer-4	AAGGCAGAATTTAAAAGTTTGA
Tarbp2-1	CCCGTGTACGACCTTCTCAAA
Tarbp2-2	CAGGATCATGGCGGGTAGCAA
Tarbp2-3	CTGTGTGTTATGGTTCTGCAA
Tarbp2-4	CAGGCTTTCATGTCAGCTAT

### 2.1.6. Vectors

- pd4eGFP-N1 (Clontech)
- pDsRed2-N1 (Clontech)
- peGFP-N1 (Clontech)
- pc 3xFLAG-CMV (Sigma)
- Topo pCR2.1 (Invitrogen)
- p QE-30 (Qiagen)

### 2.1.7. Constructs

- pIRESneo-FLAG/HA Ago1 (Addgene)
- pIRESneo-FLAG/HA Ago2 (Addgene)
- pcFLAG 2-17 FMRP, kindly provided by Dr. Yue Feng
- pc 3xFLAG – lin-41 (C- terminal part)
- pc 3xFLAG-mlin-41
- peGFP-C1-mlin-41
- pmyc-MOV10 (Addgene)
- pmyc-TNRC6B (Addgene)

### 2.1.8. Bacterial strains

- Escherichia Coli XL-1 blue cells (Stratagene)
- Escherichia Coli XL-10 gold cells

- Escherichia coli M15 (pREP4)
- Topo10 cells (Invitrogen)

### 2.1.9. Primary cells, cell lines and mouse strains

- Primary hippocampal neurons
- ES cells – murine embryonic stem cell line D3(gift of Andrea Seiler, BGW, Berlin)
- P19 EC cell– mouse embryonic carcinoma cell line (German Collection of Microorganisms and Cell Cultures, Braunschweig Germany)
- HEK293 – Human Embryonic Kidney cells (German Collection of Microorganisms and Cell Cultures, Braunschweig Germany)
- HeLa cells- Human Cervix Carcinoma (German Collection of Microorganisms and Cell Cultures, Braunschweig Germany)
- NTERA-2 cells- Human Embryonal Carcinoma, teratocarcinoma (German Collection of Microorganisms and Cell Cultures, Braunschweig Germany)
- C57Bl/6J Mouse Line (FEM Berlin)

### 2.1.10. Buffers and Solutions

Buffers and Solutions used:

<b>Cell culture solutions</b>	
Trypsin/EDTA solution, 0.25% (Gibco)	-
Penicilin/Streptomycin 100x solution (Gibco)	-
Glutamax 100x (Gibco)	-
Fetal Bovine Serum (PAN)	-
PBS, 10×, pH = 7.4	2 g/L KCl, 2 g/L KH <sub>2</sub> PO <sub>4</sub> , 80 g/L NaCl, 14.4 g/L Na <sub>2</sub> HPO <sub>4</sub> ×2H <sub>2</sub> O, to 1 L with aqua bidest
<b>Solutions used for immunostaining</b>	
Paraformaldehyde (PFA, Sigma)	4% PFA in 1xPBS
Immunocytochemistry Blocking Solution	5% normal goat serum, 1% BSA, 0.1% fish gelatine, 1xPBS
Immunohistochemistry Blocking Solution	5% normal goat serum, 1% BSA, 1xPBST (TritonX100)
Washing Solution (PBST- I)	1xPBS, 0.1% Triton X100
Washing Solution (PBST-II)	1xBBS, 0.1% Tween20
<b>Solutions used for <i>in vitro</i> processing and EMSA</b>	
Polyacrylamide-Urea Gel, 12%	80 ml: 38.4 g Urea, 18.2 ml H <sub>2</sub> O, 8 ml 10×TBE, 24 ml 40% Acrylamide/Bis 19:1, 400 µl 10% APS, 40 µl TEMED
Polyacrylamide Gel (5%)	60ml: 47 ml H <sub>2</sub> O, 3 ml 10xTBE, 10 ml Acrylamide/bis (30%), 300µl 10% APS, 20µl TEMED
TBE, 10×	1 M Tris, 1 M boric acid, 25 mM EDTA, pH=8.0
<b>Solutions used for bacteria culture</b>	

LB-medium, pH=7.4	10 g NaCl, 10 g Tryptone (Sigma), 5 g yeast extract in 1 L distilled water
SOC-medium	0.5% yeast extract, 2% tryptone, 10 mM NaCl, 2.5 mM KCl, 10 mM MgCl <sub>2</sub> , 10 mM MgSO <sub>4</sub> , 20 mM glucose
<b>Lysis Buffers for cell extracts</b>	
Lysis Buffer for <i>in vitro</i> miRNA processing assay (FMRP lysis buffer)	0.5% Nonidet P (NP-40), 150 mM NaCl, 20 mM Tris-HCl pH 7.5, 2 mM MgCl <sub>2</sub> , 10 mM sodium fluorid, 1 mM DTT, 20% glycerol, 1× protease inhibitors cocktail (Roche)
RIPA Lysis Buffer	1% NP-40, 1% sodium deoxycholate, 0.15 M NaCl, 0.01 M sodium phosphate, pH 7.2, 2 mM EDTA, 50 mM sodium gluoride, 20% glycerol, 1mM DTT, 0.2 mM sodium vanadate, 1× protease inhibitors cocktail
Immunoprecipitation buffer – 1	10mM HEPES, 10mM KoAc, 2mM Mg(OAc) <sub>2</sub> , 1mM DTT, 110mM KCL, 1% NP-40, 1x protease inhibitor
Immunoprecipitation buffer-2 (RIP-CHIP)	50mM Tris-HCL (pH 7.4), 150mM NaCl, 1mM MgCl <sub>2</sub> , 0.5% NP-40, protease inhibitor, 400µM VRC
<b>Solution used for <i>in situ</i> hybridization</b>	
Hybridization buffer 1	50% vol/vol formamide, 5x SSC, 500µg /µl yeast tRNA, 1x Denhardt's Solution
Hybridization buffer 2	
Acetylation Solution	670 µl triethanolamine, 135 µl acetic anhydride, 49 ml H <sub>2</sub> O
SSC, 20×	3 M NaCl, 0.3 M Sodium citrate, pH=7.0
Blocking Solution	5% normal goat serum, 1% BSA
<b>Solutions used for Western blot</b>	
Protease inhibitors cocktail, 10×	0.2 mg/ml Pancreas extract, 0.02 mg/ml Chymotrypsin, 5 µg/ml Thermolysin, 0.2 mg/ml Trypsin, 3.3 mg/ml Papain
Stacking gel buffer	0.5 M Tris, pH 6.8
Separation gel buffer	1.5 M Tris, pH 8.8
Stacking gel 4%	3 ml H <sub>2</sub> O, 1.25 ml Stacking gel buffer, 540 µl 37.5:1% Acrylamid/Bis (Fluka), 50 µl 10% SDS 38 µl 10% APS, 13 µl TEMED
Separation gel 7.5%	5 ml H <sub>2</sub> O, 2.7 ml Separation gel buffer, 2 ml 37.5:1% Acrylamid/Bis (Fluka), 100 µl 10% SDS, 50 µl 10% APS, 5 µl TEMED
Electrophoresis buffer for protein SDS-PAGE, 10×	0.25 M Tris (Base), 1.92 M Glycin, 1% SDS in 1 L distilled water
Western blotting buffer	192 mM Glycin, 25 mM Tris, 20% Methanol, in 1 L distilled water
PBT	1×PBS, 0.1% Tween 20
<b>Buffers used for His-tag fused protein purification</b>	
Equilibration/wash buffer	50mM sodium phosphate, 6M guanidine- HCl, 300mM NaCl, pH 7 (wash buffer) pH 8 (equilibration buffer)
Imidazole elution buffer	45mM sodium phosphate, 5.4M guanidine HCL, 270mM NaCl, 150mM imidazole, pH 7
<b>Buffers used for GST protein purification</b>	
Equilibration buffer	PBS pH 7.4
Washing buffer	PBST (1% Triton X-100)
Elution buffer	10mM reduced glutathione, 50mM Tris-HCL pH 9.5
Regeneration buffer 1	0.1M borate buffer, 0.5M NaCl, pH 8.5
Regeneration buffer 2	0.1M acetate buffer, 0.5M NaCl, pH 4.5

### 2.1.11. Media

Cell lines	medium
P19 growth medium (P19GM)	$\alpha$ modified form of Eagle's minimal essential medium ( $\alpha$ MEM, Sigma) supplemented with 10% heat inactivated fetal bovine serum (FBS, Gibco), 2 mM glutamine (Biochrom), 50 U/ml penicillin and 50 $\mu$ g/ml streptomycin (Biochrom).
P19 neural induction medium (P19IM)	$\alpha$ MEM supplemented with 5% heat inactivated FBS, 2 mM glutamine, 50 U/ml penicillin and 50 $\mu$ g/ml streptomycin.
ES cell growth medium	Dulbecco's modified Eagle's medium (DMEM, Gibco), containing 15% heat inactivated FBS, 2 mM glutamine, 50 U/ml penicillin and 50 $\mu$ g/ml streptomycin, 1% nonessential amino acids (Gibco), 0.1 mM $\beta$ -mercaptoethanol (Gibco) and 1.000 U/ml murine leukemia inhibitory factor (mLIF, ESGRO).
HEK293 and Hela cells	DMEM, containing 10% FBS, 2 mM glutamine, 50 U/ml penicillin and 50 $\mu$ g/ml streptomycin, NAAA
primary neuron culture	Neurobasal Medium without L-Glutamine (Gibco) containing B27 supplement (Gibco), 50 U/ml penicillin and 50 $\mu$ g/ml streptomycin.

### 2.1.12. Antibodies

Antibodies used for flow immunocytochemistry or western blot:

Antibody, clone, company	Immunocytochemistry working dilution	Western blotting working dilution
<b>Primary antibodies</b>		
anti-FMRP, mouse monoclonal, clone 1C3-1a, Euromedex	1/1000	1/1000
anti- $\beta$ -III Tubulin, mouse monoclonal, clone SDL.3D10, Sigma	1/800	1/1000
Anti-digoxigenin rabbit, Roche	1/2500	-
Anti-digoxigenin mouse, Roche	1/400	-
anti-NeuN, mouse monoclonal, A60, Chemicon	1/500	-
Dicer mouse monoclonal, Abcam	1/200	-
anti-Lin28 MaxPab mouse polyclonal, Abnova	1/2000	1/4000
anti-Lin28 rabbit polyclonal	1/1000	1/2500
anti-KIF17	1/500	-
anti-Oct-3/4 (C-10):sc-5279, mouse monoclonal, Santa Cruz Biotechnology	1/1000	-
Anti-Oct-3/4, goat polyclonal, Neuromics antibodies	1/200	-
Anti-Mili/Hili	1/500	-
anti-Nanog mouse monoclonal, R&D Systems	1/500	-
anti-Stella, mouse monoclonal, R&D Systems	1/1000	-
anti-GFAP, mouse monoclonal, clone G-A-5, Sigma	1/1000	-
anti-c-Kit mouse monoclonal, eBioscience	1/200	-
anti TARBP2 monoclonal antibody (M01) clone 1B1	-	1/1000
anti-SOX2 rabbit polyclonal, BIOZOL	1/1000	-
anti-Ago1, rabbit polyclonal, Upstate	1/200	1/500

anti-Ago2, rabbit polyclonal, Upstate	1/200	1/500
anti-GFAP, rabbit polyclonal, DakoCytomation	1/1000	1/1000
anti-GFP, rabbit polyclonal, Abcam	1/500	1/1000
anti-HA, mouse monoclonal, clone HA-7, Sigma	1/1000	-
anti-Flag, mouse monoclonal, clone M2, Sigma	1/2500	1/2000
Anti-CD24 mouse monoclonal, BIOZOL	1/1000	-
anti-Myc, rabbit polyclonal, Abcam	1/500	1/1000
anti-mLin-41 Serum, rabbit, Pineda Antikörper Service, Berlin	1/5000	1/5000
Anti-mLin41 Serum, rabbit, peptide, Pineda Antikörper Service, Berlin	1/200	1/400
Anti-mLin41 Serum, guinea pig, peptide, Pineda Antikörper Service, Berlin	1/100	1/100
anti- $\beta$ -actin, mouse monoclonal, clone AC-15, Sigma	-	1/5000
P70 S6 kinase (H-9): sc-8414, mouse monoclonal, Santa Cruz Biotechnology	1/250	1/1000
<b>Secondary antibodies</b>		
Alexa Fluor 488/568 F(ab') <sub>2</sub> anti-mouse IgG, Molecular probes	1/1000	-
Alexa Fluor 488/568 F(ab') <sub>2</sub> anti-rabbit IgG, Molecular probes	1/1000	-
HRP-labeled sheep anti-mouse IgG, Amersham Bioscience	-	1/5000
HRP-labeled sheep anti-rabbit IgG, Amersham Bioscience	-	1/5000
HRP-labeled donkey anti-guinea pig, Jackson ImmunoResearch	-	1/10000

## **2.2. Methods**

### **2.2.1. P19 (EC), HEK293 and HeLa cell culture methods and NS cells preparation**

All cell types were cultured at 37°C in a humidified incubator with 5% CO<sub>2</sub>.

**P19 EC cells** are pluripotent cells derived from a primary teratocarcinoma induced in the C3H/He mouse strain. These cells can differentiate into all cell types under the appropriate conditions. P19 EC cell cultures were started from a frozen stock by seeding cells into a 100-mm tissue culture dish with 10 ml of P19 growth medium (P19GM). To passage, cells were removed from the culture dish surface with a 0.25% trypsin/EDTA solution (Gibco). Trypsinization was stopped by adding P19GM. Cells were transferred into a 15-ml conical tube and pelleted in a clinical centrifuge at 1000 rpm for 3 min. They were resuspended in 5 ml of fresh medium and seeded. For immunostaining, cells were plated on 0.1% gelatin-coated coverslips in 24- or 12-well plates.

**HEK293/HeLa cells** were grown as adherent monolayers in DMEM supplemented with 10% FBS, 2 mM glutamine, 50 U/ml penicillin and 50 µg/ml streptomycin. Under optimal conditions, HEK293 cells divide every 18-24 h and therefore were normally subcultured twice a week according to the same procedure as P19 EC cells. For immunostaining, HEK293 cells were plated on poly-D-lysine or gelatin coated coverslips in 24- or 12-well plates.

**Radial glia (NS)** cultures were prepared by adaptation of dissociated E12 forebrain cells to adherent growth after a brief period of culture as neurospheres. Cells were maintained on ornithine and laminin coated tissue culture plates in defined medium (EuroMed N medium supplemented with modified N2, EGF and FGF-2), as described. The NS cell line used in these experiments is Oct-4<sup>-</sup>, GFAP<sup>-</sup>, Sox2<sup>+</sup>, RC-2<sup>+</sup>, as confirmed by RT-PCR and immunohistochemistry (data not shown), consistent with the original description. NS cells were electroporated using the Amaxa kit for neural precursors, following the manufacturer's recommendations.

### **2.2.2. Cell transfection with plasmid DNA and siRNA**

For HEK293/ Hela cells, one day before transfection  $2 \times 10^5$  cells were plated in monolayer on poly-D-lysine covered glass in 12-well plates. Cells were transfected with 1-1.6 µg of the appropriate plasmid using Lipofectamine reagent or FuGene6. Cells were processed for immunocytochemistry after 24 or 48h hours.

For RNAi experiments and ectopic miRNA expression, EC cells were transfected with Lipofectamine RNAi-Max (Invitrogen GmbH, Karlsruhe, Germany), using the manufacturer's reverse transfection protocol. RNAi duplexes were obtained from Qiagen (Hilden, Germany) and used at 50 nM. The negative control siRNA (negative universal control, medium GC) was obtained from Invitrogen. Synthetic miRNA precursors were obtained from Ambion (Ambion/Applied Biosystems, Darmstadt, Germany) and used at 50 nM.

Primary neurons were transfected 7 to 10 days after plating on 18-mm precoated coverslips with Effectene reagent (Qiagen). On the day of transfection 0.5 µg DNA was diluted in DNA-condensation buffer (EC buffer), to a total volume of 75 µl; 5 µl Enhancer was added and mixed by vortexing for 1 s. The mix was incubated at RT for 4-5 min, then 6µl Effectene was added and mixed by pipetting up and down. Samples were incubated for 7-10 min at RT. After incubation, 200 µl of growth medium was added to the tube containing the transfection complex, then the mixture was added drop-wise to the cells. After 48 hours, cells were fixed and analyzed by immunocytochemistry.

### **2.2.3. Molecular biology methods**

Standard molecular biology methods such as bacterial culturing, restriction digests, gel electrophoresis, etc. were performed according to "Current protocols in molecular biology" (Ausubel, 1994) and will not be described in detail.

#### **2.2.3.A. Total RNA isolation**

Total RNA was isolated from mouse tissue and cell lines using TRIzol reagent (Gibco) in accordance with the manufacturer's instructions. Briefly, cells were lysed by adding 1 ml of TRIzol reagent per 35-mm diameter culture dish. Mouse brain samples were homogenized in 1 ml TRIzol reagent per 100 mg of tissue. After adding 0.2 ml of chloroform the lysate was shaken by hand for 15 s, incubated at RT for 2-3 min and centrifuged at 12.000 g for 15 min at 4°C to separate the phases. The upper, aqueous phase containing RNA was collected in a new tube. RNA was precipitated by addition of 0.5 ml of isopropyl alcohol per 1 ml of TRIzol reagent by centrifugation at 12.000 g for 15 min at 4°C. Pellets were washed with 70% ethanol and dissolved in RNase-free water. RNA concentrations were measured using NanoDrop. The integrity of isolated RNA was checked by electrophoresis in a 1.5% agarose gel stained with ethidium bromide (0.1 µg/ml).

In some cases total RNA was isolated using RNeasy Plus Mini Kit (Qiagen) according to manufacturer's instructions.

### **2.2.3.B. cDNA synthesis from total RNA**

cDNA was synthesized using the Advantage RT-for-PCR kit (Clontech) or SuperScript II RT(Invitrogen).

**Using Advantage RT PCR kit**, 2 µg of total RNA were heated together with oligo(dT)<sub>18</sub> primer at 70°C for 2 min, and cooled rapidly on ice. Then the components listed below were added:

4 µl 5× reaction buffer

1 µl dNTP mix (10 mM each)

0.5 µl Recombinant RNase inhibitor, 20 U

1 µl DNase, 2 U (RNase free)

The reaction was incubated at 37°C for 30 min, then heated to 75°C for 5 min, and placed on ice. After DNase treatment, 1 µl of MMLV reverse transcriptase and 1 µl recombinant RNase inhibitor were added to the reaction, and samples were incubated at 42°C for 1 hour. To stop the cDNA synthesis, the reaction was heated at 94°C for 5 min.

**Using SuperScript II**, 0.2-4 µg of total RNA, 1 µl oligo(dT)<sub>18</sub> (500µg/ml), 1µl 10mM dNTP in 12µl volume were heated to 65°C for 5 min and quick chilled on ice. 4 µl 5x first-strand buffer, 2 µl 0.1M DTT, 1µl Ribolock (Invitrogen) were added and incubated at 42°C for 2 min followed by adding 1µl (200 units) SuperScript II enzyme. Reactions were incubated at 42°C for 50-70 min and then deactivated at 70°C for 10 min.

The cDNA was diluted to a final volume of 100 µl by adding 80 µl of RNase free water and stored at -70°C. cDNA integrity was monitored using primers specific for β-actin.

### **2.2.3.C. Polymerase Chain Reaction (PCR)**

#### **2.2.3.C.1. Semi-quantitative PCR**

DNA was amplified using a PCR block (MJ Research). PCR reactions (50 µl) were performed using either the CombiZyme DNA Polymerase mix (Invitex), GoTaq DNA polymerase (Promega) or the Phusion High-Fidelity DNA Polymerase (Finnzymes).

The following components were mixed:

**- for a CombiZyme Polymerase reaction:**

1× OptiPerform Buffer III

2.5 mM MgCl<sub>2</sub>  
 250 μM dNTPs  
 1× OptiZyme Enhancer  
 0.5 μM forward primer  
 0.5 μM reverse primer  
 15-500 ng Template DNA  
 2 U CombiZyme DNA Polymerase  
 H<sub>2</sub>O to a final volume of 50 μl

**- for Phusion Polymerase reactions:**

1× Phusion HF Buffer  
 200 μM dNTPs  
 0.5 μM forward primer  
 0.5 μM reverse primer  
 15-500 ng Template DNA  
 1 U Phusion DNA Polymerase  
 H<sub>2</sub>O to a final volume of 50 μl

**- for GoTaq polymerase reaction:**

1× GoTaq master mix  
 1 μM forward primer  
 1 μM reverse primer  
 <250 ng Template DNA  
 H<sub>2</sub>O to a final volume of 50 μl

Programs for PCR reaction with CombiZyme Polymerase Mix, GoTaq green Master Mix or Phusion Polymerase:

Steps	CombiZyme Polymerase Mix	GoTaq DNA polymerase	Phusion Polymerase
Initial denaturation	95°C for 2 min	95°C for 2 min	98°C for 2 min
Denaturation	94°C for 30-60 s	95°C for 15s	98°C for 10 s
Annealing	60-70°C for 1 min	5°C below the calculated melting temperature of the primers	58-65°C for 15-30 s
Extension	72°C for 1 min	72-74°C for 1 min	72°C for 30-45 s
Cycles	25-35	25-30	25-35
Final extension	72°C for 5 min	72°C for 5 min	72°C for 3-5 min
Storage	12°C	12°C	12°C

PCR products were analyzed by 1-2% agarose gel electrophoresis.

### **2.2.3.C.2. Real-Time PCR**

cDNA for Real-Time PCR was synthesized with the Advantage RT-for-PCR kit as described above. One  $\mu\text{l}$  cDNA was used for each reaction. Both standard housekeeping gene primers were designed with Primer-Express software (Applied Biosystems). The primers and probes for genes of interest were ordered as Custom TaqMan Gene Expression Assays from Applied Biosystems. The PCR mix for GAPDH (Glyceraldehyde-3-phosphate dehydrogenase) housekeeping gene controls contained 1  $\mu\text{l}$  cDNA template, 10  $\mu\text{l}$  2 $\times$  TaqMan Universal PCR Master Mix No AmpErase UNG (Applied Biosystems), 0.5  $\mu\text{M}$  of each primers and 0.25  $\mu\text{M}$  probe in a total volume of 20  $\mu\text{l}$ . PCR mix for genes of interest contained 1  $\mu\text{l}$  cDNA template, 10  $\mu\text{l}$  2 $\times$  Universal PCR Master Mix No AmpErase UNG, 1  $\mu\text{l}$  20 $\times$  TaqMan Gene Expression Assays Mix (containing 18  $\mu\text{M}$  primer 1, 18  $\mu\text{M}$  primer 2, 5  $\mu\text{M}$  probe) in a total volume of 20  $\mu\text{l}$ . Standard reactions were performed using an Applied Biosystems PRISM 7500 Sequence Detection System. The following cycle parameters were used: AmpliTaq activation 95°C for 10 min; PCR: denaturation 95°C for 15 s and annealing/extension 60°C for 1 min (repeated 40 times). All experiments were carried out in duplicate. The results were analyzed using TaqMan 7500 software.

### **2.2.4. Histo- and cytological methods**

#### **2.2.4.A. Immunocytochemistry**

For immunocytochemistry, cells (EC, HeLa, Hek293 cells, primary neurons) were plated on gelatin or poly-D-lysine coated coverslips. At appropriate time points cells were fixed in 4% PFA for 20 min at 4°C, washed twice with ice cold PBS, permeabilized with 0.1% Triton X and blocked for 30 min at 4°C (Blocking Solution: 5% normal goat serum, 1% BSA, 0.1% fish gelatin in 1 $\times$ PBS). Primary antibodies were diluted in Blocking Solution and incubated with cells for 2 hours at RT or overnight at 4°C. After thrice-repeated washing with ice cold PBS the cells were incubated with secondary antibodies for 1 h at RT. The antibodies used for immunocytochemistry are listed in the Table 2.1.12. Nuclei were visualized by staining with DNA specific dye DAPI for 5 min at 4°C. Cells were washed three times with ice cold PBS and fixed on glass slides with Immu-mount (Thermo Shandon).

#### **2.2.4.B. Preparation of brain and testis tissue sections and immunostaining**

For preparation of frozen sections, P4, P7, P14, P28 and adult C57BL/6 mouse testis or brains were isolated and embedded directly into Tissue-Tek O.C.T. compound (Sakura, Torrance, CA) and frozen in liquid nitrogen. 5 -10  $\mu$ m slides were prepared on the cryostat. Cryosections were fixed in 4% (w/v) paraformaldehyde/PBS solution at room temperature for 15 min and washed four times with PBS. The fixed sections were preincubated with blocking solution (5% goat serum, 1x PBS, 0.1% Triton X-100) at room temperature for 1h, and then incubated with rabbit anti-mLin41 antibody. To examine the cell phenotype of Lin41 expression, double immunofluorescence was applied using cell type-specific markers, including anti- C-kit receptor (stem cell factor receptor) antibody (eBioscience, Netherlands) for germ cell, anti Müllerian Hormone Receptor for the testis intrastromal wall. For the brain slides: anti-glial fibrillary acidic protein (GFAP) antibody (Sigma, St. Louis, MO, USA) for astrocytes, and anti-prominin antibody for SVZ and anti-nestin for neuroprogenitor cells were used. In brief, the sections were incubated in the following order: rabbit anti-mLin41 antibody overnight at 4 °C, and Alexa-568 anti-rabbit IgG (Sigma) for 1 h at RT. The sections were then washed and blocked with 5% normal goat serum for 1 h at RT, incubated overnight at 4 °C with either the mouse monoclonal anti C-kit, or anti-GFAP antibody for the brain sections or the anti c-kit receptor antibody for the testis sections. After three washes, the slides were stained with Alexa-488 labeled goat anti-mouse IgG (Sigma). The double immunofluorescence-stained specimens were examined with a fluorescence microscope.

#### **2.2.4.C. Immunofluorescence staining for early stage mouse embryos**

Mouse embryos were isolated at E7.5 to E7.8 of development. The midday of the vaginal plug was considered as Day 0.5 post coitum. Embryos were fixed for 10 min in 4% PFA in PBS and permeabilized with 0.1% Triton X-100 in PBS for 10 min at RT. The fixed embryos were blocked overnight at 4°C in 1% BSA, 0.1% TritonX-100 in PBS, and then incubated for 2-3h at RT (or o.n. in 4°C) in the blocking solution with the primary antibodies, followed by several washes times (3x in 0.1ml blocking solution), incubation with the secondary antibody for 1-2h at RT, and staining with DAPI. After the final washes the embryos were equilibrated in 10-20 $\mu$ l mounting medium (Vectashield). A small drop of the medium was put on the cover slip and gently put over the drop with the embryos. After 5 min. the cover slip was sealed with nail polish.

#### **2.2.4.D. Immunohistochemistry with floating brain sections for electron microscopy**

For preparation of floating sections, P14, P28 and adult C57BL/6 perfused mouse brains were isolated, fixed overnight in 4% PFA, washed 2x with PBS and embedded in 20% gelatine. Brains were sectioned on vibratome into 50  $\mu$ m slides. Sections were treated for 20 min with 1% H<sub>2</sub>O<sub>2</sub> to block endogenous peroxidase activity, followed by 5 washes with 0.1M PB and then blocked for 1h with blocking solution BS (2% BSA, 5% normal goat serum, +/- 0.1% TritonX100). The blocking solution was replaced with antibody solution and incubated at RT overnight with stirring or at 4°C over 2 days. Slides were washed 5x with PB and incubated for 2h with biotinylated secondary antibodies, followed by several washes with PB and development with DAB (ABC reaction).

ABC reaction:

1. AB solution: 10 ml PB + 90 $\mu$ l solution A + 90 $\mu$ l solution B, incubated for 1h in dark, followed by several washes with PB
2. C solution: - solution-1: 25 ml PB + 17.5 mg DAB (stirred and shortly sonicated), + 80  $\mu$ l of NH<sub>4</sub>Ni-SB<sub>4</sub> and 100  $\mu$ l of CoCl<sub>2</sub>  
- solution-2: 9.9 ml distilled water + 0.1 ml H<sub>2</sub>O<sub>2</sub>

Solution C was prepared by adding 165  $\mu$ l of solution-2 to solution-1 and incubated with slides. The reaction was stopped by several washes in PB.

#### **2.2.4.E. Immunostaining with paraffin embedded tissue**

Human brain tumor paraffin sections were dewaxed with Xylene 3x 5min and then dehydrated through an ethanol series (2x 100%-2min each, 2x 95%-2 min, 1x 70%-2min, 1x 50%-2min, 1x30%-2 min, 3x PBS). Slides were backed in the microwave 2x 5min in 0.01M NaCl and allowed to cool down to the room temperature at least for 15 min. Endogenous peroxidase activity was blocked by a 5 min incubation with 3% H<sub>2</sub>O<sub>2</sub>, followed by several washes with PBS. Slides were blocked for at least 1h with blocking buffer (5% NGS, 1% BSA, 0.1% TritonX100), followed by o/n incubation with primary antibody. Slides were washed several times with PBST and incubated for 2h with secondary biotinylated antibody, followed by several washes with PBS. ABC reagent was prepared according to the manufacturer's description, and incubated on the slides for 30-45min. Slides were washed 5x 5min and incubated with DAB reagent (10mL of water, one tablet of UREA Hydrogen and one tablet of DAB (Sigma)). The reaction was stopped by washing slides several times with cold PBS, followed by o/n washing. Slides were dehydrated

through an ethanol series, cleared in xylene and mounted with Xylene Substitute Mountant medium (Shandon).

#### 2.2.4.F. Preparation of mouse skin cryostat sections

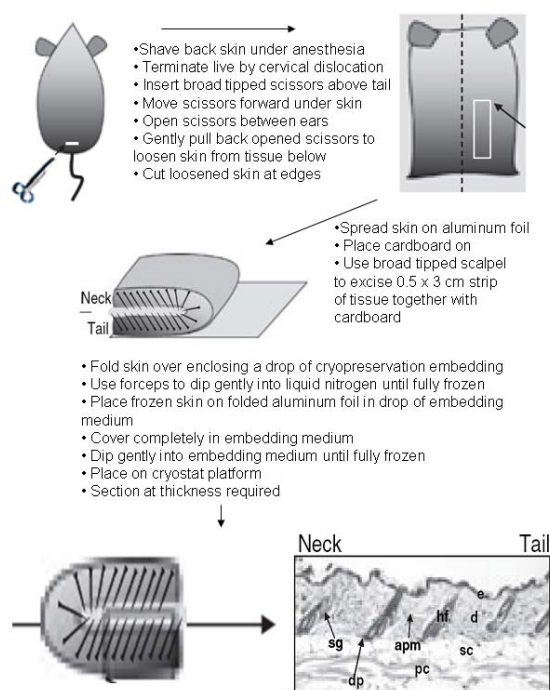


Figure 2.1. **Guide to perpendicular skin harvesting.** This schematic representation demonstrates how skin can be harvested to provide exact and reproducible histology. Abbreviations: apm, arrector pili muscle; d, dermis; dp, dermal papilla; e, epidermis; hf, hair follicle; pc, panniculus carnosus; sc, subcutis and sg, sebaceous gland (Adapted from Hendrix et al., 200).

#### 2.2.5. Fluorescent and Confocal microscopy

Slides were photographed with an Olympus BX 51 BX 50 microscope using the Magnafire program. Confocal images were acquired with an upright laser microscope (Leica DM 2500) equipped with a 63x objective (oil-immersion) using sequential scanning with the 405-nanometer spectral line of a blue diode laser, the 488-nanometer line of an argon-ion laser and the 532-nanometer line from a green helium-neon laser. During the processing stage individual image channels were pseudocolored with RGB values corresponding to each of the fluorophore emission spectral profiles. All images were collected, merged and compiled with the aid of Image J and Adobe Photoshop. Brightness and contrast were adjusted in Image J, equivalent settings were used for control and test images.

### **2.2.6. *in situ* hybridization**

#### **2.2.6.A. *in situ* hybridization on mouse testis/brain slides**

LNA probes (Exiqon) were labelled with terminal transferase and digoxigenin-ddUTP (DIG-3'-end labelling kit, Roche), followed by purification with MicroSpin G-25 columns (Amersham Biosciences). Cryosections of mouse testis were acetylated for 10 min at RT, washed 3 times in PBS, dehydrated in an ethanol series (30,70, 90,100%) and prehybridized in hybridization buffer (10 mM HEPES pH 7.5, 600 mM NaCl, 100 mM dithiothreitol, 50%(v:v) formamide, 1mM EDTA,10% dextran sulfate, 1x Denhardt's solution, 100µg/ml salmon sperm DNA) at 20°-22°C below the calculated probe T<sub>m</sub>. After 2h the prehybridization solution was replaced with hybridization buffer (HB) containing 10 µl (around 10 pm/slide) of purified probe and hybridized overnight. One 15 min wash step in 1xSSC at hybridization temperature was followed by 3x washes with 0.1 x SSC at hybridization temperature for 15 min each. Further wash steps in PBST were performed at RT followed by blocking in PBST plus 5% goat serum and 2 mg/ml BSA. Slides were then incubated with anti-DIG antibody (1:5000) for 2h at RT and washed 4 x with PBST for 30min each, 2x in NTMT (100mM Tris-HCL pH 9.5, 50mM MgCl<sub>2</sub>, 100mM NaCl, 0,1% Tween) and stained with BCIP/NBT.

#### **2.2.6.B. *Cells in situ* hybridization.**

Cells were plated on gelatin covered slides. After 12-24h cells were fixed with 4% PFA for 20 min in RT, washed with PBS and stored in 70% ethanol at 4°C at least overnight and for up to 1 month. Cells were rehydrated in 2x SSC (2x 15 min wash) and then prehybridized in hybridization buffer [50% (vol/vol) formamide, 5xSSC, 500 mg/ml yeast tRNA, 100ug/ml salmon sperm DNA, 1x Denhardt's solution] for 1h in 37°C. Prehybridization buffer was replaced with hybridization buffer containing 2 pmol of DIG labeled probe/100ul/slide and hybridized overnight in 37°C. Coverslips were then washed 3x 15 min at 55°C (washing temperature was adjusted according to annealing temperature of the probe) with 30% formamide in 2xSSC, then 2x 15 min 2xSSC at RT and 2x 15 min PBS at RT. Cells were incubated for 10 min with 3% (vol/vol) H<sub>2</sub>O<sub>2</sub> to block endogenous peroxidase activity, washed 3x with PBS and blocked for 1h with blocking solution (1xPBS, 1% BSA,3% normal goat serum). Primary anti DIG antibody were diluted in blocking solution and incubated for 2h (monoclonal for fluorescent 1:400 or sheep for colorimetric detection 1:2500). Slides were washed 3x 15 min with PBST (1xPBS, 0,1% TritonX100). For fluorescent detection slides were incubated with Alexa568 coupled secondary antibody for 1h, washed 3x with PBST and stained with DAPI. For

colorimetric detection slides were washed 2x with AP buffer and incubated with NBT/BCIP in AP buffer. Slides were mounted in Prolong Gold Antifade (Invitrogen, Carlsbad, CA) and allowed to dry overnight in the dark at 20–21°C before observation and imaging.

#### **2.2.6.C. Whole mount *in situ* hybridization**

Mouse embryos were dissected in ice-cold PBS. The extra-embryonic membranes were removed and the heart, brain and optic vesicles were punctured with a sterile steel needle. Embryos were fixed in 4% PFA overnight at 4°C, washed with PBS and dehydrated on ice through a methanol series (25%, 50%, 75%, 2x 100%). Embryos were bleached in methanol/H<sub>2</sub>O<sub>2</sub> (4:1) for 1h at -20°C, washed 2x with 100% methanol and stored in -20°C up to several months.

Embryos were dehydrated through a methanol/PBS series (75%, 50%, 25%) , washed 2x with PBST (PBS+ 0.1% Tween-20), treated with 10 µg/ml proteinase K in PBST (10 min for E9.5, 15 min for E10.5, 20 min-E11.5 embryos). Embryos were washed briefly with PBST, post- fixed for 20 min in 4% PFA, washed 2x with PBST and 1x with prehybridization solution/BBST (1:1) and 1x with prehybridization solution. Prehybridization was carried on for 2h at 20-25°C under the annealing temperature of the LNA probe. The prehybridization solution was replaced with prewarmed hybridization solution contain DIG labelled LNA probe and incubated overnight at hybridization temperature.

Embryos were washed as followed:

- 2x 5 min prewarmed hybridization solution
- 2x 30 min prewarmed hybridization solution/ 0.1x SSC
- 3x 0.1xSSC at hybridization temperature
- 2x 2x SSC at RT

Embryos were blocked for 2h with a blocking solution (5% NGS, 1% BSA in PBST or with 2% Boehring Blocking Reagent in MABT ( 100mM Maleic acid, 150mM NaCL, 0.5% Tween-20) buffer), followed by overnight incubation with anti-DIG antibody in blocking solution. Embryos were washed for several hours with PBST (PBST exchange every 30 min) than 2x with NTMT (pH 9.5) buffer and finally developed with NBT/BCIP solution. The reaction was stopped, at the moment when first staining appeared, by several washes with PBST. Embryos were washed overnight and the staining procedure was repeated until clear signal appeared. Embryos were post-fixed with 4% PFA, washed with PBS and stored at 4°C in 80% glycerol solution in PBS.

### **2.2.7. DNA cloning methods**

- Gel extraction:

DNA fragments were purified from agarose gels using the QIAquick Gel Extraction Kit (Qiagen) according to the manufacturer's instructions.

- Plasmid linearization and dephosphorylation:

Vectors used for cloning were linearized with the appropriate restriction enzymes and 5' phosphates were removed when necessary using Shrimp Alkaline Phosphatase (SAP, Promega). Both restriction enzymes and SAP were heat-inactivated for 15 min at 65°C.

- Ligation:

Insert restriction fragments were ligated into the linearized and dephosphorylated vectors using T<sub>4</sub> DNA Ligase (BioLabs) in 20 µl reaction volume overnight at 16°C. T<sub>4</sub> DNA Ligase was inactivated by heating at 65°C for 15 min and the vectors were transformed into chemically competent *E. coli* cells.

- *E. coli* transformation:

XL-10 gold or Topo10 chemically competent *E. coli* cells were thawed on ice, 200-400 ng of plasmid DNA were added to 50 µl cells and incubated on ice for 30 min. The heat shock step was carried out at 42°C for 30 s, 250 µl SOC-Medium was added and the cells were incubated at 37°C for 1 h on a shaker. 100 µl from transformed bacterial cells were plated onto LB-plates containing ampicillin (100 µg/ml) or kanamycin (30 µg/ml) to select transformed bacteria. Plates were incubated at 37°C overnight. Individual colonies were picked and grown in LB-medium with appropriate antibiotics for plasmid DNA preparation.

- Extraction of plasmid DNA:

Small-scale preparations of plasmid DNA were performed in 3 ml of LB-medium by Plasmid-Mini Kit (SeqLab). Medium culture (25 ml) or large culture (100-200 ml) preparations were carried out using Plasmid-Midi and Plasmid-Maxi kits (NucleoBond Macherey-Nagel) respectively, according to the manufacturer's protocols.

- Restriction enzyme digestion:

To check the presence and the orientation of the insert of interest, plasmid DNA was digested with the appropriate restriction endonucleases at 37° C for 1-2 hours in 10-30 µl reaction volume. The product size was analyzed by agarose gel electrophoresis using 100-bp DNA Ladder, extended (Roth).

### 2.2.8. Plasmid constructs cloned for this work

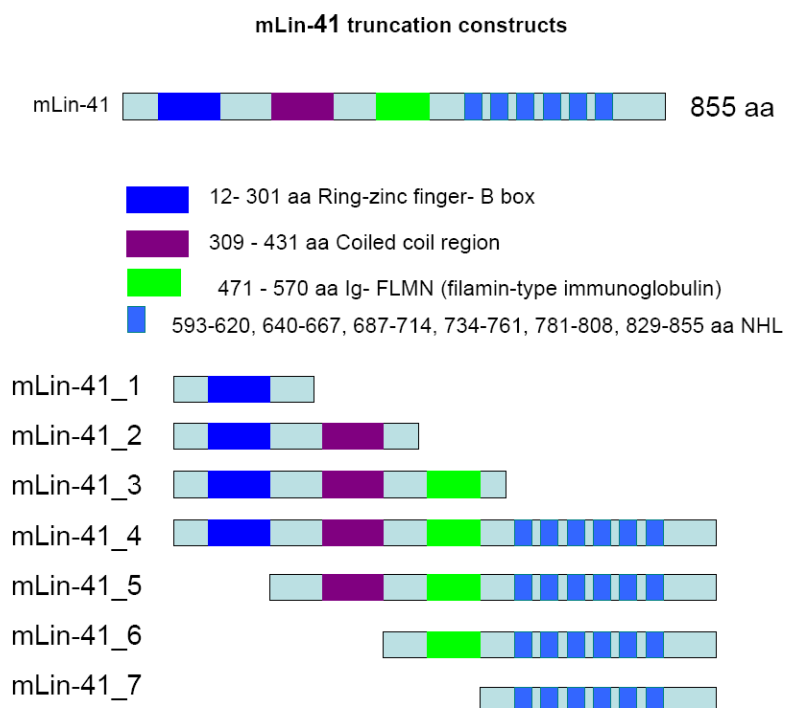


**Figure 2.2. mLin-41 truncation constructs.**

For all the GFP Lin-41 truncation constructs, the primer used for amplification contained a Sall (forward primer) and BamHI (the reverse primer) restriction sites. The resulting PCR fragments: 1-900bp, 2-1300bp, 3-1700bp, 4-1800bp, 5-1650bp, 6-1200bp, 7-820bp, were precloned into the pCR2.1 TOPO Vector using the TOPO-kit (Invitrogen), followed by excision with Sall and BamHI. Fragments were then gel-purified and inserted into the peGFP-C1 vector.

### 2.2.9. *In vitro pre-miRNA transcription*

About seventy base pair templates for *in vitro* transcription were amplified using specific primer pairs from table 2.1.4.C. *pre-let7e*, *mir-128*, *mir-291*, *mir-125* were amplified from a genomic mouse DNA fragment subcloned in Topo pCR2.1 vector, *pre-let7a* – by nested PCR from mouse genomic DNA. The PCR products were purified from a 2.5% agarose gel using the QIAquick Gel Extraction kit and 1 µg of each template was transcribed by T7 RNA polymerase (MaxiScript SP6/T7) in the presence of [ $\alpha$ - $^{32}$ P]UTP (25 µCi at concentration of 10 µCi/µl). The reactions were incubated at 37°C. After 2 hours pre-miRNAs were purified by phenol/chloroform extraction and precipitated with 100% isopropanol in the presence of 0.3 M ammonium acetate.

Pellets were dissolved in RNase free water at 20.000 cpm/ $\mu$ l. RNAs were stored at  $-80^{\circ}\text{C}$ . *In vitro* transcribed pre-miRNAs were used for the EMSA and the *in vitro* miRNA processing assay.

### 2.2.10. RNA labelling for microarrays

Total RNA was isolated from cell lines using TRIzol reagent (Gibco) as described above.

- The first strand synthesis was performed for 1h at  $42^{\circ}\text{C}$ , in the following reaction mix:

1 $\mu$ l of oligo-dT-T7	}	denaturated at $70^{\circ}\text{C}$ , 10 min
16 $\mu$ g of total RNA		
up to 11 $\mu$ l Millipore II water		

added:

4  $\mu$ l 5x first strand buffer

2  $\mu$ l 0.1M DTT

1  $\mu$ l 10mM dNTPs

- The synthesis of second strand was performed in the following reaction mix:

71 $\mu$ l Milli II water	}	incubate at $16^{\circ}\text{C}$ for 2h
30 $\mu$ l second strand buffer		
3 $\mu$ l 10mM dNTPs		
1 $\mu$ l E.coli DNA ligase		
4 $\mu$ l E.coli DNA polymerase		

1  $\mu$ l E.coli Rnase H

2  $\mu$ l of T4 DNA polymerase was added, and incubated for an additional 15 min at  $16^{\circ}\text{C}$ , followed by addition of 10  $\mu$ l 0.5M EDTA.

- cDNA purification

cDNA was cleaned up with phenol/chlorophorm extraction and phase-lock tubes purification according to manufacturers description. cDNA was precipitated with 80% ethanol, and the pellet was resuspended in 12  $\mu$ l of Milli II water.

- *in vitro* transcription (GeneChip® IVT Labeling Kit, Affymetrix) was performed overnight at 16°C, in the following reaction mix:

4 µl cDNA

6 µl Milli II

2 µl IV labeling buffer

6 µl IVT labeling NTP mix

2 µl IVT enzyme mix

The reaction mix was cleaned up with spin columns, and RNA was eluted 2x with 15 µl of H<sub>2</sub>O. The quality of the transcription reaction was checked on an agarose gel. 15 µg of labeled RNA in a volume of 30 µl H<sub>2</sub>O was sent to the microarray facility at the MDC (Buch). Microarray analysis was performed on the GeneChip® Mouse Expression Set 430 (Affymetrix)

### **2.2.11. Biochemical methods**

#### **2.2.11.A. Protein electrophoresis and Western blots**

Protein extracts were prepared from P19 EC, HeLa, HEK293, NS cells or primary neurons. Cells were resuspended in RIPA Lysis Buffer or Lysis Buffer used for *in vitro* miRNA processing in the presence of a protease inhibitor cocktail (Roche). Lysates were clarified by centrifugation at 14.000 rpm, 4°C for 20 min. Supernatants were snap-frozen in liquid nitrogen and stored at -80°C. The total protein concentration in the extracts was measured by the BCA protein assay kit (Pierce) according to the manufacturer's description. Briefly, BSA (25 µg/ml – 2000 µg/ml) was used as a standard. The measurement was performed in 96-well plates in the ratio of sample to working reagent 1:8. After 30 min incubation at 37°C, the absorbance was measured at 562 nm on a plate reader (Biotech Instruments).

Ten to twenty µg of protein extract in SDS sample loading buffer were denaturated at 95°C for 10 min, separated by SDS-PAGE and transferred to an Immobilon P membrane (Millipore) in Western blotting buffer at 10 V for 20 min. The transfer efficiency was determined by Ponceau Red staining for 5 min at RT.

To block non-specific binding to the membranes, they were incubated overnight at 4°C in Blocking Solution (3% BSA in PBT). The primary antibodies were diluted in Blocking Solution according to the manufacturer's recommendation and incubated with membranes for 2 hours at RT. After 3 15 min washing steps with PBST, horseradish peroxidase conjugated secondary anti-mouse or anti-rabbit antibodies (Amersham Biosciences) were applied for 1 hour. The

membranes were washed as above. For visualization of immuno-reactive bands chemiluminescent detection ECL reagents (Amersham Biosciences) were used as recommended by the manufacturer. The membranes were then exposed to ECL Hyperfilm (Amersham Biosciences). To reprobe membranes, the old antibody complexes were stripped in 0.2 M glycine, 0.1% SDS, 1% Tween20, pH 2.2 for 3 hours at RT prior to blocking.

#### **2.2.11.B. Immunoprecipitation**

Cells were homogenized in immunoprecipitation buffer (50mM Tris-HCl pH 7.5, 10mM KoAc, 2mM Mg(OAc)<sub>2</sub>, 1mM DTT, 110mM KCl, 1% NP-40, 1x Protease Arrest / Calbiochem). After incubation for 30 min on ice, the homogenates were centrifuged, and the cell lysates were spun at 15,000×g in an for 10 min at 4 °C, to pellet the unbroken cells. The protein concentrations were determined using the BioRAD protein assay, with BSA as the standard. The lysate supernatant was precleared by incubation with preimmune IgG and protein A-Sepharose for 1h. Precleared cell lysates were incubated with primary antibodies and 20 µl of the 50% slurry of protein A-Sepharose or G-Sepharose for 4-24 h. The immune complex was collected by low-speed centrifugation and washed five times with ice-cold immunoprecipitation buffer. One volume of 2x SDS sample buffer was added and the mixture was boiled. The recovered proteins were separated by SDS-polyacrylamide gel electrophoresis.

#### **2.2.11.C. Protein overexpression for anti-mLin-41 antibody generation**

The N-terminal and C-terminal fragments of mLin-41 protein were expressed as a 6xHis-tagged fusion proteins using pQE-30 . In parallel glutathione *S*-transferase (GST) fusion proteins were generated pGEX-P3. After growth in LB medium at 37° to an optical density of 0.6, induction was carried out with 0.1 mM isopropyl β-d-thiogalactopyranoside for 2 h and harvested by centrifugation at 5000 ×g for 10 min at 4°. Cells were re-suspended in STE buffer containing 10% sarcosyl for lysis by sonication on ice. The sonicate was centrifuged at 14,000 ×g for 20 min at 4°C. The supernatant was mixed with glutathione-Agarose Beads (Sigma) for His-tagged proteins or TALON Methal Affinity Resin (BD Bioscience) for GST-tagged protein, incubated 4h at 4°C. The mixtures were diluted and loaded onto a mini-column and washed with 30 volumes of washing buffer. The GST-Lin41-N fusion protein was eluted with PBS containing 5 mM reduced glutathione and the His-tagged protein with 150mM imidazole.

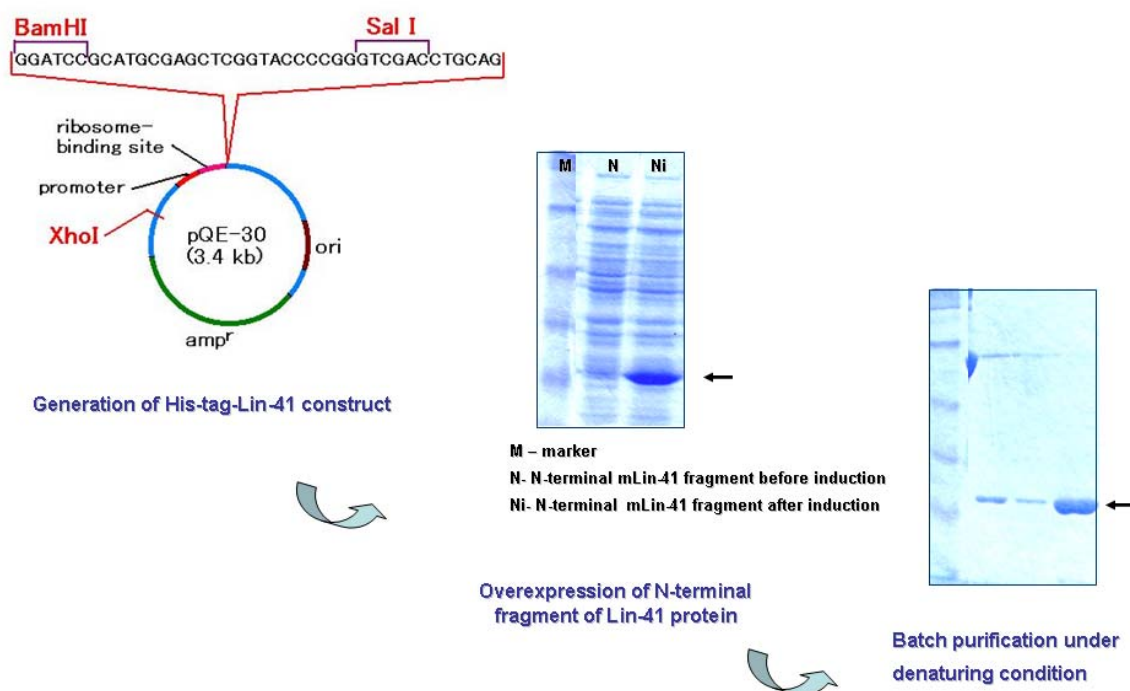


**Figure 2.3. N-terminal fragment of mLin-41 protein overexpression and purification for antigen production.**

The N-terminal Lin41-His-tagged protein was used as an antigen for antibody generation. Standard methods of immunization, boosting and bleeding of rabbits were carried out by Pineda-Antikörper-Service.

Crude sera were affinity purified using cross-linked GST beads, prepared according to standard protocols. After centrifugation to remove aggregated proteins ( $12,000 \times g$  5 min), the serum supernatant was diluted with an equal volume of PBST (PBS, 0.2% Tween20) and incubated over night with 800  $\mu$ l of cross-linked GST beads. The preparation was applied to a column by gravity flow. The column was washed with 30 ml PBST (PBS, 0.2% Tween20) After the final wash with 10 ml PBS, the IgG fraction was eluted with 0.2 M glycine pH 2.5. The IgG elution was collected in 750  $\mu$ l fractions in 1.5 ml conical tubes containing 250  $\mu$ l of 1 M  $K_2HPO_4$  to neutralize the sample. Sodium azide was added to a final concentration of 0.02%. The specificity of purified sera was tested by Western Blot and Immunohistochemistry.

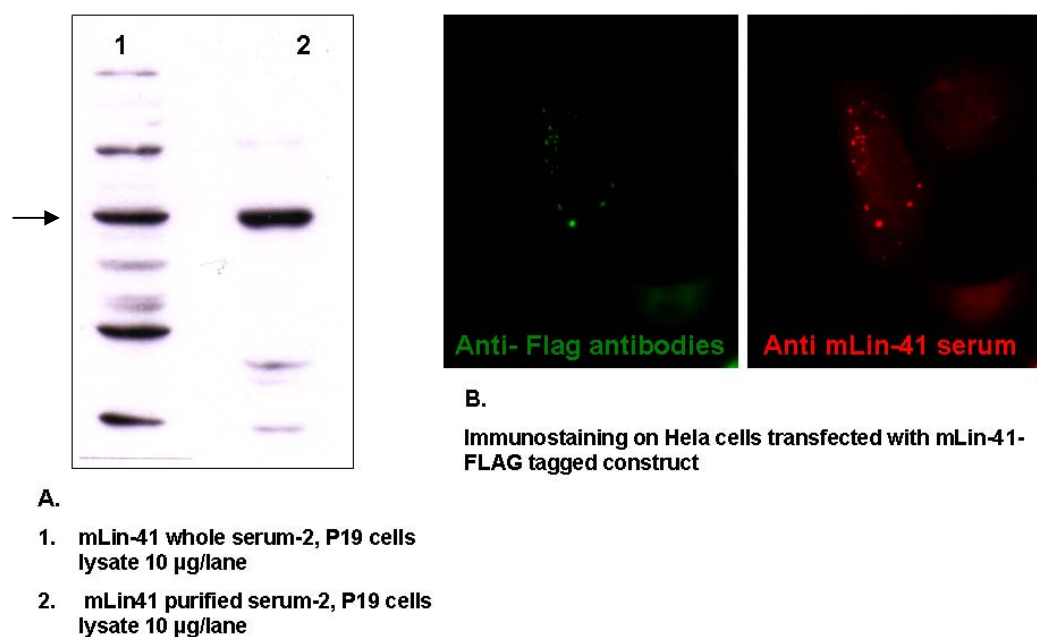


Figure 2.4. Lin-41 serum test by Western Blot (A) and Immunocytochemistry (B).

#### 2.2.11.D. *In vitro* miRNA processing assay

pre-miRNA templates were transcribed *in vitro* in the presence of [ $\alpha$ - $^{32}$ P]UTP. Cytoplasmic extracts for the *in vitro* reaction were prepared from undifferentiated or neural differentiated P19 EC cells, ES cells, primary neurons and astrocytes in Lysis Buffer (0.5% Np-40, 150 mM NaCl, 20 mM Tris-HCl, pH 7.5, 2 mM MgCl<sub>2</sub>, 10 mM sodium fluoride, 1 mM DTT, 20% glycerol and 1× protease inhibitors cocktail (Roche)). Cell pellets were resuspended in Lysis Buffer. Extracts were cleared by centrifugation at 14,000 rpm for 20 min at 4°C. Supernatants were collected in fresh tubes and immediately frozen in liquid nitrogen. The quantification of proteins in the extracts was performed using the BCA protein assay reagent kit.

For the *in vitro* miRNA processing assay 10 µg of protein extracts of interest were incubated for 90 min at 37°C with 20,000 cpm pre-miRNA in 75 mM NaCl, 20 mM Tris-HCl, pH 7.5, 3 mM MgCl<sub>2</sub> and 0.1 U/µl RNase inhibitor. As a control pre-miRNA was digested with recombinant Dicer (0.1 U/reaction) with the same conditions. Reaction products were resolved by 12% denaturing gel electrophoresis. Subsequently, gels were stained with ethidium bromide to visualize size standards (100 nt RNA marker and 22 nt siRNA duplex), vacuum dried and visualized by autoradiography.

#### **2.2.11.E. *In vitro* ubiquitination assay**

Full length mLin-41 and truncation variants were generated by PCR (see section 2.1.4.). PCR fragments were engineered to contain T7 promoter and Kozak regulatory sequence. *In vitro* transcription/translation reactions were performed in reticulocyte lysate contained <sup>35</sup>S labeled Met at 30°C for 2 h (T7 TNT kit, Promega). 2 µl of the translation reaction was added to a 20µl ubiquitination mix containing:

- 0.5ug E1 enzyme (Boston Biochem)
- 0.5µg E2 enzyme (UbcH2, UbcH5a, Ubc5Hb, UbcH5c, UbcH6, UbcH7, or UbcH10)
- 50mM Tris pH 7.5,
- 5mM MgCl<sub>2</sub>,
- 1mM DTT,
- 10mM ATP
- 2µM MG 132 (Boston Biochem)
- 1µM ubiquitin aldehyde (Calbiochem),
- 2µg ubiquitin (Boston Biochem)

The reaction was incubated for 2h at 37°C and stopped by the addition of SDS sample buffer and heating at 90°C for 10 min. Reaction products were separated by SDS-PAGE gel electrophoresis. The gels were then fixed in fixation solution followed by 15 min incubation in enhancing solution (Ambion). Dried gels were exposed to X-ray film, at -80° overnight.

#### **2.2.11.F. *In vivo* ubiquitination assay**

For the *in vivo* mLin-41 ubiquitination assay, a HeLa 100-mm dish cells was transfected with Flag-tagged mLin-41 expression plasmid. Twenty four h after transfection, cells were treated with the proteasome inhibitor MG132 (20 µM) for 4 h. Cells were then collected, pelleted by centrifugation, lysed in 200 µl of preheated lysis buffer [50 mM Tris-HCl (pH 7.5), 0.5 mM EDTA, 1% SDS, and 1 mM DTT], and further boiled for an additional 5 min. Lysates were clarified by centrifugation at 14,000 rpm on a microcentrifuge for 10 min. Supernatant was diluted 10 times with 0.5% NP40 buffer and immunoprecipitated with anti-Flag antibody. Immunoprecipitates were washed 5 times and resolved by 8% SDS-PAGE, followed by immunoblotting with anti-mLin-41 or anti-ubiquitin antibodies (Assay Designs).

**2.2.11.G. *Electro Mobility Shift Assay (EMSA)***

Cells extracts and labeled precursors were prepared as described for *in vitro* miRNA processing assay. 0.5-2 µg of protein were incubated with 20,000 cpm <sup>32</sup>P-labeled precursor RNAs for 30 min at 37°C in 20mM Tris-HCl, pH 8.0, 100mM KCl, 1.5 mM MgCl<sub>2</sub> , and 1mM DTT. Ficoll was added to 2%, followed by electrophoresis on a 5% polyacrylamide gel. Gels were vacuum dried and visualized by autoradiography (Wulczyn et al., 2007).

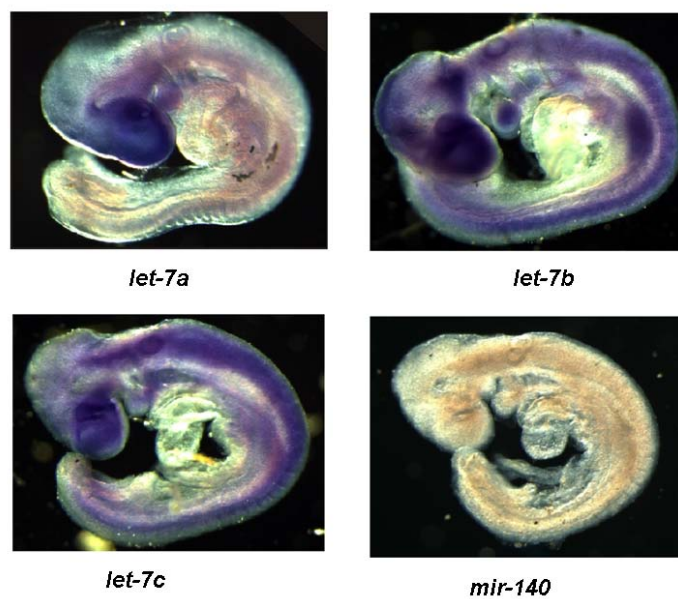
### 3. RESULTS

#### 3.1. Characterization of *let-7* miRNA expression by *in situ* hybridization

The *let-7* miRNA was originally discovered in the nematode *C. elegans* where it regulates cell proliferation and differentiation, but subsequent work has shown that both its sequence and its function are conserved in mammals. In humans and mice, the *let-7* family consists of 12 precursor genes that encode nine distinct, mature 22 nucleotide sequences. The mature forms differ at one to four positions from the canonical *let-7a* sequence. Lagos-Quintana et al. were the first to demonstrate that *let-7* family members are highly enriched in miRNA populations from mouse brain (Lagos-Quintana et al., 2002; Rauhut et al., 2002). Moreover, expression of *let-7* in the developing nervous system of the zebrafish has been characterized by *in situ* hybridization (Wienholds, Kloosterman et al., 2005) and the technique has been extended to mouse embryogenesis (Kloosterman, 2006). However, the function of *let-7* during brain development has not been specifically addressed.

As a starting point for this thesis, the regulation of several highly expressed neural miRNAs, including *let-7*, in embryonic brain development and neural differentiation of ES and EC cells had already been described (Smirnova et al., 2005). We began by employing recently developed protocols for *in situ* hybridization (ISH) of miRNAs (Wienholds, 2005) to early mouse embryos. For three *let-7* isoforms tested (*let-7a*, *let-7c*, and *let-7e*), very similar expression patterns were obtained in whole mounts of E9.5 embryos. We have not excluded the possibility of cross-hybridization between the related *let-7* probes; however, the LNA-modified probes used have been shown to be sensitive to single-nucleotide exchanges (Kloosterman, 2006). Staining was observed primarily in the neuroepithelium of the brain and spinal cord, the first and second branchial arches, and the forelimb primordia (Figure 3.1.1). In the case of *let-7a* but not *let-7c* or *let-7e*, most embryos demonstrated weaker signal in the developing heart and vasculature. The staining pattern obtained was strikingly similar to that observed with two brain-specific miRNAs, *mir-124* and *mir-128*, and the brain-enriched *mir-125* (Figure 3.1.1).

A.



B.

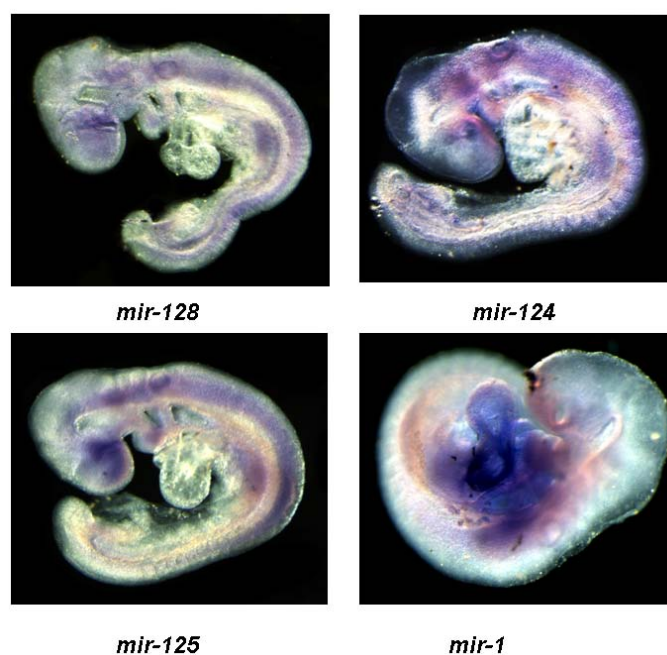


**Figure 3.1.1. Whole mount *in situ* hybridization.** E 9.5 mouse embryos were hybridized with digoxigenin-labelled LNA oligonucleotides and developed with NBT/BCIP. **Panel A:** Hybridization with probes directed against *let-7* isoforms a, c,e and control *mir-140* (cartilage specific). **Panel B:** Hybridization with probes specific for neural enriched miRNAs (*mir-124*, *mir-125* and *mir-128*), and the control miRNA *mir-1* (mesoderm-specific).

To demonstrate specificity of the hybridization conditions, *mir-1* strongly and specifically stained the heart and major vessels but not the neuroepithelium and no signal was obtained for *mir-140*, a cartilage-specific miRNA (Figure 3.1.1, Panel A). These results are consistent with an extensive *in situ* hybridization study in zebrafish and with many expression studies in the mouse using northern blotting or microarray technologies (Wienholds, 2005).

Tissue specificity was examined in sections of a representative E9.5 embryo stained for *let-7e*. In Figure 3.1.2, three different levels of coronal section are presented. At the level of the hindbrain (Figure 3.1.2, A) the neuroepithelium of the hindbrain, neural tube and DRG are stained. The sections shown in the Figure 3.1.2, B provide an overview at the level of the midbrain and the Figure 3.1.2, C at the level of heart, branchial arches and optic vesicles. The neuroepithelium of the midbrain and forebrain are uniformly stained, as are the mandibular and maxillary parts of the first branchial arch. *let-7e* expression was not detected in heart muscle or vasculature. For each of the *let-7* probes tested staining was evenly distributed throughout the hindbrain, midbrain and forebrain, as well as the otic and optic vesicles. Staining of the branchial arches is consistent with the initiation of expression in cells of the migrating neural crest. At the level of the forelimb bud (Figure 3.1.2, C), *let-7* was expressed in the limb bud mesoderm, as well as the ventral and dorsal neural tube. Within the somites, staining was most intense in the dorsal and lateral cell layers of the dermomyotome.

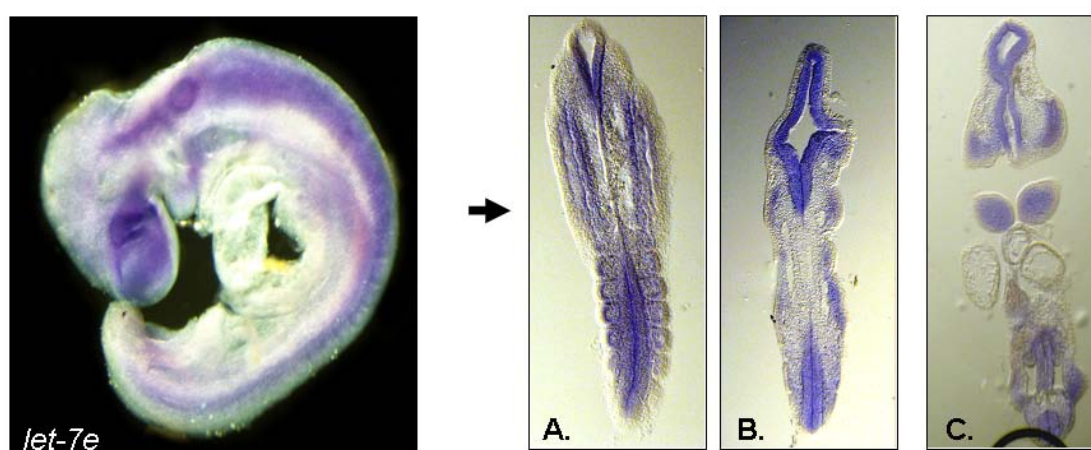


**Figure 3.1.2.** *let-7e* expression in E9.5 embryo. **Panel A** is a coronal section through neural tube, DRG. **Panel B**: section through hindbrain, neural tube. **Panel C**: present details staining of the midbrain, optic vesicles, first branchial arch, heart chambers spinal cord, somites and hindgut at the level of the forelimb bud.

To follow expression at later time points, we employed ISH with  $^{35}\text{S}$ -labelled LNA probes. Staining of a sagittal section of a whole Day 12 embryo for *let-7a* revealed widespread expression, most prominently in the neuroepithelium of the brain and spinal cord, and the cranial and dorsal root ganglia (Figure 3.1.3). Expression in the limb buds was also conspicuous, particularly in the cartilage. Organs of the gut stained less intensely, and the heart and lungs showed the lowest levels of expression. In the brain between P3 and P7, the highest level of expression was observed in the hippocampus and the cortical layers. In the adult brain overall expression was reduced in comparison to the neonate, with high levels of expression restricted to the neuron-rich layers of the hippocampus and cerebellum. Representative results for *let-7a* are shown in Figure 3.1.3. These results are consistent with a northern blot analysis of *let-7* expression during brain development (Wulczyn et al, 2007), in which 22 nt forms of *let-7* increase in parallel with the major period of neurogenesis between E13 and E18. Postnatally, expression in the cortex declined slightly while increasing in the cerebellum.

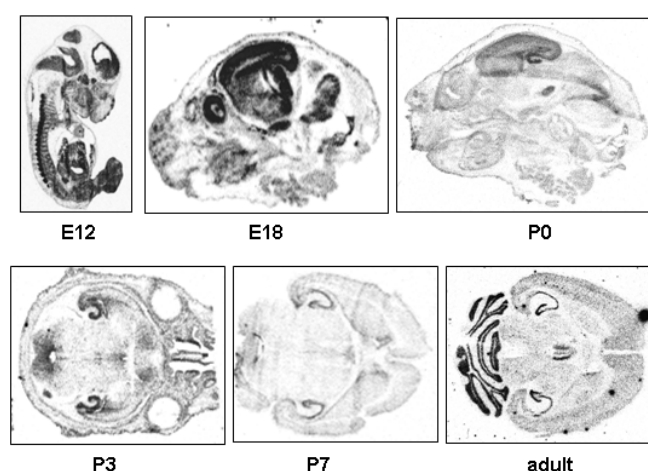
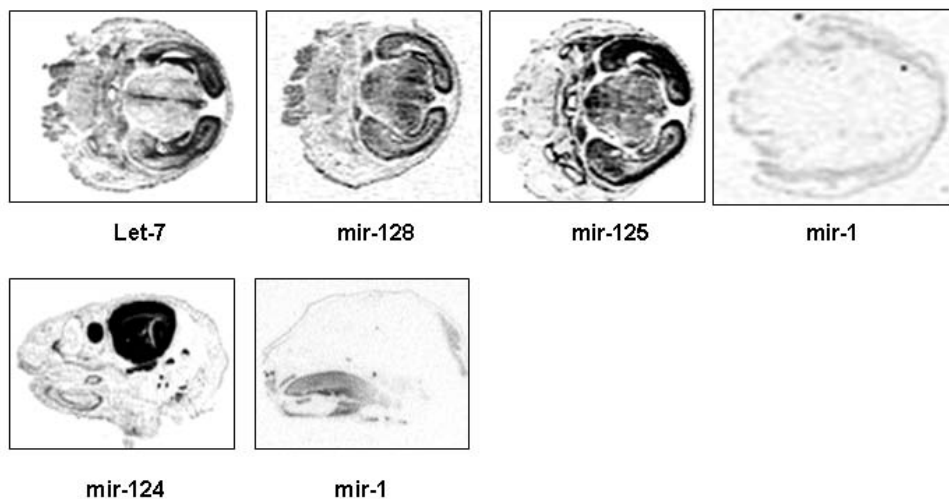


**Figure 3.1.3. *let-7* expression in embryonic and postnatal brain.** Radioactive *in situ* hybridization was performed on embryonic (E12 and E18) and postnatal mouse brain (P0, P3, P7, adult) using *let-7*  $^{35}\text{S}$ -labelled LNA probe. The hybridization pattern is described in the text.

We next compared the expression of *let-7* miRNA to brain specific miRNAs in P0 and adult mouse brain. At P0, *let-7* expression was restricted to the cortical plate, hippocampal formation and cerebellum, while *mir-125* and *mir-128* showed more widespread expression including the thalamus and striatum (Fig 3.1.4, Panel A). In the adult mouse brain *let-7* was ubiquitously expressed in the neuron rich regions of the cerebral cortex and hippocampus. In the hippocampal formation the most intense expression was observed in CA1, and in the cerebellum in Purkinje cells and the granular layer. The signal was absent from the white matter, suggesting that *let-7*

may be preferentially expressed in neurons. A similar pattern was obtained for *mir-128*, with the exception of the Purkinje cells, which did not express *mir-128*.

**A.**



**B.**

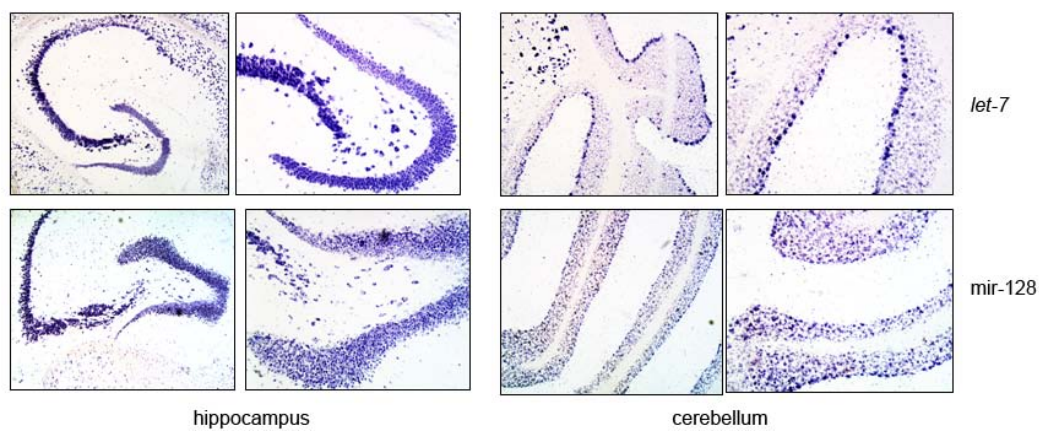


**Figure 3.1.4. Let-7 expression in P0 and adult brain in comparison to brain specific miRNA- mir-128. Panel A:** Autoradiograph of *in situ* hybridization on P0 mouse brain using probes indicated below each image. **Panel B:** *In situ* hybridization on adult mouse brain using the miRNA probes indicated on the right. High magnification of hippocampal formation and the cerebellum are shown.

### 3.2. Identification of *let-7* target genes in pluripotent cells

To elucidate *let-7* function, we focused on the identification of genes regulated by *let-7*. The finding that miRNA targeting frequently leads to mRNA destabilization (Lim et al, 2005) established microarray screening as a new strategy for the identification of miRNA targets. To identify genes regulated by *let-7* in early development, we used microarray profiling to determinate the influence of ectopic *let-7* expression on mRNA levels in EC cells (Fig 2.1). These cells are pluripotent, do not express any of the mature *let-7* miRNAs in the undifferentiated state, but efficiently induce *let-7* upon induction of neural differentiation (Wulczyn et al., 2007).

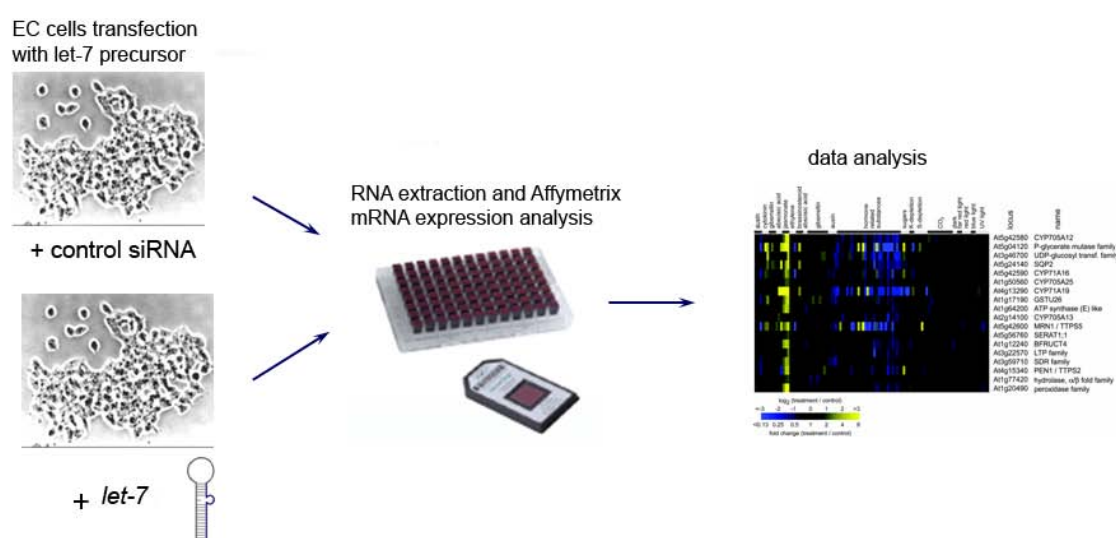


**Figure 3.2.1. Scheme of microarray analysis after ectopic *let-7* expression.** EC cells (P19) were transfected with *let-7a* precursor or control RNA, total RNA was extracted and analyzed by Affymetrix microarray.

Using two-fold changes as a threshold, we found that transfection of EC cells with a synthetic *let-7a* precursor leads to downregulation of 38 distinct mRNAs and upregulation of 128 distinct mRNAs. The Gene Ontology (GO) database was used to provide an overview of the probable functions of the downregulated genes. The major categories are transcriptional regulation (10), DNA binding (9) and growth control (9). A list of the downregulated genes is provided in Table 3.2.1.

Table 3. 2.1. The strongly downregulated genes after ectopic *let-7* expression

	Probe Set ID	Gene ID	Gene Symbol	Gene Title
1	1437571_at	<u>58180</u>	<u>Hic2</u>	hypermethylated in cancer 2
2	1423526_at	<u>56380</u>	<u>Arid3b</u>	AT rich interactive domain 3B (Bright like)
3	1460731_at	<u>228875</u>	<u>Slc35c2</u>	solute carrier family 35, member C2
4	1456572_x_at	<u>12464</u>	<u>Cet4</u>	chaperonin subunit 4 (delta)
5	1428826_at	<u>14536</u>	<u>Nr6a1</u>	nuclear receptor subfamily 6, group A, member 1
6	1456673_at	<u>102639</u>	<u>Trim71</u>	tripartite motif-containing 71
7	1455223_at	<u>140486</u>	<u>Igf2bp1</u>	insulin-like growth factor 2 mRNA binding protein 1
8	1428825_at	<u>14536</u>	<u>Nr6a1</u>	nuclear receptor subfamily 6, group A, member 1
9	1449210_at	<u>140486</u>	<u>Igf2bp1</u>	insulin-like growth factor 2 mRNA binding protein 1
10	1424457_at	<u>225372</u>	<u>Apbb3</u>	amyloid (A4) precursor protein-binding
11	1453599_at	<u>636931</u>	<u>Trim71</u>	tripartite motif-containing 71
12	1433844_a_at	<u>75590</u>	<u>Dusp9</u>	dual specificity phosphatase 9
13	1424448_at	94088	<u>Trim6</u>	tripartite motif protein 6
14	1424448_at	94088	<u>Trim6</u>	tripartite motif protein 6
15	1440185_x_at	<u>56459</u>	<u>Sae1</u>	SUMO1 activating enzyme subunit 1
16	1452208_at	<u>72843</u>	<u>Prdm4</u>	PR domain containing 4
17	1449880_s_at	<u>12095</u>	<u>Bglap2</u>	bone $\beta$ -carboxyglutamate protein, related sequence 1
18	1422851_at	<u>15364</u>	<u>Hmga2</u>	high mobility group AT-hook 2
19	1438952_x_at	<u>21357</u>	<u>Tarbp2</u>	TAR (HIV) RNA binding protein 2
20	1447933_at	<u>238403</u>	<u>Kif26a</u>	kinesin family member 26A
21	1448782_at	<u>106200</u>	<u>Txndc11</u>	thioredoxin domain containing 11
22	1429850_x_at	<u>72041</u>	<u>Alkbh4</u>	alkB, alkylation repair homolog 4 (E. coli)
23	1419140_at	<u>11481</u>	<u>Acvr2b</u>	activin receptor IIB
24	1450781_at	<u>15364</u>	<u>Hmga2</u>	high mobility group AT-hook 2
25	1439523_at	<u>399584</u>	<u>G24Rik</u>	RIKEN cDNA D330027G24 gene
26	1454944_at	<u>58180</u>	<u>Hic2</u>	hypermethylated in cancer 2
27	1453301_a_at	<u>72041</u>	<u>Alkbh4</u>	alkB, alkylation repair homolog 4 (E. coli)
28	1437994_x_at	<u>70427</u>	<u>Mier2</u>	mesoderm induction early response 1, family member 2
29	1427941_at	<u>192119</u>	<u>Dicer1</u>	Dicer1, Dcr-1 homolog (Drosophila)
30	1442768_at	<u>268739</u>	23Rik	RIKEN cDNA E130112L23 gene
31	1418585_at	<u>66671</u>	<u>Ccnh</u>	cyclin H
32	1427213_at	<u>18639</u>	<u>Pfkfb1</u>	6-phosphofructo-2-kinase/fructose-2,6-biphosphatase 1
33	1417865_at	<u>21927</u>	<u>Tnfaip1</u>	tumor necrosis factor, alpha-induced protein 1
34	1456411_at	<u>269955</u>	<u>Rccd1</u>	RCC1 domain containing 1
35	1418887_a_at	<u>28081</u>	<u>Wsu99e</u>	DNA segment, Chr 11,
36	1433899_x_at	<u>21807</u>	<u>Tsc22d1</u>	TSC22 domain family, member 1
37	1429388_at	<u>71950</u>	<u>Nanog</u>	Nanog homeobox
38	1439856_at	<u>11481</u>	<u>Acvr2b</u>	activin receptor IIB
39	1454737_at	<u>75590</u>	<u>Dusp9</u>	dual specificity phosphatase 9
40	1420984_at	<u>18559</u>	<u>Pctp</u>	phosphatidylcholine transfer protein
41	1434204_x_at	<u>108037</u>	<u>Shmt2</u>	Serine hydroxymethyl transferase 2 (mitochondrial)
42	1456614_at	<u>71238</u>	<u>Acn9</u>	ACN9 homolog (S. cerevisiae)
43	1423616_at	<u>21357</u>	<u>Tarbp2</u>	TAR (HIV) RNA binding protein 2
44	1453324_at	<u>76155</u>	<u>Nip7</u>	nuclear import 7 homolog
45	1457078_at	<u>243963</u>	<u>Zfp473</u>	zinc finger protein 473
46	1417593_at	<u>80385</u>	<u>Tusc2</u>	tumor suppressor candidate 2
47	1439764_s_at	319765	<u>Igf2bp2</u>	insulin-like growth factor 2 mRNA binding protein 2
48	1425404_a_at	<u>69179</u>	<u>Tmem110</u>	transmembrane protein 110
49	1419168_at	<u>50772</u>	<u>Mapk6</u>	mitogen-activated protein kinase 6

Analysis of the downregulated genes using three published miRNA target gene prediction databases PicTar (P) (Krek et al., 2005), TargetScan (T) (Lewis et al., 2005), and RNA22 (Miranda et al., 2006) revealed that twenty-two of the thirty-eight genes have been identified as putative *let-7* targets by at least one algorithm. In particular, *Hic-2*, *Arid3b*, *Nr6a1*, and *Hmga2* are the four highest ranking *let-7* target predictions according to the PicTar program, and regulation of *Hmga2* by *let-7* has recently been experimentally confirmed (Young and Narita, 2007). Similarly, *Trim71/Lin-41* is the mammalian homolog of the original *C. elegans* target gene *lin-41*, and its regulation by *let-7* has also been demonstrated (Kanamoto et al., 2006). Also of note are the presence of *Dicer1* and *Tarbp2*, which act together in the miRNA pathway at the pre-miRNA cleavage step. According to PicTar, the *Tarbp2* mRNA has two *let-7* binding sites and *Dicer* has one. Two of the ten most strongly regulated genes lack predicted binding sites: *Slc35c2*, and *Cct4*. However, using RNA22 at relaxed stringency two potential binding sites can be found in the 3'UTR of *Slc35c2*, and 5 sites within the coding region of *Cct4*.

Analysis of the upregulated genes using the prediction databases suggest that these mRNAs are not directly influenced by *let-7*-mRNA interactions, as few contain potential *let-7* binding sites in their 3'UTRs. There was also no recognizable bias in the number or identity of potential binding sites for other miRNAs. Ninety-four of the upregulated genes have GO annotations, the most frequent included development, cell differentiation or morphogenesis (27), regulation of transcription (23), cell signaling (19) and nervous system development (13). The 25 most strongly upregulated genes are listed in Table 3.2.2.

**Table 3.2.2. The strongest upregulated genes after ectopic *let-7* expression**

	Probe Set ID	Gene Symbol	Gene Title	Gene ID
1	1443836_x_a	Wdr48	WD repeat domain 48	67561
2	1460465_at	A930038C0	RIKEN cDNA A930038C07 gene	68169
3	1455907_x_at	Phox2b	Phox2b paired-like homeobox 2b	18935
4	1448293_at	Ebf1	early B-cell factor 1, Olfactory Neuronal Transcription Factor	13591
5	1416211_a_at	Ptn	Pleiotrophin, Neurite Outgrowth-Promoting Factor	19242
6	1436791_at	Wnt5a	wingless-related MMTV integration site 5A	22418
7	1423436_at	Gsta3	glutathione S-transferase, alpha 3	14859
8	1421399_at	Insm1	insulinoma-associated 1	53626
9	1427256_at	Vcan/Cspg	chondroitin sulfate proteoglycan 2, versican	13003
10	1458370_at	Bmp2k	BMP2 inducible kinase	140780
11	1455865_at	Insm1	insulinoma-associated 1	53626
12	1455512_at	Gm879	gene model 879, (NCBI)	380702
13	1422530_at	Prph1	peripherin 1	19132
14	1435683_a_at	Abcc5	ATP-binding cassette, sub-family C (CFTR/MRP)	27416
15	1436876_at	Rgs7bp	regulator of G-protein signalling 7 binding protein	52882
16	1450806_at	Tlx3	T-cell leukemia, homeobox 3; respiratory neuron homeobox	27140

17	1448254_at	Ptn	pleiotrophin; heparin-binding neurite promoting factor	19242
18	1429896_at	5830408B19	Mus musculus adult male thymus cDNA,	74756
19	1450625_at	Col5a2	procollagen, type V, alpha 2	12832
20	1456783_at	Zdbf2	Zdbf2 zinc finger, DBF-type containing 2	73884
21	1455739_at	6430704N06	EG245190 predicted gene	245190
22	1456725_x_at	Vil2	villin 2	22350
23	1422659_at	Camk2d	calcium/calmodulin-dependent protein kinase II, delta	108058
24	1416688_at	Snap91	synaptosomal-associated protein 91	20616
25	1420719_at	Tex15	testis expressed gene 15	104271

We next sought to verify the results of the screen by RT-PCR using cells transfected with precursor RNAs for *let-7a*, *let-7e*, *mir-125* or *mir-128*. Representative results from three independent experiments are presented in Figure 3.2.2.

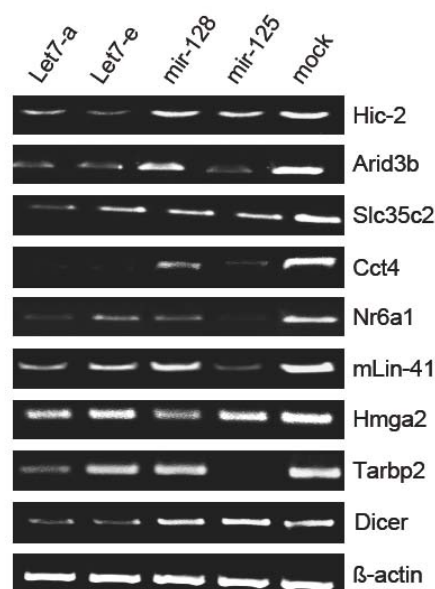


**Figure 3.2.2. Semi-quantitative RT-PCR analysis of genes downregulated by *let-7a* miRNA.** cDNA samples were prepared from EC cells transfected with RNA precursors for *let7a* (Lane 1), *let-7e* (Lane 2), *mir-128* (Lane 3) or *mir-125* (Lane 4). Mock transfection is shown in Lane 5. cDNA integrity was monitored using primers specific for  $\beta$ -actin. Gene names are given on the right. All amplifications were performed in triplicate, representative results are presented.

In all experiments, transcripts for each of the downregulated genes tested were reduced by *let-7a*. A similar result was obtained with *let-7e*, with the exception of *Hmga2* and *Tarbp2*, which were not significantly reduced. *mir-125* was also tested, as *mir-125* is known to participate in the regulation of *lin-41* in *C. elegans*. In addition to *mLin-41*, the *Arid3b*, *Nr6a1* and *Tarbp2* mRNAs were downregulated in response to *mir-125*. Predicted binding sites are present for *mir-125* in the 3'UTRs of *mLin-41*, *Arid3b* and *Nr6a1*. Together with the mock transfection, *mir-128* serves as a negative control for these experiments, as none of the genes tested are predicted targets for this miRNA. As an additional control, we chose *mLin-41* as the best understood *let-7* target gene for

confirmation using Real-Time PCR. Levels of *mLin-41* RNA were reduced approximately three-fold by *let-7a* and *let-7e*, as well as *mir-125*. Transfection with *mir-128* had no effect compared to a mock transfection (Figure 3.2.3)

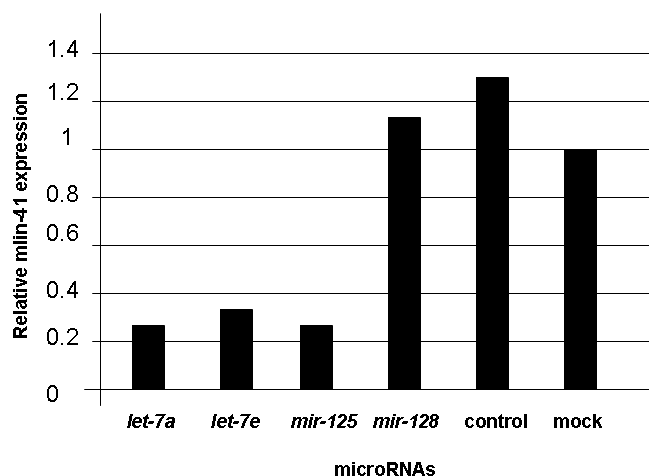


**Figure 3.2.3. Real-Time quantitative RT-PCR analysis of *mlin-41* expression.** All amplifications were performed in duplicate and normalized using  $\beta$ -actin as a standard, expression relative to the mock transfection is shown. The level of *mlin-41* RNA was reduced three-fold by *let-7a* and *let-7e*, as well as *mir-125*. No effect was observed with the *mir-128a* control miRNA compared to mock transfection.

Using RT-PCR, we also confirmed the microarray results for 7 upregulated genes of particular developmental interest (Figure 3.2.4). In each case, ectopic *let-7* expression led to a clear increase in message levels. These genes were not subjected to further analysis, but may provide clues to downstream effects of *let-7* on gene expression during stem cell differentiation.

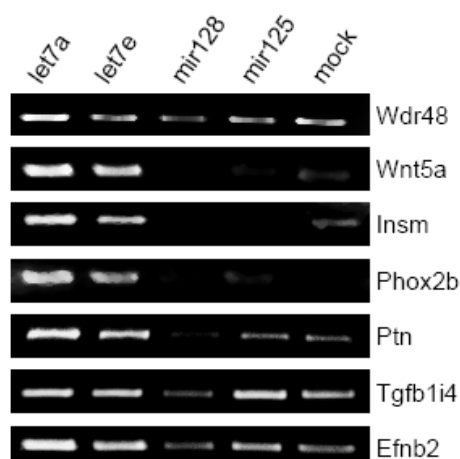


**Figure 3.2.4. Representative results from RT-PCR of genes upregulated by *let7a* in EC cells.** RT-PCR analysis was performed A for a selection of genes listed in Table 3.2.2.

Taken together, the results of the RT-PCR assay suggest that the microarray screen successfully identified strong candidates for *let-7* target genes in stem cell differentiation. To further characterize *let-7*-target gene interactions, we choose to examine regulation and function of the *mLin-41* gene in greater detail.

### 3.3. Characterization of mouse *lin-41* expression and function

The *C. elegans* heterochronic gene *lin-41* is one known target of *let-7* miRNA (Slack et al., 2000). *Lin-41* null mutations cause precocious expression of adult fates at larval stages. Increased *Lin-41* activity causes the opposite phenotype, reiteration of larval fates. *let-7* mutations cause similar reiterated heterochronic phenotypes that are suppressed by *Lin-41* mutations, showing that *Lin-41* is negatively regulated by *let-7*. Our group and others identified and cloned the mammalian homolog of *lin-41*, which we will refer to as *mLin-41* (Entrez Gene Symbol Trim71) (Lancman et al., 2005; Schulman et al., 2005; Kanamoto et al., 2006). The mouse *Lin-41* protein contains an N-terminal RING finger domain followed by a pair of B-Box-type Zinc fingers and the B-Box coiled coil domain, a filamin-type immunoglobulin domain and a C-terminal NHL domain (Figure 3.3.1) (Kanamoto et al., 2006). This combination of RING finger and B-Box domains, termed tripartite domain (Trim), is found in a large number of proteins and is thought to mediate protein-protein interactions (Reymond et al., 2001). The combination of Trim and NHL domains is found in a subset of the Trim family. The NHL domain was first recognized as a repetitive structural motif in the Ncl-1, HT2A and *Lin-41* proteins (Slack et al., 2000). The role of the *Lin-41* NHL domain is unknown, but the presence of the RING domain is associated with E3 ligase activity, implicated in ubiquitination (Meroni and Diez-Roux, 2005).

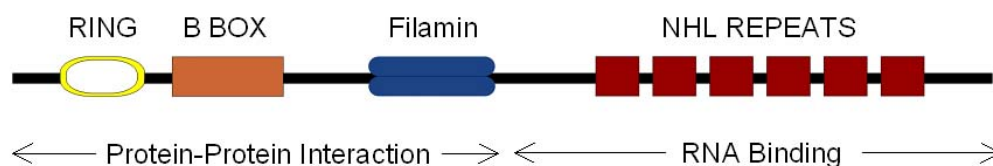


**Figure 3.3.1. *Lin-41* protein structure**

### 3.3.1. *mLin-41* is expressed in undifferentiated stem cells and in the mouse epiblast

Using RT-PCR, we found that the *mlin-41* mRNA was readily detected in undifferentiated EC cells, and strongly downregulated during the course of neural differentiation induced by RA (Wulczyn et al., 2007; Rybak et al., submitted).

We next generated affinity-purified rabbit sera against a recombinant fragment of the mLin-41 protein. Using these antibodies, we confirmed that the protein is expressed in undifferentiated EC cells as a single band at a molecular weight of approximately 95 kD (Figure 3.3.2). The protein could not be detected eight days after RA-induced neural differentiation.

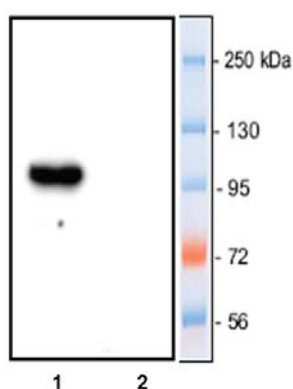


**Figure 3.3.2. Downregulation of mLin-41 protein during RA induction of EC cells.** Western blot analysis was performed using a polyclonal anti-mLin-41 antibody (described in Materials and Methods). The full blot is shown, to demonstrate the specificity of the antibody. The mLin-41 protein was expressed in undifferentiated cells (Lane 1), but not after RA-treatment (Lane 2).

Similar results were obtained for ES cells: the mLin-41 protein was also lost upon neural differentiation. In whole embryo extracts, mLin-41 was detected at E8.5 and E9.5, and significantly downregulated at E10.5 and E12.5 (Figure 3.3.3). This corresponds well to the time course of *let-7* induction (Wulczyn et al., 2007) and to downregulation of *mlin-41* mRNA during embryogenesis as determined by northern blot (Schulman et al., 2005).

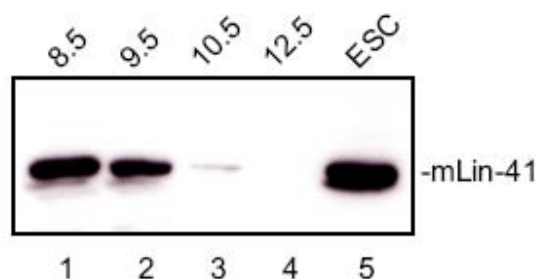
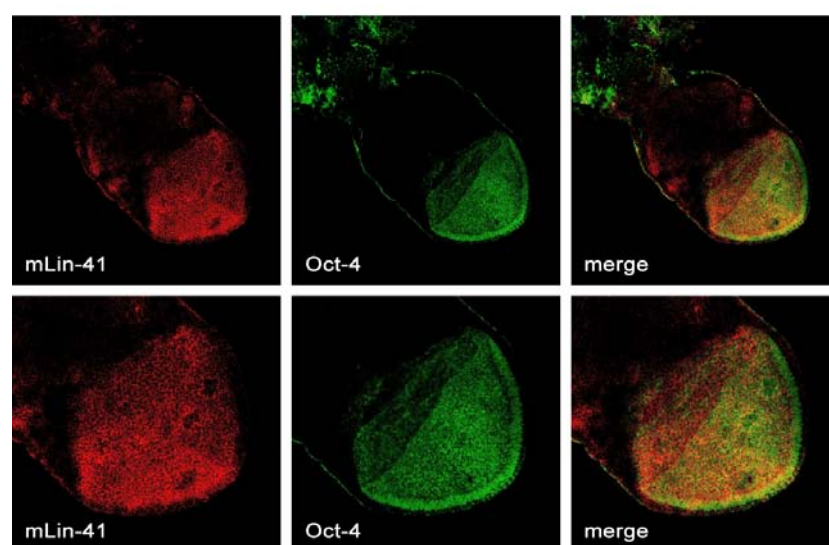


**Figure 3.3. mLin-41 expression during mouse embryonic development.** Whole embryo extracts were analyzed by Western blot. mLin-41 protein was highly expressed at E8.5 and E9.5 (Lanes 1, 2) and largely extinguished at E10.5 and E12.5 (Lane 3, 4). ES cell extract was used as a positive control (Lane 5).

A full description of *let-7* expression in early mouse embryogenesis is not yet available. PCR profiling suggests that *let-7* is supplied as a maternal miRNA in the mouse but is rapidly lost between the one and eight cell stage (Tang et al., 2007). We therefore examined mLin-41 protein expression in the early mouse embryo. Using whole mounts of E7 embryos, strong mLin-41 staining was obtained in the embryonic ectoderm and in the ectoplacental cone, with little to no staining in the extraembryonic tissues (Figure 3.3.4, Panel A, red). The expression pattern closely resembles that of the central regulator of pluripotency, Oct-4 (Figure 3.3.4, Panel A, green). In the merged view, mLin-41 staining is seen to be granular and perinuclear. Staining of the tall columnar cells of the embryonic ectoderm was verified in sections of E7 embryos prepared *in situ* (Figure 3.3.4, Panel B).

A.



B.

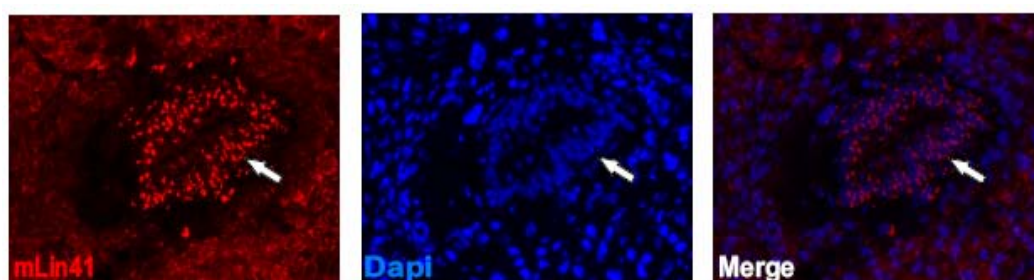


**Figure 3.3.4. mLin-41 expression in the postimplantation embryo.** Panel A. mLin-41 expression in early post-implantation embryos. Whole mount immunohistochemistry of E7 mouse embryos was performed with anti-mLin-41 (red) and Oct-4 (green) antibodies. mLin-41 protein showed high expression in embryonic ectoderm and in the ectoplacental cone (indicated with arrows). Overview and detailed view of embryonic ectoderm are provided. Panel B. mLin-41 expression in embryonic ectoderm. mLin-41 immunofluorescence analysis on cryostat sections of E7 mouse embryos (red). An arrow indicates staining of the tall columnar cells of the embryonic ectoderm. Cell nuclei were counterstained with DAPI (blue).

Similar results were obtained for the mLin-41 mRNA using a DIG-labeled LNA probe (Figure 3.3.5).

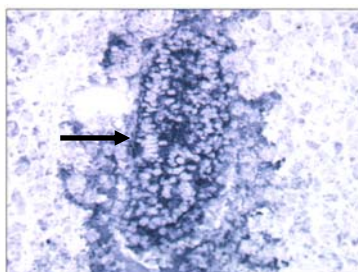


**Figure 3.3.5. mLin-41 mRNA expression in postimplantation embryos.** mLin-41 *in situ* hybridization on the cryostat sections of E7 mouse embryo using LNA probe directed against mLin-41 mRNA. Arrow indicates signal in embryonic ectoderm.

### **3.3.2. mLin-41 expression during embryonic and postnatal developmental stages**

Using antibodies raised against recombinant mLin-41 for immunohistochemistry and LNA probes for *in situ* hybridization, we have extensively characterized mLin-41 expression during embryonic mouse development and in adult mouse.

#### **3.3.2.A. mLin-41 expression during embryonic development**

mLin-41 protein and mRNA are ubiquitously expressed in the neuroepithelia through E10. At E12 expression is apparent in the neural tube, DRGs and in the embryonic brain (Figure 3.3.6). Expression of mlin-41 mRNA and *let-7* in the ventricular and mantle zones of the spinal cord was also compared at E12 (Figure 3.3.7). The staining pattern was found to be roughly reciprocal, mLin-41 high in the ventricular progenitor zone and *let-7* more prominent in the differentiating cells of the mantle zone.

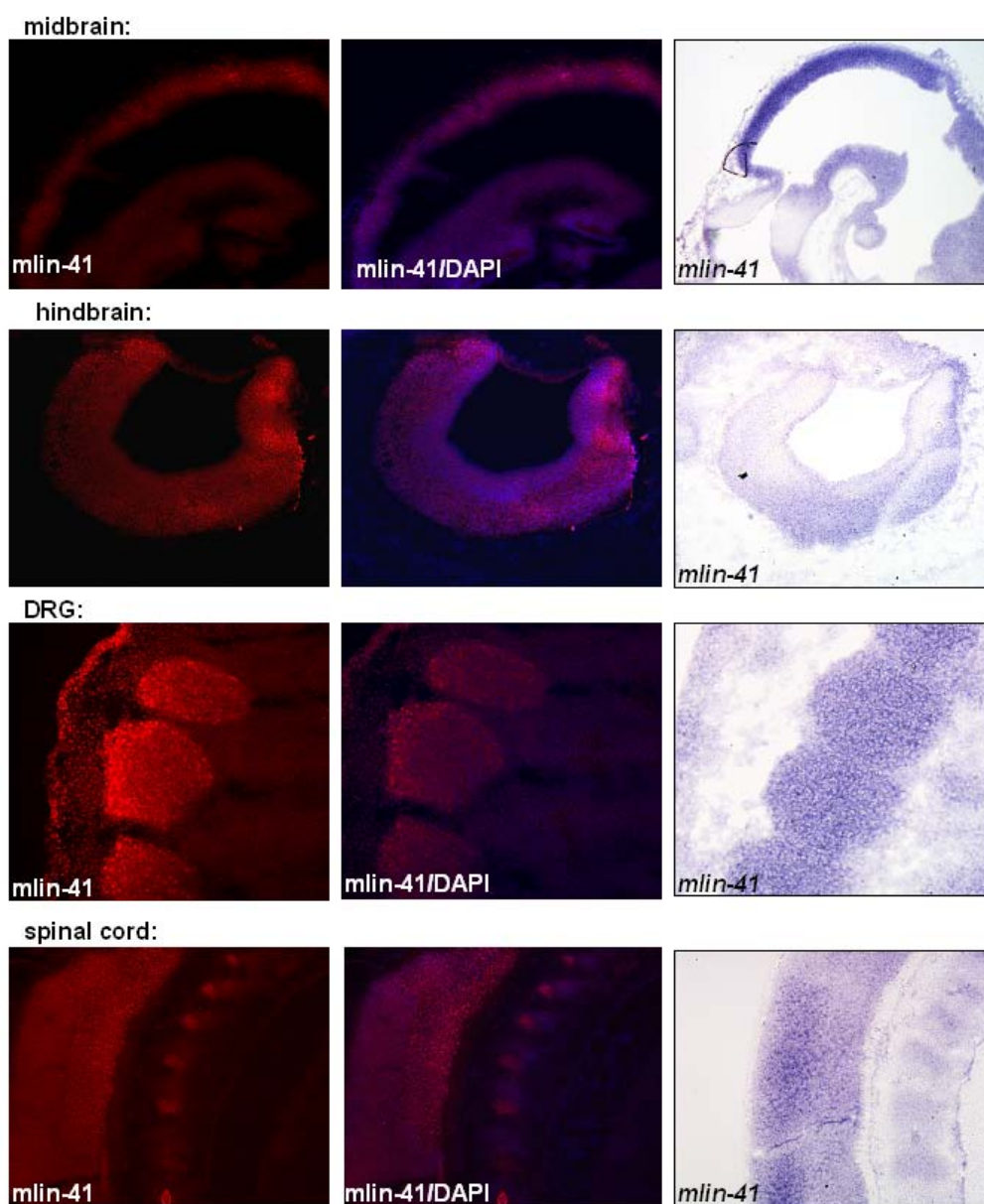


**Figure 3.3.6. mLin-41 expression in developing nervous system.** Immunostaining (left side) and in situ hybridization (right side) were performed on sagittal sections from E12 mouse embryo. Each row represents a different region; midbrain, hindbrain, DRG, spinal cord

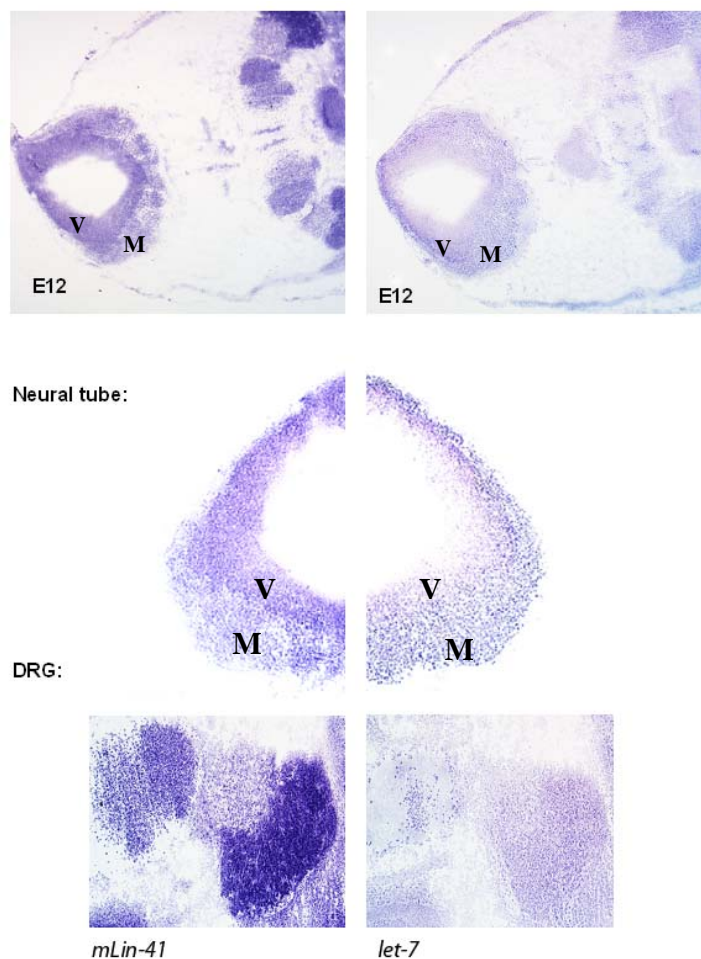


**Figure 3.3.7. Reciprocal expression of *mlin-41* and *let-7* in developing nervous system.** *In situ* hybridization was performed with LNA probes directed against *mLin-41* (right side) and *let-7* (left side) on transversal sections from E12 mouse embryo. High magnification of neural tube and DRG is provided. V- ventricular zone, M-mantle zone.

In later stages *mLin-41* is strongly downregulated in developing mouse brain. mRNA levels are close to undetectable in whole brain between E16 and P0, but begin to rise again beginning at P5 (Figure 3.3.8).

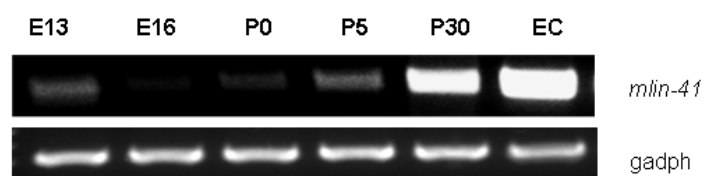


**Figure 3.3.8. *mlin-41* expression in mouse brain.** Total RNA was isolated from whole mouse brains representing embryonic days (E13, E16), postnatal days (P0, P5,P30) or embryonic carcinoma cells (EC) and RT PCR was performed with primers specific for *mlin-41* gene or *gapdh* as a control.

Overall, mLin-41 was strongly downregulated in E16 brain, however, expression was evident in extraocular muscle (Figure 3.3.9), nasal olfactory epithelium (Figure 3.3.10), and the basal layer of embryonic skin and hair and whisker follicles (Figure 3.3.11). All of these regions are potential stem cell niches in postnatal mice. Extraocular muscle represents a rare anatomical niche that contains a high proportion of stem cells in adult tissue, with more myogenic and proliferative potential than skeletal muscle. An interesting aspect of extraocular muscle cell biology is that it is spared from various skeletal muscle disorders compared with limb skeletal muscle (Budak et al, 2005). The olfactory epithelium (OE) is also one of sites of adult neurogenesis. The multipotent stem cells of OE possess the ability to differentiate into either mature olfactory receptor neurons or non-neuronal support cells; however the identity of its stem cell is still debated (Schwob and Jang, 2007). The basal layer of skin harbors stem cells, which can divide to produce daughter stem cells and transit amplifying (TA) cells that go on to differentiate and cornify (Fuchs and Raghavan, 2002). The control of the cell cycle and asymmetric cell division by the interfollicular stem cell is not yet understood.

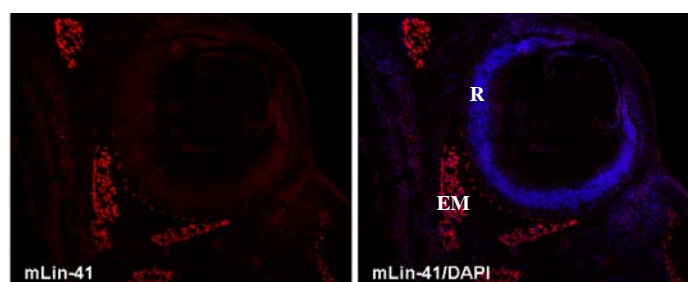


**Figure 3.3.9. mLin-41 expression in extraocular muscle.** Immunostaining on horizontal sections from E16 mouse head was performed with anti-mLin-41 antibody and costained with DAPI. R- retina, E- extraocular muscle.

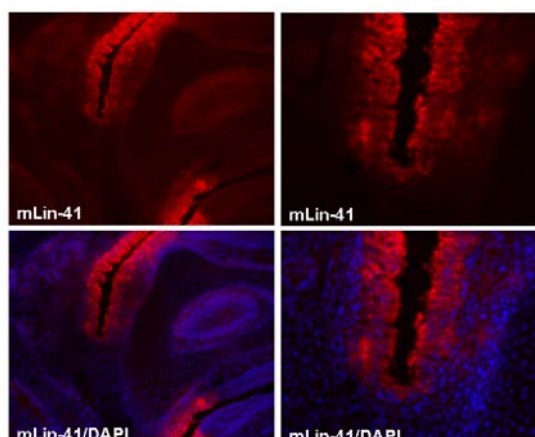
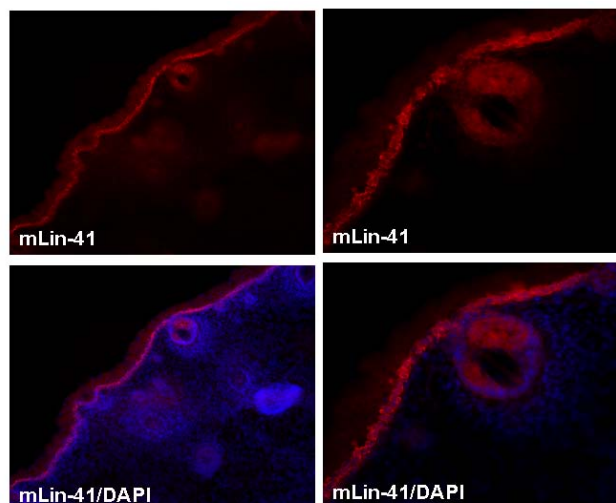


**Figure 3.3.10. mLin-41 expression in nasal olfactory epithelium.** mLin-41 staining was performed on sagittal section from E16 mouse embryo and costained with DAPI. An overview and higher magnification view are provided.

A)



B)

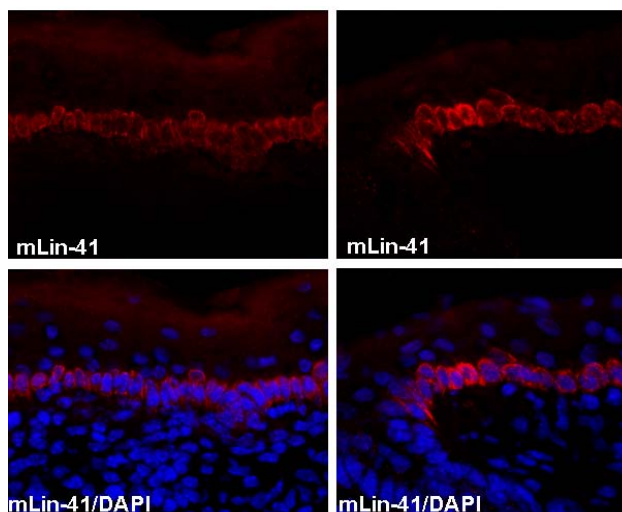


**Figure 3.3.11. mLin-41 expression in embryonic epidermis .** Immunostaining on E16 mouse skin sections was performed with anti-mLin-41 antibody and costained with DAPI to visualize nuclei. Panel A presents a staining of facial epidermis and during whisker follicle development; Panel B presents high expression of mLin-41 in the basal layer of embryonic epidermis.

### 3.3.2.B. *mLin-41* expression in the postnatal mouse brain

mLin-41 expression was then studied in the postnatal mouse brain, which revealed that the staining was restricted to the walls of the lateral and third ventricles. Prominent staining was also seen in the subcallosal zone, an embryological remnant of the lateral ventricle pressed between the hippocampal formation and the corpus callosum (Figure 3.3.12).

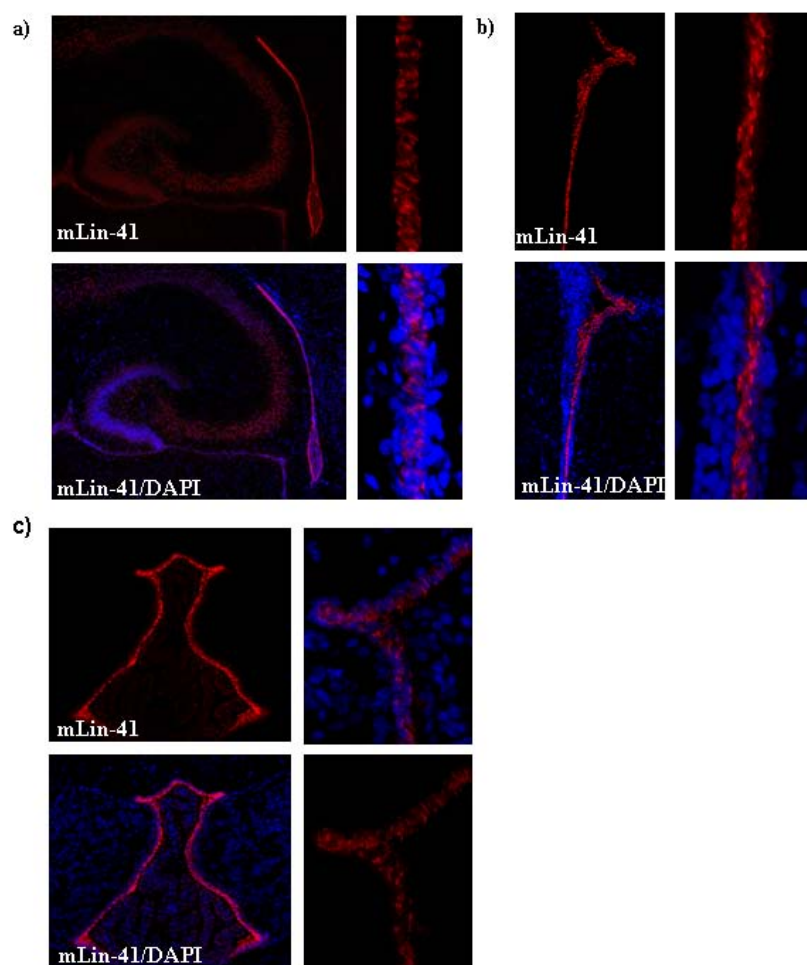


**Figure 3.3.12. mLin-41 expression in postnatal brain.** Immunostaining was performed on coronal sections from P7 mouse brain. Panel: a) represent the subcallosal zone, b) lateral ventricle region, c) 3th ventricle. An overview and detail view is provided.

In an attempt to determine the cell type expressing mLin-41 protein, we performed colocalization studies with several well characterized markers for the different cell types potentially present in these regions: GFAP (Astrocytes), Prominin (Ependymal subsets), and Nestin (Neuronal Progenitors). However the results were not conclusive (data not shown). Since mLin-41 positive cells appear to line the ventricle wall with morphology most consistent with ependymal cells; we performed electron microscopy as a definitive test. Figure 3.3.13 demonstrates the region subject to study, taken from P28 brain and including a part of the subcallosal zone. Based on higher magnification pictures, mLin-41 positive cells were found to represent a simple, cuboidal, ciliated epithelium typical for ependymal cells.

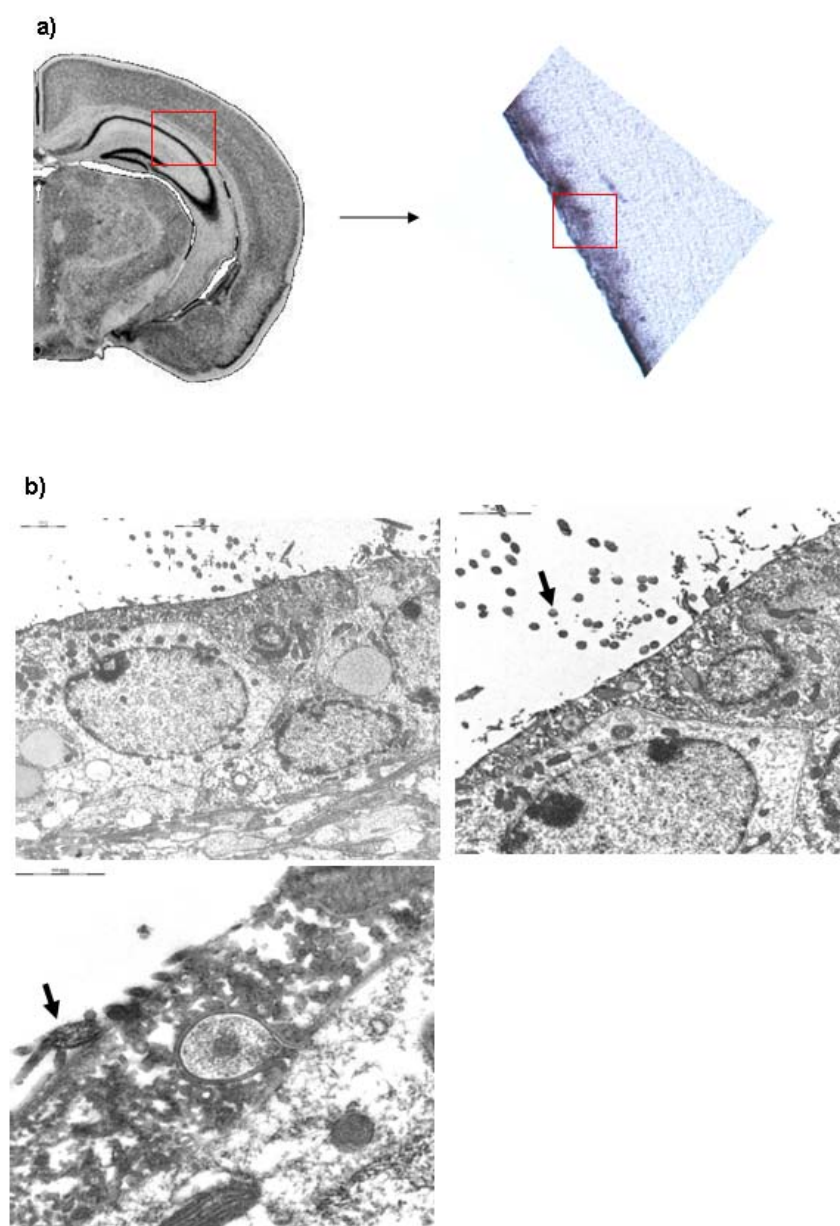


**Figure 3.3.13. Electron microscopy study revealed that mLin-41 positive cells are the ependymal cells.** Electron microscopy was performed on subcallosal region of the postnatal mouse brain as indicated in panel a). Panel b) represent electron microscopy pictures of mLin-41 positive cells lining the ventricular wall. Arrows indicate cilia.

Ependymal cells (also called ependymocytes) are a specialized neuroglia cell, thought to be a terminal differentiation product of radial progenitors. These cells arise primarily at E14-16 with functional maturation in the early post-natal period (Spassky et al., 2005). Fetal ependymal cells participate in developmental processes such as neurogenesis, neuronal differentiation/axonal guidance, metabolite transport and trophic support. Maturation of the ependyma is not complete until the postnatal period (Sarnat, 1992; Bruni et al, 1998). Johansson et al (1999) have presented

evidence that ependymal cells are neural stem cells. They have reported that ependymal cells proliferate dramatically in response to spinal cord injury and generate migratory cells that differentiate into astrocytes (Gleason et al., 2008). Cancer cells arising from ependymal cells are called ependymomas, a rare neoplasm that occurs predominantly in children. Using material kindly provided by Dr F. Heppner (Institute for Neuropathology, Charité) we tested if mLin-41 is also expressed in tumor cells originating from ependyma. Figure 3.3.14 presents an example of mLin-41 staining obtained on human ependymoma with two different anti-mLin-41 antibodies. mLin-41 was strongly and specifically expressed in the solid tumor tissue, characterized by cells with large rounded nuclei in compact, cell-rich areas clearly demarcated from normal tissue, with the presence of pseudorosettes (arrows). However, additional experiments have to be performed in order to verify mLin-41 expression, accompanying development of ependymoma. This would be particularly interesting in regard to recent data showing that *let-7* and *mir-125* expression correlate with many different types of cancer (Table 3.3.1). Moreover, in many cases it was demonstrated that reduction in *let-7* maintains the stem cell character of tumor initiating cells (Yu et al., 2007).

**Table 3.3.1. *let-7* and *mir-125* expression in different types of cancer**

Cancer type	Potential target	reference
<i>let-7</i>		
Lymphoma (Burkitt Lymphoma)	myc	Sampson et al., 2007
Breast cancer	RAS, HMGA2	Lee et al., 2007
Lung cancer	RAS	Esquela-Kerscher A., 2008
Esophageal cancer	???	Zhang et al., 2007
germ cell tumor	cyclin, CDK4	Schultz et al., 2008
<i>mir-125</i>		
Neuroblastoma (mir125a,b)	??	Reneve et al., 2007
Thyroid cancer (mir125a)	ERBB2, ERBB3	Scott et al., 2007
Prostatic cancer	Bak1, eIF4EBP1	Ozen et al., 2007
cervical cancer	??	Lorio et al., 2007

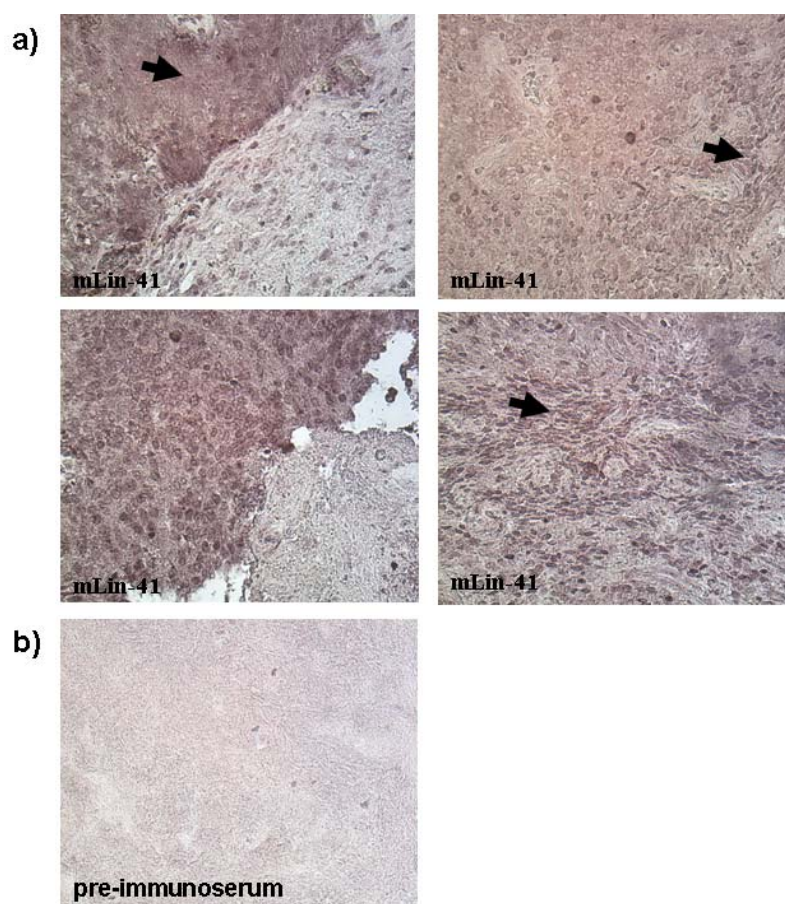


**Figure 3.14. mLin-41 expression in human ependymoma tissue.** DAB- staining was performed on paraffin sections from human ependymoma tissue with two different antibodies directed against mLin-41 protein. **Panel a)** represent the positive stained tissue, with morphology characteristic for ependymoma; clear cut border, presence of pseudorosettes (indicated with arrows). **Panel b)** represents control, ependymoma tissue stained with pre-immunoserum.

### 3.3.2.C. Expression of *mLin-41* in male germ cells and reproductive tract

Based on est data, we expected *mLin-41* to be primarily embryonic, although there is some evidence for expression in the germ line. This pattern was confirmed in a tissue screen for *mLin-41* mRNA by RT-PCR, with cDNAs kindly provided by Dr C. Hagemeyer, (Department of Pediatrics, Charité). The results confirmed expression in the brain, and revealed strong expression in the placenta and testis. All other tissues examined were negative, as shown in Figure 3.3.15 for liver and spleen.

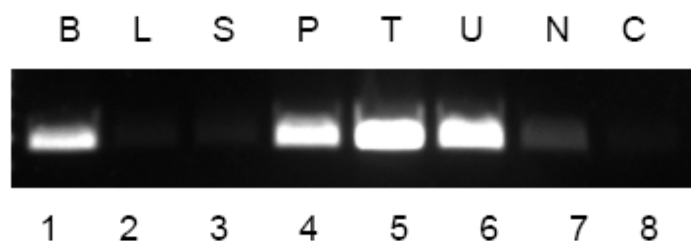


**Figure 3.3.15. *mlin-41* expression in adult tissue.** cDNAs were amplified from: brain (B, Lane 1), liver (L, Lane 2), spleen (S, Lane 3), placenta (P, Lane 4), testis (T, Lane 5), undifferentiated EC cells (U, Lane 6), and EC cells after neuronal differentiation (N, Lane 7). Control reaction with mock cDNA is shown in Lane 8 (C). Strong expression was observed in brain, testis, placenta and in undifferentiated stem cells.

We next examined mLin-41 protein expression during the period of perinatal testis development between P7 and adult. mLin-41 is expressed throughout the postnatal period of mouse testis maturation (Figure 3.3.16).



**Figure 3.3.16. Western blot analysis of mLin-41 protein expression in mouse testis at different developmental stages.** mLin-41 was observed throughout the early postnatal period (P7, P14 Lanes 1, 2) of mouse testis maturation with low, but detectable, signal at P28 and the adult (P28, Adult Lanes 3 and 4). ES cell lysate was loaded as a positive control (ESC, Lane 5)

The decline in protein levels with age could be due to downregulation of the gene, or to expression in specific cell populations that become comparatively less abundant during development. To address this question, we first compared *let-7* and *mlin-41* mRNA staining in the P14 testis, near the peak of protein expression, and found a reciprocal staining pattern (Figure 3.3.17).

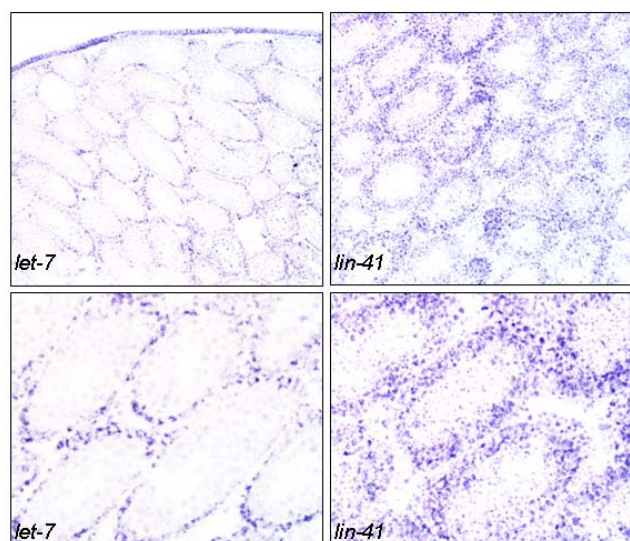


**Figure 3.3.17. Reciprocal expression of *let-7* and *mlin-41* in mouse testis.** Panel shows results from *in situ* hybridization of cryostat sections of P14 mouse testis, using DIG- labeled LNA modified probe for *mlin-41* and *let-7*. An overview and detailed view of seminiferous tubules are provided.

*let-7* stained a basal layer of cells, while *mlin-41* staining was highest in the germinal epithelium. We observed a similar correlation for three other *let-7* target genes: *Arid3b* (DNA-binding domain), *Hic-2* (hypermethylated in cancer 2), and *Nr6a1* (nuclear receptor subfamily 6, group A, member 1) (Figure 3.3.18). This observation is consistent with a contribution of *let-7* to the regulation of these genes in the testis.

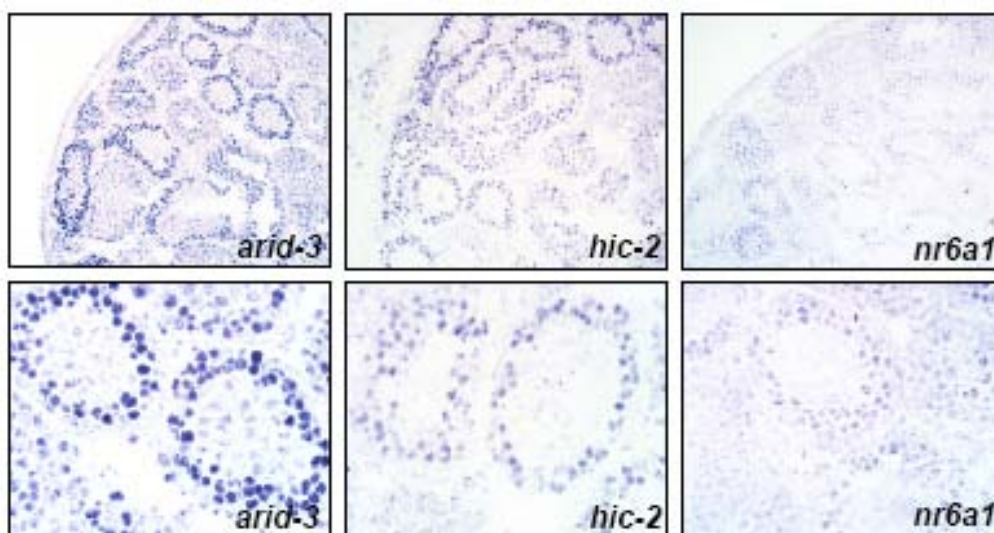


**Figure 3.3.18. Arid-3, Nr6a1, Hic-2 expression in postnatal mouse testis.** Panel shows results from *in situ* hybridization on cryostat sections of P14 mouse testis, using DIG- labeled LNA modified probes for *Arid-b3*, *NR6A1*, *Hic-2*.. An overview and detailed view of seminiferous tubules are provided.

To positively identify the cell type expressing mLin-41, testis sections from P4, P7 and P14 were co-stained with mLin-41 and c-Kit antibodies, a standard marker for germ line stem cells. At P4, c-Kit is not yet expressed by germ line cells but is restricted to the interstitial cells. mLin-41, in contrast, stained the gonocytes at this stage of seminiferous tubule formation (Figure 3.3.19).

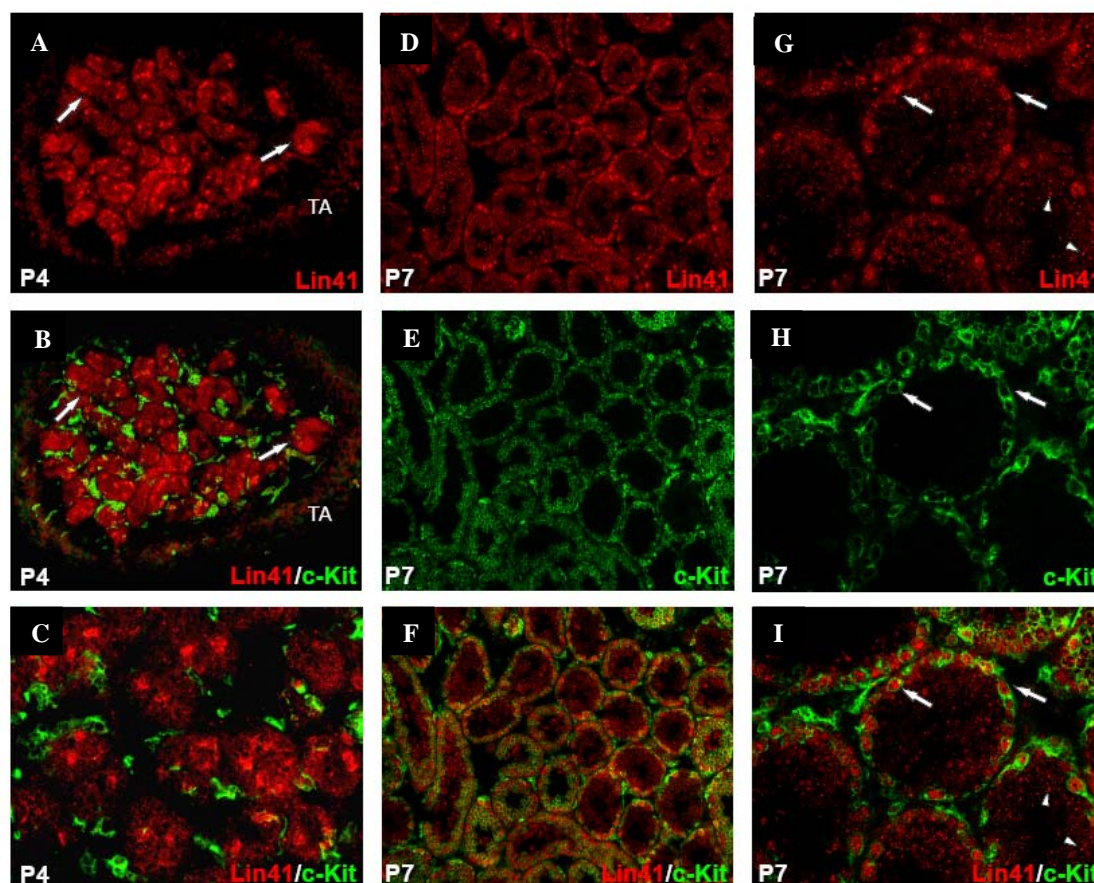
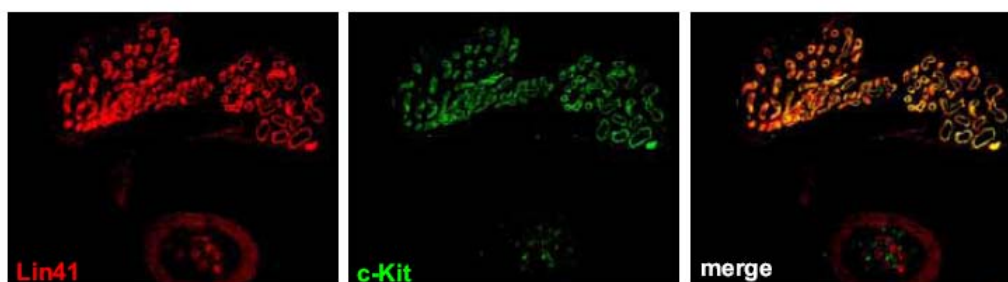


**Figure 3.3.19. mLin-41 expression in mouse testis development.** Cryosections of mouse testis at P4 (A-C) and P7 (D-F) were stained with anti-mLin-41 (red) and anti-c-Kit receptor antibodies (green). At P4, c-Kit does not overlap with mLin-41 staining of the gonocytes (indicated with arrows). Panels A and B show a cross section through a whole testis, Panel C is a higher magnification view. At P7, c-Kit and mLin-41 co-localize in spermatogonial stem cells in the basal layer of the seminiferous tubules (indicated with arrows), two magnifications are shown. Granular staining in luminal cells is indicated by arrowheads.

At the P7 stage of tubule maturation c-Kit expression is taken up by the early spermatogonia (Yoshinaga *et al.*, 1991), and these cells also express mLin-41 (Figure 3.3.19). Marked co-staining was maintained at P14, as the seminiferous tubules progress towards functional maturity. These results establish mLin-41 as a novel marker for c-Kit positive spermatogonial stem cells. Co-staining of c-Kit and mLin-41 was also observed in the epithelium of the epididymis, suggesting that the epididymis is an additional niche in which stem cell-specific messages can escape suppression by *let-7* (Figure 3.3.20).

A.



B.

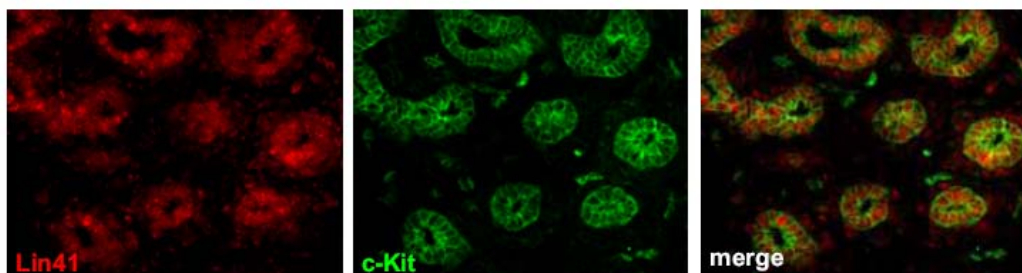


**Figure 3.3.20. mLin-41 expression, in the epithelium of the P4 epididymis.** Cryosections were stained with anti-mLin41 (red) and c-Kit (green) antibodies. mLin41 colocalizes with c-Kit expression in the epithelium (yellow). **Panel A** presents an overview of the epididymis, **Panel B** a higher magnification of epithelial staining.

### 3.3.3. *mLin-41* co-localizes to *P*-bodies.

We also compared the mLin-41 staining pattern with a second marker for male germ cells, Mili. The results suggested that the two proteins are expressed in a similar population of spermatocytes, with a strikingly similar intracellular staining pattern (data not shown). Because Mili is part of the testis-specific piRNA (Piwi interacting RNA) pathway (reviewed in Kotaja and Sassone-Corsi, 2007), this finding prompted us to examine intracellular localization of the mLin-41 protein. In EC and ES cells, immunofluorescent staining of the endogenous protein revealed a concentration of the protein in perinuclear foci that was not observed with preimmune serum (Figure 3.3.21).

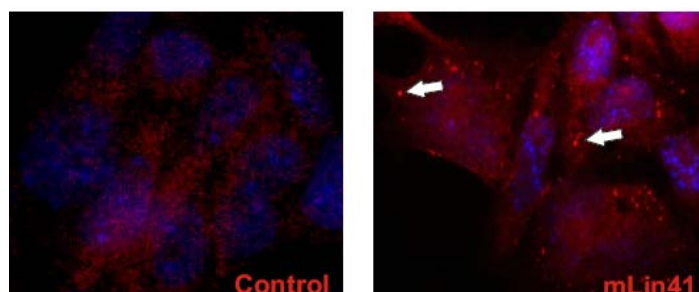


**Figure 3.3.21. Immunofluorescent staining of endogenous mLin-41 protein.** EC cells were fixed and stained with anti-mLin-41 antibody. Preimmune serum was used as a negative control. DAPI staining indicates location of nuclei.

To confirm the co-localization of mLin-41 protein to P-bodies, we performed transfection assays with proteins known to localize to P-bodies in association with the miRNA processing machinery. HeLa cells were used to transfect a full-length mLin-41 expression construct carrying an N-terminal Flag epitope tag. The resulting staining pattern of multiple, bright staining cytoplasmic foci closely resembles that obtained with P-body markers associated with the miRNA pathway, Ago-2 and MOV10 (Figure 3.3.22).

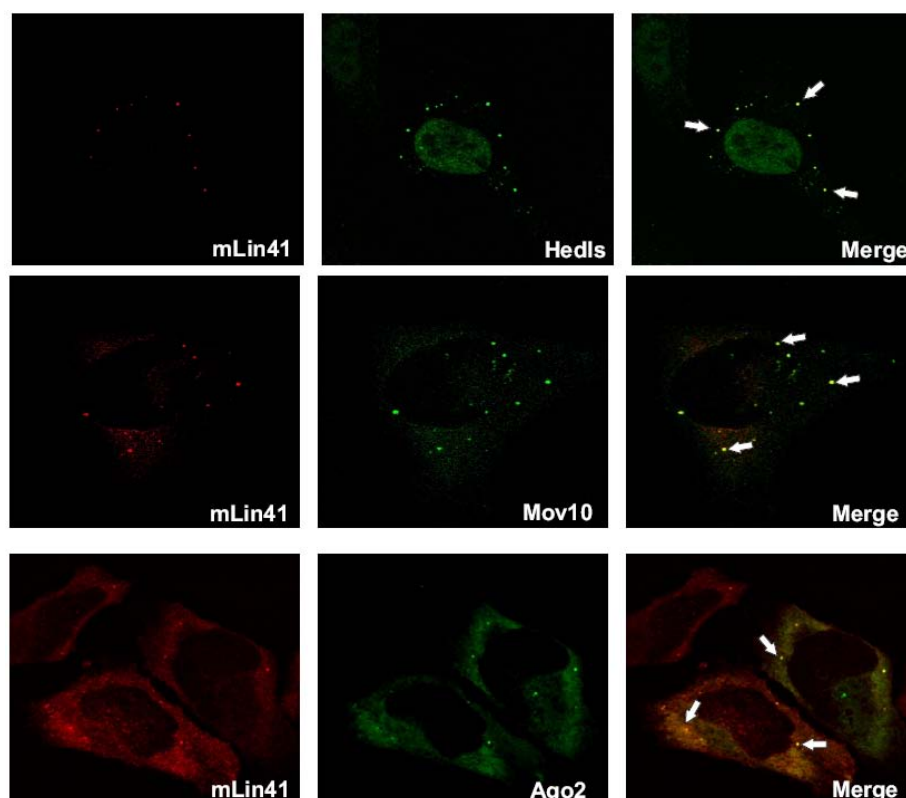


**Figure 3.3.22. Cellular localization of mLin-41 protein.** GFP- tagged Ago-2, Myc-tagged MOV10 and Flag-tagged mLin-41 (**green**) were expressed in HeLa cells and stained with rabbit anti-Myc and mouse anti-Flag antibodies, as well as with the endogenous P-bodies marker hedls. DAPI counterstaining visualized nuclei (**blue**). The mLin-41 protein localized to cytoplasmic foci and the staining closely resembled that of the P-body markers Ago-2, MOV10 and hedls. Examples are marked by arrows.

In co-transfections, substantial co-localization was observed between mLin-41 and MOV10 as well as Ago-2 (Figure 3.3.22). To confirm co-localization, we repeated the co-transfections using primary hippocampal neurons, where we have previously detected dendritic foci containing MOV10, TNRC6B, as well as Ago-2 and FMRP (Wulczyn et al., 2007). mLin-41 was found to localize to discreet, round to oblong foci in the cell bodies and dendrites of hippocampal neurons. The cellular distribution was indistinguishable from that of MOV10 and TNRC6B (Figure 3.3.23). As in HeLa cells, after co-transfection mLin-41 was found to co-localize with both of the

P-body markers, results for MOV10 are shown in Figure 3.3.23. The finding that mLin-41 traffics to P-bodies is interesting in the light of the *let-7* target gene screen in which two essential miRNA pathway genes, Dicer and Tarbp2, were also downregulated in response to *let-7*.

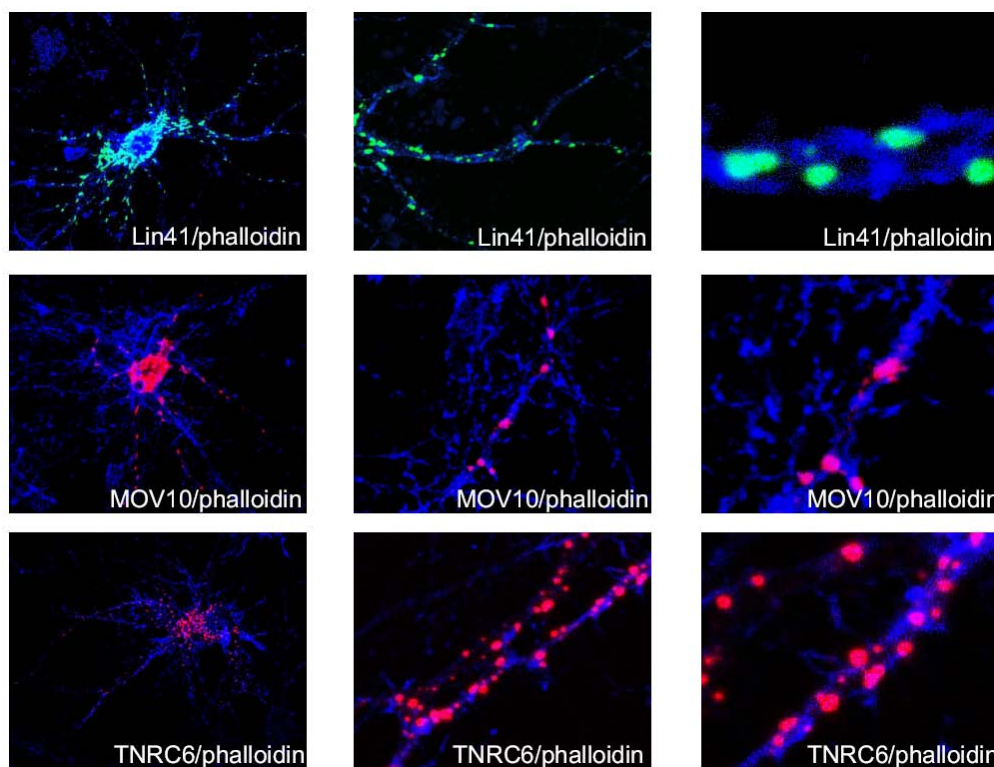


**Figure 3.3.23.A. Localization of mLin-41 protein in primary hippocampal neurons.** Neurons were transfected with expression vectors for Flag-tagged mLin-41 and c-Myc-tagged MOV10/TNRC6B. mLin-41 was visualized with mouse anti-Flag mAb (**green**), MOV10/TNRC6B with rabbit anti-Myc (**red**). To visualize dendritic morphology, cytoskeleton was stained with labelled phalloidin (**blue**). mLin-41 protein localizes to discrete foci in the cell bodies and dendrites, examples are marked with arrows.

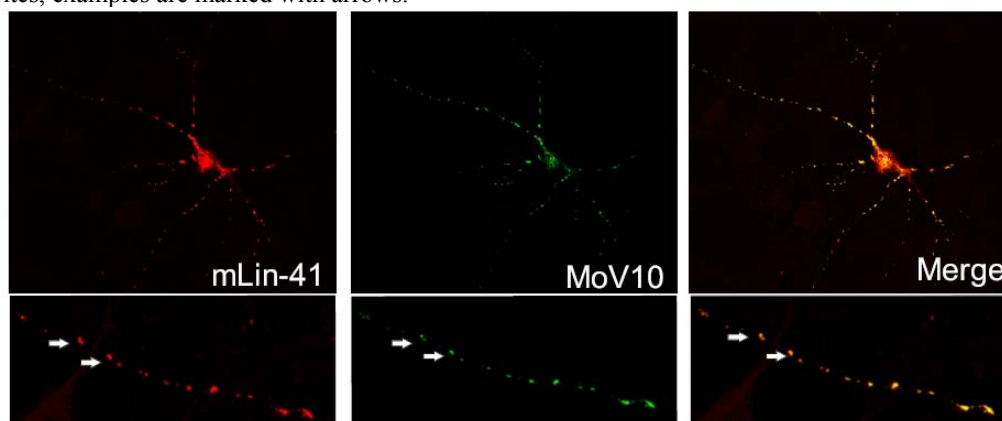


**Figure 3.3.23.B. Overlapping staining of mLin-41 and P-body markers in dendrites.** Neurons were co-transfected with expression vectors for Flag-tagged mLin-41 and c-Myc-tagged MOV10. mLin-41 was visualized with anti-Flag mAb (**red**), MOV10 with rabbit anti-Myc (**green**). An overview and detailed view of dendritic staining are provided, regions of interest are marked with arrows. For the sake of clarity, phalloidin staining is not depicted in co-transfections.

### 3.3.4. *mLin-41* function

The finding that *mLin-41* colocalizes with miRNA pathway proteins raised a question: what is the role that *mLin-41* plays in the P-bodies? Does it directly regulate protein synthesis or does it regulate the ‘regulators’- the P-body proteins? To answer these questions, first of all we performed immunoprecipitation to look for direct interactions between *mLin-41* and miRNA pathway proteins.

To identify potential interaction partners for *mLin-41* in P-bodies, we performed co-precipitation experiments in HeLa cells after transfection with epitope-tagged *mLin-41* and Ago-2, Dicer, Mov10 or TNRC6B. In the case of Ago-2-*mLin-41* and Dicer-*mLin-41* a reciprocal co-precipitation was observed (Figure 3.3.24)

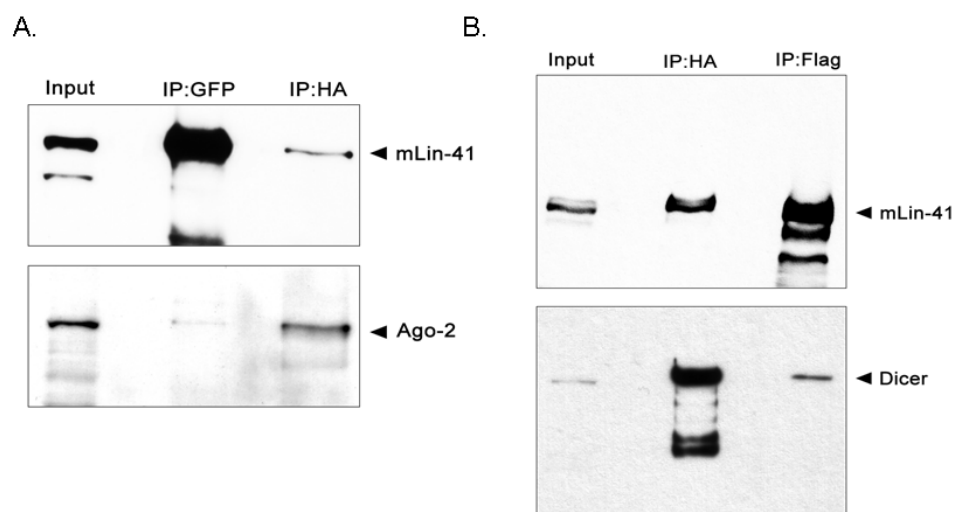


**Figure 3.3.24. Panel A. GFP-tagged *mLin-41* coimmunoprecipitates Ago-2 protein.** HA/Flag- tagged Ago-2 and GFP-tagged *mLin-41* were co-expressed in HeLa cells. *mLin-41* protein were immunoprecipitated with anti-GFP antibody and Ago-2 with anti-HA, in both cases coimmunoprecipitation was observed. **Panel B *mLin-41* coimmunoprecipitates Dicer protein.** HA- tagged Dicer and Flag-tagged *mLin-41* were coexpressed in H293 cells. *mLin-41* protein were immunoprecipitated with anti-Flag antibody and Dicer with anti-HA, in both cases coimmunoprecipitation was observed.

As a further control, Ago-2 did not co-precipitate after co-transfection with Flag-Lin-28, another *let-7* miRNA target known to be present in P-bodies (Figure 3.3.25).

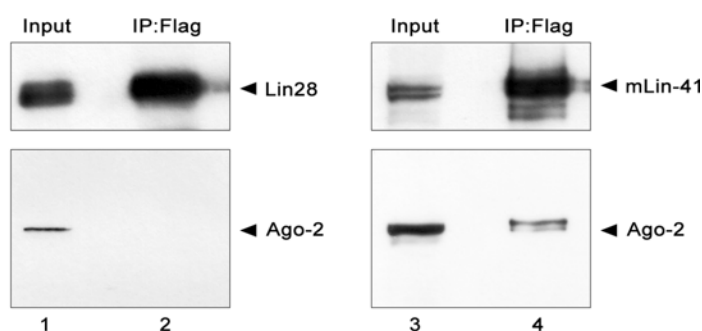


**Figure 3.3.25. Flag- tagged mLin-41 but not flag- tagged lin28 coprecipitates Ago-2.** Flag-tagged mLin-41 and flag-tagged lin-28 were expressed in P19 cells. Flag tagged proteins were purified with  $\alpha$ -Flag agarose beads. Immunoprecipitates were subjected to SDS-PAGE and analysed by Western blot for the presence of Ago-2 protein. mLin-41 (lane 4), but not Lin-28 (lane 2) coprecipitates Ago-2 protein.

Co-precipitation of the endogenous proteins could also be demonstrated in EC cells, using polyclonal anti-Ago-2 serum to precipitate mLin-41 and an anti-peptide antiserum against mLin-41 to precipitate Ago-2 (Figure 3.3.26). Neither protein was precipitated when preimmune serum was used in place of specific serum.

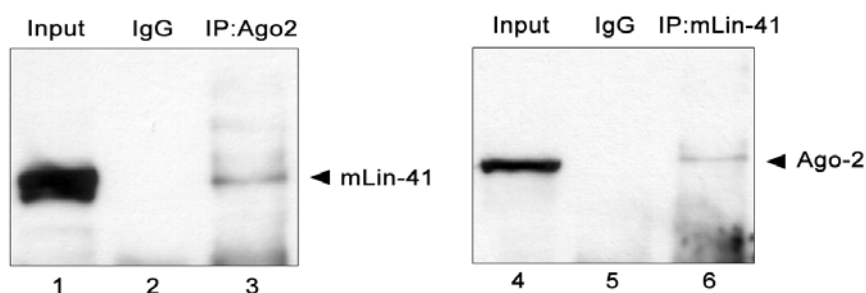


**Figure 3.3.26. Coimmunoprecipitation of endogenous mLin-41 and Ago-2 proteins.** Endogenous proteins were precipitated from P19, EC cells, using anti-Ago-2 or anti-mLin-41 antibodies. The precipitates were analysed by immunoblotting with anti-mLin-41 or anti-Ago-2 antibodies, as indicated. Input- lane 1,4, precipitation with control serum- lane 2,5, immunoprecipitation with Ago-2- lane 3 and with mLin-41 antibodies-lane 6.

Recently, E3 ligase activity has been demonstrated for many Trim proteins, including Trim2. Trim-2 deficiency results in an ataxic, neurodegenerative phenotype with axonopathy affecting several brain areas (Balastic et al., 2008).

Ubiquitination is a posttranslational modification involving at least three classes of enzymes: an E1 Ubiquitin activation enzyme (E1), an E2 Ubiquitin conjugation enzyme (E2) and an E3 Ubiquitin ligase (E3). The mammalian genome encodes only one E1 enzyme, 20-30 E2 enzymes and hundreds of E3 Ubiquitin ligases, which function alone or in multidomain complexes as

substrate recognition modules. There are two main types of E3 Ubiquitin ligases, the RING (Really Important New Gene) class and the HECT (Homologous to the E6-AP Carboxyl Terminus) class. The attachment of Ubiquitin to a target protein comes in different flavors; the linkage of one molecule, i.e. monoubiquitination, or attachment of polymers of different topology. These different modes of Ubiquitin attachment result in different readouts and are responsible for the great functional diversity of the Ubiquitin system. Monoubiquitination has been functionally implicated in endocytosis, transcriptional regulation and nuclear-cytoplasmic transport (Haglund et al., 2003). Polyubiquitination represents an assembly of multiple ubiquitin chains, wherein one Ubiquitin moiety is linked to the target protein and further Ubiquitins are linked to one of the seven lysine (K) residues within Ubiquitin itself. These Ubiquitin chain formations are named by indicating the branching lysine within Ubiquitin. K48 branching is the best-characterized form of polyubiquitination, and is recognized by the proteasome, a multiprotein complex that catalyzes degradation of K48 Ubiquitin-tagged proteins (Ciechanover, 1998; Ciechanover and Schwartz, 1998; Hershko and Ciechanover, 1998). K63 linked Ubiquitin chains are involved in cellular processes such as DNA repair, endocytosis and signal transduction (Chan and Hill, 2001). Ubiquitin chains branching at other residues as well as mixed chains have been observed *in vivo* and *in vitro* but little is known about the downstream biochemical mechanisms. Posttranslational regulation of protein components in RNA silencing has not been investigated so far.

It has been observed that many of the TRIM/RBCC proteins can mediate their autoubiquitination *in vitro*. To check if mLin-41 also possesses E3 autoubiquitination activity, we performed an *in vitro* ubiquitination assay. We synthesized mLin-41 protein *in vitro* using a rabbit reticulocyte-based coupled transcription-translation (TNT) reaction in the presence of S[35] methionine. The resulting S[35] labeled mLin-41 was incubated with purified Ubiquitin, E1 enzyme, and a set of different recombinant E2s in the presence of the proteasome inhibitor MG132. In presence of UbcH5a, but not other tested E2s (UbcH2, UbcH5b, UbcH5c, UbcH6, UbcH10), mLin-41 became ubiquitinated (Figure 3.3.27).

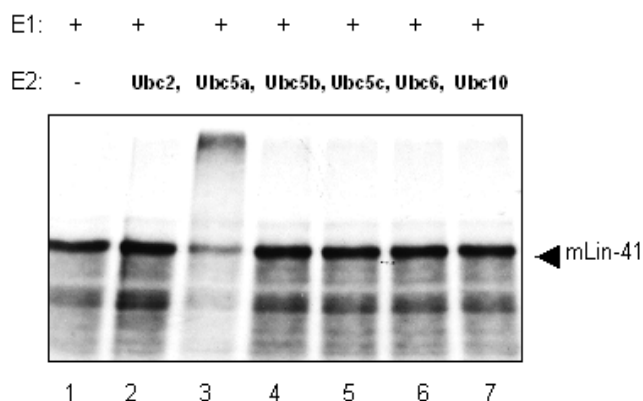


**Figure 3.27. In vitro ubiquitination assay confirmed mLin-41 E3 ligase activity.** In vitro synthesized, S[35] labeled mLin-41 protein was incubated with E1 enzyme and different types of E2 enzymes. Self ubiquitination was observed in presence of E2- UbcH5a.

As the mentioned before, mLin-41 protein contains several functional domains (Ring finger, B-box, coiled coil, filamin and six NHL repeats). In all characterized E3 ubiquitin-protein ligases activity of the Trim family was intrinsic to the RING domain. To test if the RING-finger domain is responsible for the ubiquitination activity of mLin-41, we generated truncation mutants lacking either the N-terminal RING-finger, the RING-finger and B-box domain together, or the C-terminal NHL domain. In addition, a mutant containing a deletion in the RING-finger domain was tested. We could detect ubiquitination activity using full-length mLin-41, the RING-finger/B-box domains, or the RING-finger domain. No activity was observed in the case of the mutant lacking the N-terminal fragment or the RING-finger deletion mutant (Figure 3.3.27). These data taken together indicate that the RING-finger domain is necessary for mLin-41 ubiquitination activity.

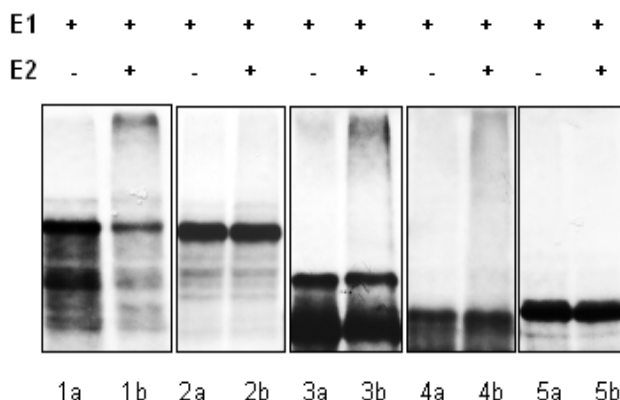


**Figure 3.3.27. In vitro autoubiquitination of full length and mutant mLin-41 in the presence (a) or absence (b) of Ubc5a.** The autoubiquitination activity was observed in case of full length mLin-41(1b) and mutants containing the RING finger domain (lane 3b,4b), but not in mutant lacking the RING-finger domain (5b) or containing a mutation in it (2b).

To confirm mLin-41 autoubiquitination *in vivo*, Flag-tagged mLin-41 protein was overexpressed in HeLa cells. 24h after transfection the cells were treated with the proteasome inhibitor MG132, and immunoprecipitated with anti-Flag antibody. Immunoprecipitated proteins were separated by SDS-PAGE and immunoblotted with anti-Ubiquitin or anti-mLin-41 antibodies. Higher molecular weight forms representing ubiquitinated protein were observed in the presence of MG132 (Figure 3.3.28).

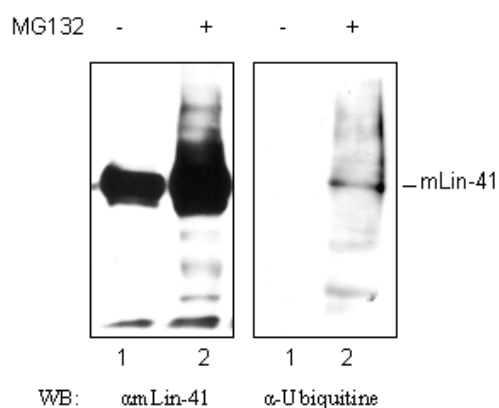


**Figure 3.3.28. *In-vivo* ubiquitination of mLin-41-flag tagged protein.** mLin-41 flag-tagged proteins were expressed in HeLa cells. 24 h after transfection proteins were treated for 4h with MG132 (lane 2) or DMSO as a control (lane 1). Proteins were immunoprecipitated and subjected to SDS-PAGE followed by Western Blot with  $\alpha$ -ubiquitin or  $\alpha$ -mLin-41 antibody.

To determine if mLin-41 has E3 ligase activity towards interaction partners in P-bodies, Flag-tagged mLin-41 was affinity-purified after expression in HEK293 cells. Flag-tagged Lin-28 was purified in parallel as control. Purified proteins were incubated with immunoprecipitates of Ago-2 protein in a reconstituted *in vitro* ubiquitination reaction. After elution of the immunoprecipitate, reaction products were analysed by western blot using anti-Ago-2 antibody. A ladder of high molecular weight forms was observed from reactions containing mLin-41 but not Lin-28. Omission of Ubc5a from the reconstituted reaction strongly reduced Ago-2 ubiquitination, as expected (Figure 3.3.29).

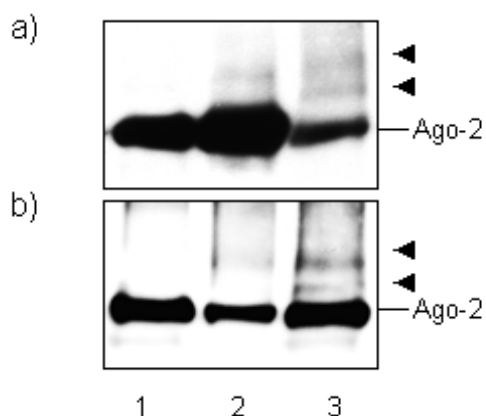


**Figure 3.3.29. mLin-41 ubiquitinates Ago-2 protein *in vitro*.** **a)** Ago-2 proteins were overexpressed in Hek293 cells. Purified protein were incubated with purified mLin-41 in the presence (lane 3) or absence (lane 2) of Ubc5a, or with purified Lin-28 as a control (lane 1). **b)** Purified Ago-2 protein was incubated with *in vitro* synthesized mLin-41 in the presence (lane 3) or absence (lane 2) of Ubc5a, reticulocyte lysate was used as a control (lane 1).

Ago-2 was also found to be ubiquitinated *in vivo* upon co-expression of the two proteins in H293 cells. Cells were transfected with Ago-2 or with Ago-2 plus mLin-41, followed by treatment with proteasome inhibitor MG132. Ago-2 was precipitated with anti-HA antibody, and analysed by western blot using anti-HA or anti-ubiquitin antibodies. Ago-2 ubiquitination was not observed in immunoprecipitates from Ago-2 transfected cells, either in the presence or absence MG132 despite efficient Ago-2 pulldown. After co-transfection with mLin-41, a ladder of ubiquitinated protein at approximately 100kDa and above was detected. Reprobing the blot with anti-ubiquitin antibody confirmed the accumulation of ubiquitinated Ago-2 in the presence of mLin-41 and MG132.

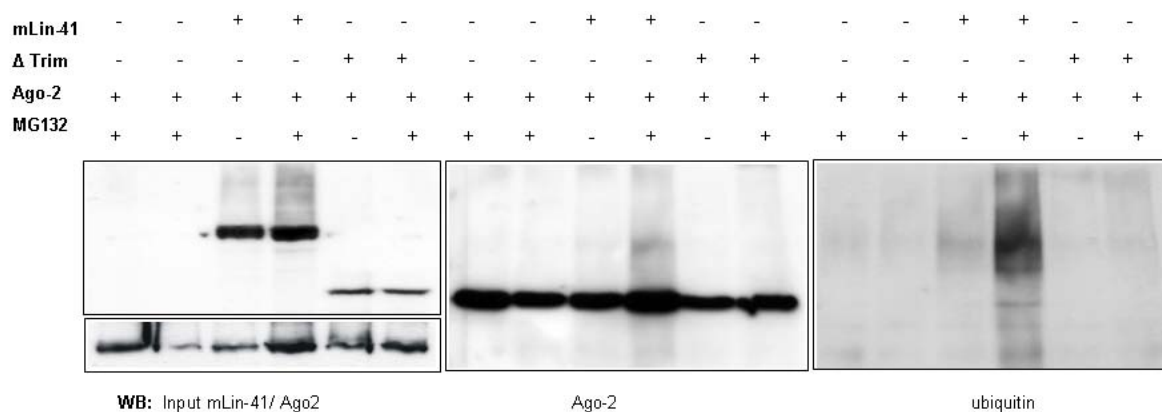


**Figure 3.3.30. mLin-41 enhances Ago-2 ubiquitination *in vivo*.** H293 cells were transfected with HA-tagged Ago-2 singly or in combination with mLin-41 or mLin-41 lacking Ring domain ( $\Delta$ Trim). One half of each transfection was treated with MG132 prior to harvest, as indicated. Cells were lysed in the presence of 1% SDS, extracts were then diluted and Ago-2 immunoprecipitated using anti-HA antibody. A western blot of the mLin-41/Ago-2 input for each precipitation is shown in the **Left Panel**. Precipitates were analysed by western blot using anti-Ago-2 antibody (**Middle Panel**) or anti-ubiquitin antibody (**Right Panel**), as indicated below.

### 3.4. Mechanism regulating *let-7* expression

We next focused on the mechanisms regulating *let-7* expression during stem cell commitment. In principal, miRNA biogenesis can be regulated on three different levels: transcription, nuclear pri-miRNA processing or cytoplasmic pre-miRNA processing. There is increasing evidence that post-transcriptional mechanisms contribute to miRNA regulation during development and in carcinogenesis. It was shown by Thompson et al. that nuclear processing activity is limiting at early stages of development. In the case of *mir-138*, there is also evidence for developmental regulation at the next step: pre-miRNA precursor processing (Obernosterer et al., 2006). Similarly, based on *in vitro* processing assays as well as precursor RNA binding activity, we proposed a model for *let-7* regulation at the level of precursor RNA processing during stem cell differentiation. This proposal was strongly supported by the observation of disparity between accumulation of the precursor and mature forms in different cell lineages (Wulczyn et al., 2007). Comparing *let-7* expression between undifferentiated and differentiated EC cells, strong induction of ~22 nt mature *let-7* forms was observed after differentiation. Meanwhile, the precursor form was present at a constant level in both undifferentiated and differentiated cell samples. This observation was the first evidence that the cytoplasmic precursor processing step can be an important and perhaps essential element of *let-7* regulation.

#### 3.4.1. *let-7* binding complexes

Given the evidence for differential processing activity as a function of differentiation state, we reasoned that developmentally regulated RNA-binding proteins might influence *let-7* maturation. We therefore examined pre-*let-7* precursor-binding activity in an electrophoretic mobility shift assay (EMSA). We first tested EC cell extracts using pre-*let-7a* as substrate (Figure 3.4.1). Apart from a slowly migrating binding activity designated Complex A observed in all lanes, neural differentiation after stimulation with RA was accompanied by a shift in the pattern of bound complexes. With undifferentiated extracts, a single major complex was formed (Complex C) (Figure 3.4.1, Lane 2). Levels of Complex C decreased during the course of neural differentiation. In differentiated cells, Complex C was supplanted by an alternative complex with slower mobility, designated B (Figure 3.4.1 Lanes 3-4). For comparison, extracts prepared from cells induced under conditions favouring differentiation to cardiomyocyte-like cells were also tested. In contrast to neural cells, these cells displayed a more modest shift from Complex C to B over the course of the experiment (Figure 3.4.1, Lanes 5-6). In competition experiments, all three

complexes were inhibited by addition of a ten-fold excess of unlabelled pre-*let-7e* RNA, but not an unrelated RNA fragment transcribed from the eGFP gene (data not shown).

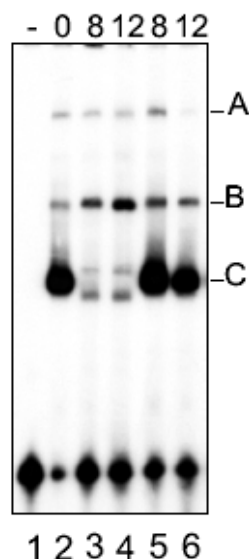


**Figure 3.4.1. Analysis of miRNA precursor binding complexes.** Labeled *pre-let-7a* RNA was incubated either without extract (**Lane 1**), or with extract from undifferentiated EC cells (**Lane 2**), or EC cells stimulated with RA and harvested after 8 (**Lane 3**) or 12 days (**Lane 4**). For comparison, EC-derived cardiomyocytes were tested after 8 (**Lane 5**) and 12 (**Lane 6**) days of differentiation.

As a further test for specificity, we determined the sensitivity of binding to sense and antisense 2'-O-methyl modified oligoribonucleotides (2'OM-ORN). In control experiments (Figure 3.4.2, Lanes 1-3), addition of the *let-7a* 2'OM-ORN to a binding reaction in the absence of protein extract had no effect on the migration of the labeled precursor. Addition of the anti-*let-7a* 2'OM-ORN led to formation of a band with reduced mobility, indicating that the antisense molecule could invade the stem and compete with the *let-7a* complementary sequence for *let-7a* (Figure 3.4.2, Lane 3). Interestingly, the two 2'OM-ORN had differential effects on Complex B and C binding. Addition of the *let-7* surrogate to a reaction containing undifferentiated cell extract eliminated Complex C formation without reducing Complex B (Figure 3.4.2, Lane 5). The interference was sequence specific; as anti-*let-7* did not affect Complex C and a control 2'OM-ORN complementary to *mir-128* was also ineffective as an inhibitor (Figure 3.4.2, Lanes 6-7).

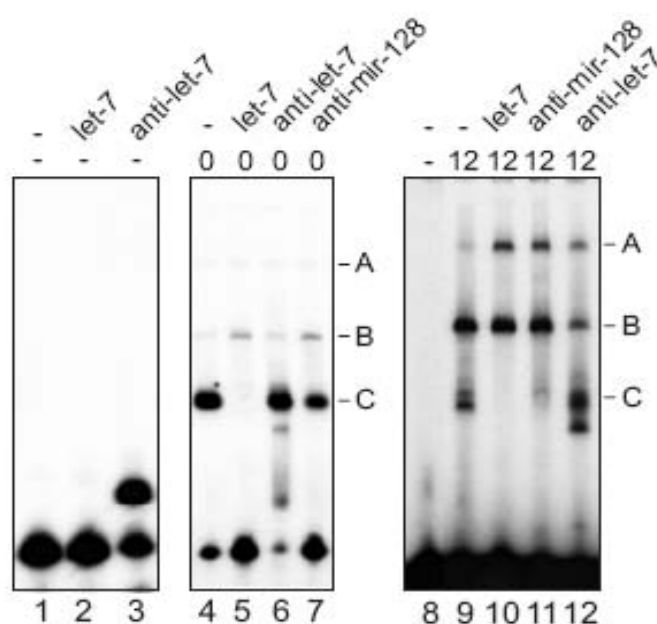


**Figure 3.4.2. The sensitivity of binding to synthetic 2'OM-ORN.**

Free pre-*let-7a* probe was incubated either with synthetic *let-7a* 2'OM-ORN (**Lane 2**) or with an 2'OM-ORN complementary to *let-7a* (**Lane 3**). Duplex formation leads to a slower migrating band in **Lane 3**. Undifferentiated EC cells extracts (**Lanes 4-7**) or extracts from Day 12 (**Lanes 8-12**) were incubated with labeled pre-*let-7a* RNA without 2'OM-ORN (**Lanes 4 and 9**), with *let-7a* analog 2'OM-ORN (**Lanes 5 and 10**), with a 2'OM-ORN complementary to *let-7a* (**Lanes 6 and 12**) or with control oligoribonucleotide, complementary to *mir-128* (**Lanes 7 and 11**).

The pattern of inhibition observed for Complex B was the inverse of Complex C. Neither the *let-7* surrogate (Figure 3.4.2, Lanes 5 and 10), nor anti-*mir-128* (Figure 3.4.2, Lanes 7 and 11) significantly interfered with Complex B formation. However, addition of anti-*let-7* strongly reduced Complex B formation (Figure 3.4.2, Lane 12). These results are consistent with a functional role for Complex B in processing, as antisense but not sense 2'OM-ORN strongly inhibit miRNA function *in vivo*.

These results suggest that the anti-*let-7* oligoribonucleotide may interfere with an early step in the recognition of the precursor by the processing machinery. To directly link the RNA binding activity to the miRNA biogenesis pathway, we challenged neural complexes with antibodies to several known miRNP components (Figure 3.4.3). Addition of Protein A purified anti-Argonaute1 antibody, a core miRISC protein (Ago1, Lane 3) reproducibly reduced formation of Complex B. As a control, binding was unaffected by addition of either an unrelated antibody preparation (Protein A purified anti-H3) or an antibody specific for the RNA helicase Gemin3 (Figure 4.3, Lanes 4 and 5). Furthermore, a monoclonal antibody specific for the miRISC-associated Fragile X Mental Retardation protein (FMRP, Lane 8) reproducibly reduced formation

of Complex B. Control reactions contained isotype matched antisera that did not affect binding (Figure 3.4.3, Lanes 9 and 13)

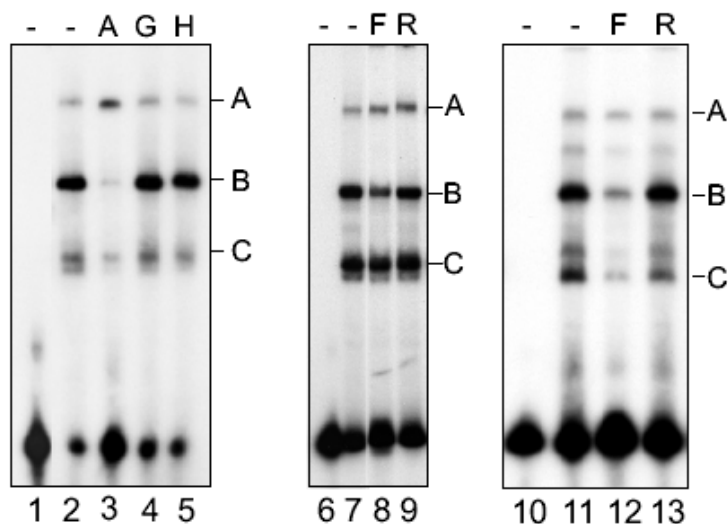


**Figure 3.4.3. Antibodies against miRNP components reduce complex B formation.** Differentiated EC cells extracts from Day 12 (**Lanes 2-5; 11-13**) or Day 8 (**Lanes 7-10,**) were preincubated either without antibody (**Lanes 2, 7 and 11**); with anti Ago1 pAb (A, **Lane 3**); anti-Germin3 mAb (G, **Lane 4**), or with anti-histone3 H3 mAb (H, **Lane 5**); anti-FMRP mAb 7G1-1 (F, **Lanes 8 and 12**); or anti-Rip1 mAb (R, **Lanes 9 and 13**) prior to addition of labeled pre-*let-7e*. Migration of free pre-*let-7e* probe is shown in **Lanes 1, 6 and 10**. Anti-Ago1 and anti-FMRP specifically reduced formation of Complex B.

We next compared pre-*let-7* binding activity in EC-derived neurons to primary cortical neurons (Figure 4.4). In primary neurons we observed two RNA-binding activities with mobility indistinguishable from Complexes A and B. The embryonic Complex C was not present. Preincubation with anti-FMRP antibody strongly and specifically inhibited formation of the neuronal Complex B compared to control (Figure 3.4.4, Lanes 5 and 6), consistent with the presence of FMRP in a neuron-enriched miRNP.

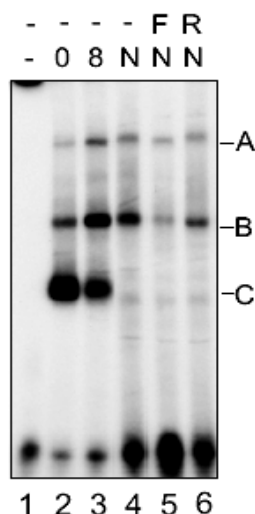


**Figure 3.4.4. Comparison of binding complexes between he EC cells and neurons.** Binding complexes were formed after incubation of labeled pre-*let-7a* with extracts from undifferentiated (**Lane 2**) or Day 8 (**Lane 3**) EC cells or primary embryonic neurons (N, **Lanes 4-6**). Migration of free probe is shown in **Lane 1**. Neuronal extracts were preincubated with anti-FMRP antibody (F, **Lane 5**) or control anti-Rip1 mAb (R, **Lane 6**). Two prominent complexes are seen using neuronal extracts, labeled A and B to the right. Note similar mobility to Complex A and B from neuronal EC cells. Complex B is sensitive to anti-FMRP antibody (**Lane 5**) but not control antibody (**Lane 6**).

We next compared the pattern of protein binding to three different precursor RNAs: the ubiquitously expressed *let-7a*, the neuron-specific *mir-128*, and the stem cell specific *mir-291*. Using pre-*mir-128* as probe, we observed a binding activity of the same mobility as Complex C that was also restricted to undifferentiated EC cells (Figure 3.4.5, Lane 2). In addition, a low mobility complex resembling Complex A was observed in all cells tested. However, there was no Complex B formed on pre-*mir-128* (Figure 3.4.5, Lanes 3 and 4). We next examined binding complexes using pre-*mir-291* - miRNA exclusively expressed in embryonic stem cells (Figure 3.4.5). For pre-*mir-291*, a single binding activity was observed with mobility similar to Complex A. Importantly, there was no detectable Complex C, and differentiation state had no influence on the pre-*mir-291* binding pattern.

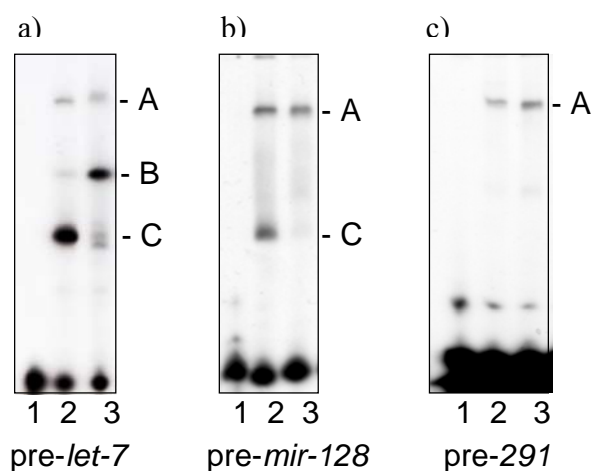


**Figure 3.4.5. Comparison of miRNA binding complexes between *let-7a*, *mir-128*, *pre-291*.**

Characterization of pre-*let-7a* (Panel a), pre-*mir-128* (Panel b) and pre-*mir-291* (Panel c) RNA binding by EMSA. Binding reactions contained extracts from undifferentiated EC cells (EC, Lanes 2) or EC cells after neural differentiation (EC+RA, Lanes 3). Lane 1 is a mock binding reaction without added cell extract showing migration of free probe. The position of RNA-binding complexes referred to in the text is indicated to the right. Note the prominent Complex C in undifferentiated EC cells formed on pre-*let-7a* (Panel a, Lane 2) and pre-*mir-128* (Panel b, Lane 2), but not pre-*mir-291* (Panel c, Lane 2). Complex B is a pre-*let-7*-specific complex found in EC-derived neurons (Panel a, Lanes 3 and 4).

For each of the cell types tested, there was a clear inverse correlation between Complex C expression on the one hand, and *let-7* expression and processing activity on the other. This data supported our previous suggestion that Complex C might be a specific inhibitor of pre-*let-7* processing. Since the protein component or components of Complex C are specific to pluripotent cells, this correlation also raised the possibility of an autoregulatory loop between *let-7* and Complex C. In this scenario, *let-7* might regulate its own processing by targetting the putative inhibitor responsible for Complex C.

To test if levels of Complex C are regulated by *let-7*, we artificially overexpressed several miRNAs in EC cells. We found that ectopic expression of *let-7a*, *mir-125*, or a combination of the two reproducibly reduced binding of Complex C compared to a negative control miRNA. As a further control, ectopic *mir-128* did not reduce levels of Complex C. The reduction in Complex C was observed using either pre-*let-7a* or pre-*mir-128* as substrate for the binding reaction (Figure 3.4.6).

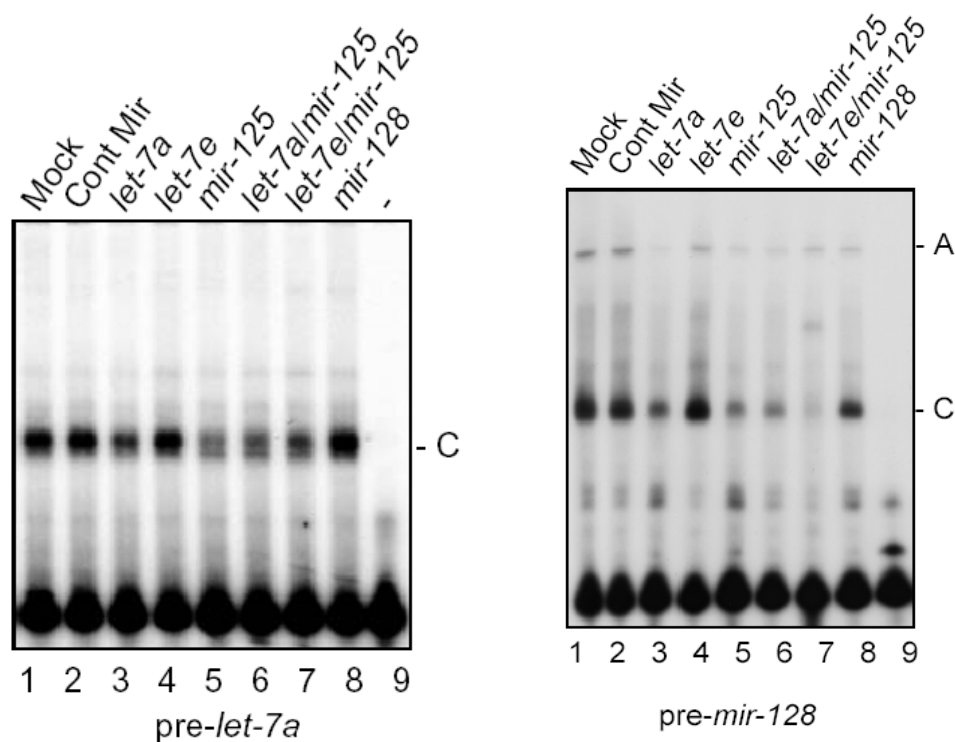


**Figure 3.4.6. Complex C is regulated by *let-7* and *mir-125*.**

EC cells were transfected with precursor RNA as indicated above each lane. Undifferentiated EC cells were Mock transfected (Mock, **Lane 1**) or transfected with negative control precursor (Cont Mir, **Lane 2**), *let-7a* (**Lane 3**), *let-7e* (**Lane 4**), *mir-125* (**Lane 5**), *let-7a* and *mir-125* (**Lane 6**), *let-7e* and *mir-125* (**Lane 7**), or *mir-128* (**Lane 8**). Free probe is shown in **Lane 9**. Complex C was downregulated by *let-7a* and *mir-125* but not *let-7e* or *mir-128*. Complex A was not consistently affected by any miRNA tested. Similar regulation of pre-*mir-128* binding complexes is shown.

### 3.4.2. Pre-*let-7* binding protein

To identify candidates for Complex C, we compared the microarray profiling of the EC response to ectopic *let-7* (Results, chapter 3.2) and *let-7* target gene prediction databases. This analysis suggested a number of candidates, including Lin-28, Lin-28B, Lin-41, Dicer, Tarbp2/Trbp and Tnrc6B. We performed overexpression and siRNA-mediated silencing experiments of candidate genes and assayed the influence on precursor RNA binding. In the case of Lin-41 we did not observe any changes in comparison to the control. However, we observed a dramatic reduction in Complex C after treatment of EC cells with any of four specific siRNA duplexes directed against Lin-28. Representative results are shown for pre-*let-7a* in Figure 3.4.7, Panel A, and for pre-*mir-128* in Figure 3.4.7, Panel B. In contrast, siRNA-mediated silencing of either Dicer or Tarbp2 specifically interfered with Complex A, but had no effect on Complex C.

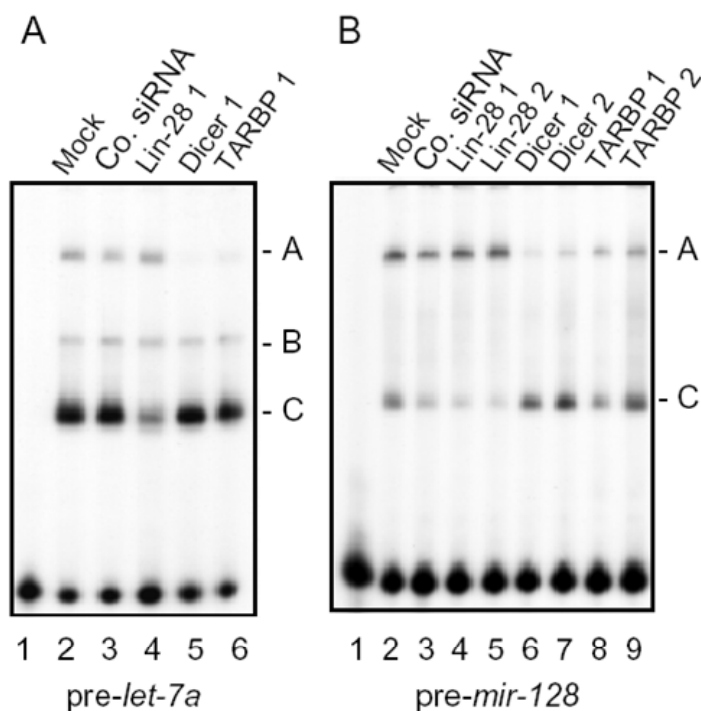


**Figure 3.4.7. siRNAs directed against *lin-28* inhibit Complex C.** siRNAs directed against *dicer* and *tarbp2* inhibit Complex A. Undifferentiated EC cells were transfected with siRNA duplexes as indicated above each lane. Lin28 1, Lin28 2, Dicer 1, Dicer 2, Tarbp1 and Tarbp 2 represent two distinct siRNAs for each gene. Four siRNA duplexes were tested for each gene with similar results (not shown). RNA binding complexes specific for pre-*let-7a* (**Panel A**) or pre-*mir-128* (**Panel B**) were analysed after 24 hours.

Silencing of Dicer also reduced binding of Complex A with the pre-*mir-291* probe. siRNA efficacy and specificity was confirmed by Western blot (Figure 3.4.8). The demonstration that reduction in two essential miRNA pathway proteins (Dicer and Tarbp2) affects precursor binding suggests that the binding complexes observed in the EMSA are physiologically relevant.

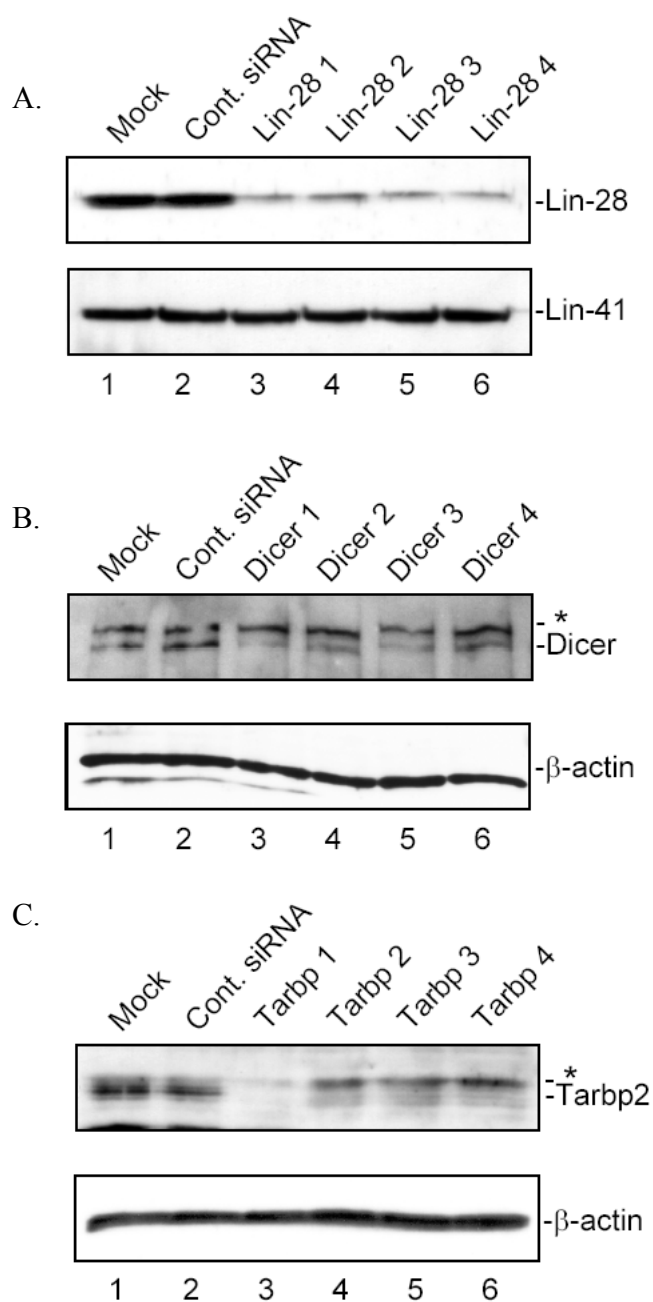


**Figure 3.4.8. Western blot analysis of siRNA efficacy and specificity against Lin-28, Dicer or Tarbp protein.** For each mRNA, four siRNA duplexes were tested. Silencing efficiency is compared to transfection of water (Mock **Lane 1**), negative control siRNA (Cont. siRNA, **Lane 2**), and each specific siRNA duplex as indicated above each lane (**Lanes 3-6**). **Panel A.** Silencing of Lin-28, compared to the control protein Lin-41. **Panel B.** Silencing of Dicer, compared to the control protein β-actin. **Panel C.** Silencing of Tarbp2, compared to the control protein β-actin. A non-specific band is indicated by an asterisk to the right. Duplexes 1 and 2 were used in the experiments reported here.

### 3.4.3. Lin-28 as pre-let-7 binding protein in undifferentiated cells

To confirm the physical presence of Lin-28 in Complex C, an EMSA gel was blotted onto a PVDF membrane and probed with antibodies for Lin-28 and, as control, Lin-41. The results demonstrated that Lin-28 is a component of Complex C. First, two bands were seen; the lower band corresponded in migration to complex C as revealed by autoradiography. Second, the Lin-28 was present in pluripotent but not differentiated cells, and was specifically downregulated in response to ectopic *let-7* and *mir-125* overexpression.

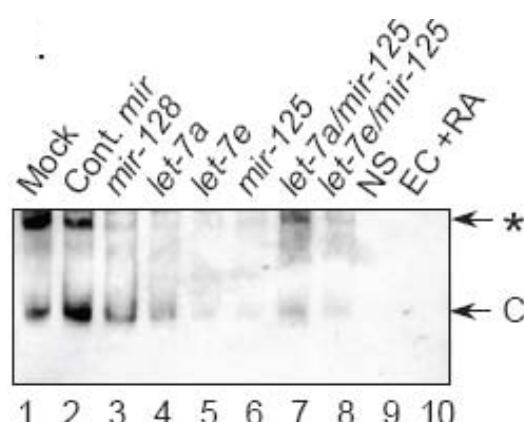


**Figure 3.4.9. Shift-Western experiment demonstrating the presence of Lin-28 in Complex C.** An EMSA using pre-*let-7a* as probe was performed with EC cell extracts transfected with synthetic precursor RNAs. For comparison, extracts from NS cells (NS) and RA-treated EC cells (EC+RA) without transfection were also tested. The Lin-28 signal was reduced by overexpression of *let-7a* (Lane 4), *let-7e* (Lane 5), *mir-125* (Lane 6) and combinations thereof (Lanes 7 and 8), but not the control precursor (Cont Mir, Lane 2) or *mir-128* (Lane 3) compared to mock control (Lane 1). No signal was obtained in NS cells (Lane 9) and RA-treated EC cells (Lane 10), neither of which express Lin-28.

We then affinity purified Lin-28 to directly assay for binding to pre-*let-7* and pre-*mir-128*. In Figure 3.4.10 Flag-purified Lin-28, but not Flag-purified Lin-41 prepared in parallel, bound with high affinity to either pre-*let-7* or pre-*mir-128* RNA.

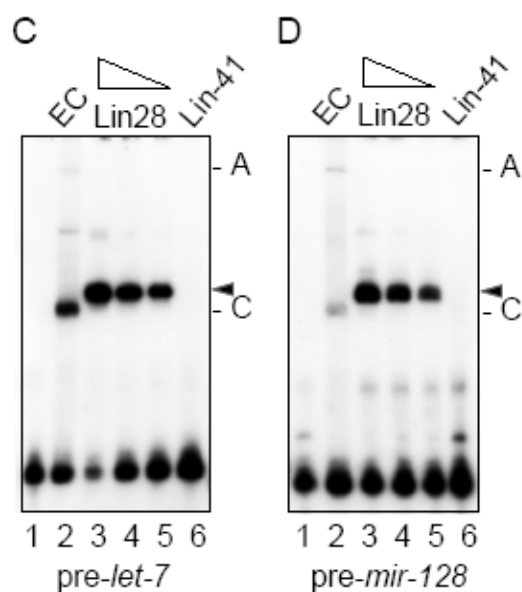


**Figure 3.4.10. Flag-purified Lin-28, but not Lin-41 binds precursor let-7a and mir-128.** A dilution series (1:50 to 1:100) of Lin-28 was tested for each precursor (lane 3-5). In each panel lane 2 presents binding obtained with undifferentiated EC extracts, the position of the complex C is indicated on the right. The mobility shift of the purified protein (black arrowhead) relative to complex C corresponds to the epitope tag. Mobility of the free probe is shown in lane 1.

#### 3.4.4. *lin-28* as *let-7* target gene

The mouse *lin-28* mRNA is known to be a target for *mir-125*, but our results indicated it might be also targeted by *let-7* as well (Figure 3.4.11). Consistent with this, overexpression of *let-7* in EC cells led to a reduction in the endogenous Lin-28 mRNA and protein of a magnitude similar to that observed with *mir-125* (Figure 3.4.11).

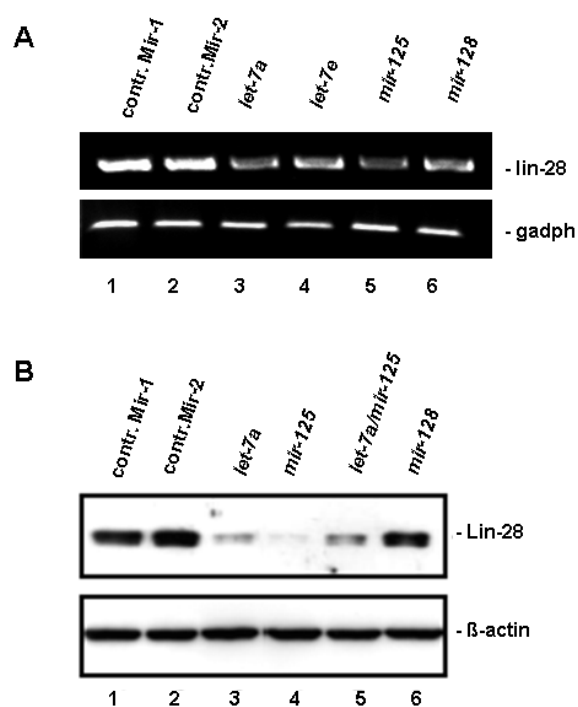


**Figure 3.4.11. Endogenous Lin-28 protein is downregulated after overexpression of Let-7a or mir-125 in EC cells.** RT-PCR (A) and Western blot (B) of Lin-28 48h after transfection with precursor miRNA showing: mock transfection, negative control miRNA (Control Mir), *let-7a*, *let-7e*, *mir-125* and *mir-128*. Lin-28 was effectively silenced on both mRNA and protein level by *let-7* and *mir-125*.

This result is consistent with the presence of four conserved *let-7* binding sites in the mouse *lin-28* 3'UTR (According to the current PicTar database of predicted miRNA binding sites). The activity of these sites was verified in our laboratory (Rybak et al. 2008).

### 3.4.5. *Lin28/pre-let-7* interaction study

To learn more about the Lin-28/*pre-let-7* interaction, we compared the sensitivity of EC cell extracts or affinity-purified Lin-28 to tRNA and EDTA. Lin-28 binding from either source was resistant to 500-fold molar excess of tRNA, but was reduced in the presence of 10 mM EDTA (Figure 3.4.12). Sensitivity to EDTA most likely reflects a requirement of correct substrate secondary structure for binding.

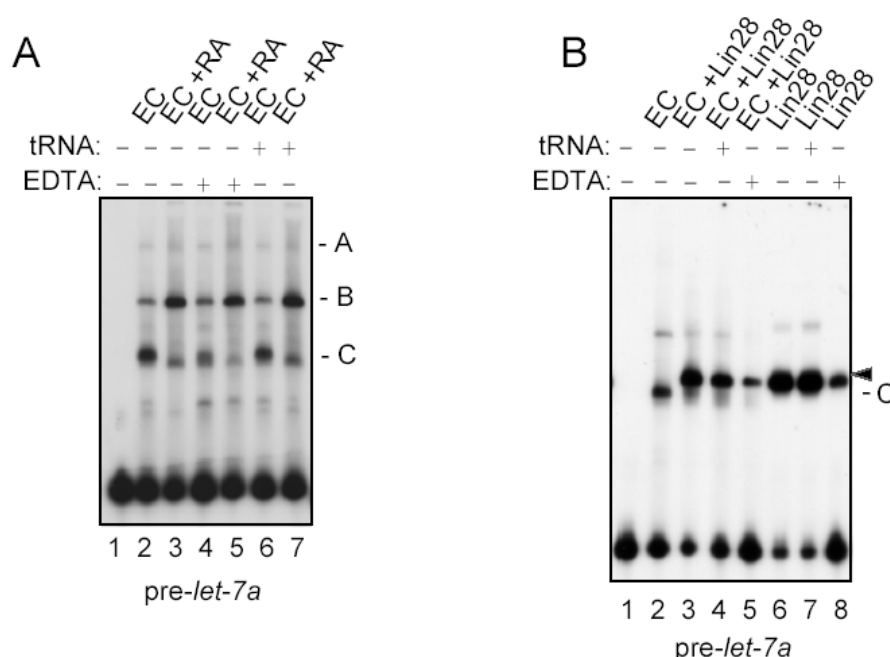


**Figure 3.4.12. Sensitivity of pre-let-7 binding complexes to tRNA and EDTA.** In **Panel A**, extracts from undifferentiated and RA-stimulated EC cells were tested, as indicated above each lane. In **Panel B**, complexes formed by control EC cells (**Lane 2**), EC cells overexpressing Lin-28 (**Lanes 3-5**) or affinity-purified Lin-28 (**Lanes 6-9**) were challenged with tRNA or EDTA, as indicated above each lane. Binding reactions were assembled under standard conditions, or in the presence of 250 ng tRNA or 1.5 mM EDTA.

We then performed competition experiments with a series of synthetic RNA oligoribonucleotides described in Figure 3.4.13. Dividing pre-let-7 into 5' stem, loop, and 3' stem, we found that the 5' stem (identical to 22 nt *let-7*) and the loop RNAs efficiently competed for binding by Lin-28/Complex C. In contrast, the 3' stem sequence (identical to *let-7* star) was unable to compete for binding (Figure 3.4.13). To further delineate contacts between Lin-28 and *let-7*, competitor RNAs spanning nucleotides 1-14 and 9-22 of *let-7* were tested. Although both RNAs reduced Lin-28 binding, the RNA containing the conserved 5' seed was more effective. As further evidence for specific contacts to the seed region, a mutated *let-7* RNA with 3 nucleotide exchanges in the seed sequence was shown to be less effective as competitor compared to the wild type sequence (Figure 3.4.13).

A.

## Competitor RNAs

let-7 1-67

UGAGGUAGUAGGUUGUAUAGUUUAGAGUUACAUCAAGGGAGAUAAACUGUACAGCCUCCUAGCUUUCC

5' 1-22 (let-7)

UGAGGUAGUAGGUUGUAUAGUU

5' 1-22 M

UAGGGCAGUAGGUUGUAUAGUU

Loop 23-43

UAGAGUUACAUCAAGGGAGAU

3' 46-67 (let-7 star)

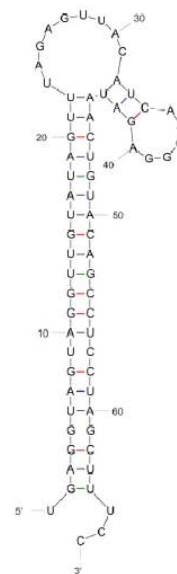
CUGUACAGCCUCCUAGCUUUCC

5' 1-14

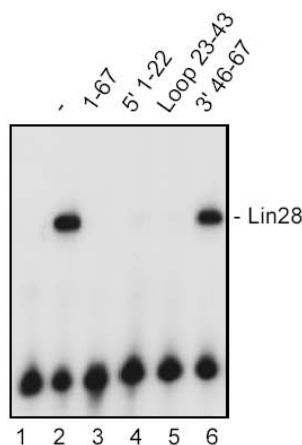
UGAGGUAGUAGGUU

5' 9-22

UAGGUUGUAUAGUU



B.



C.

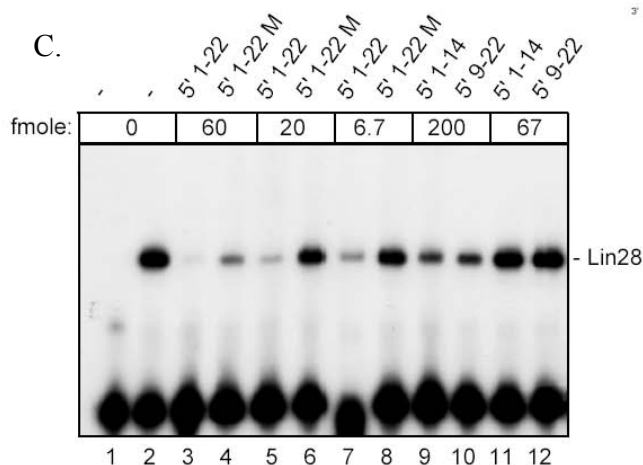


**Figure 3.4.13. Mapping the contact site of let-7- lin-28 interaction.** **Panel A.** RNA's used to delineate recognition elements for Lin-28 in Panels B and C are described. Nucleotide exchanges are shown in red type. The predicted structure of pre-let-7a-2 as determined by mfold1 is shown at the right. **Panel B.** RNA's corresponding to 22 nt let-7a RNA, or the let-7a-2 loop sequence, but not let-7a star compete for Lin-28 binding. **Lanes 1 and 2** display free pre-let-7a probe and probe plus affinity-purified Lin-28 in the absence of competitor RNA, respectively. In **Lanes 3-6**, EMSA reactions contained affinity-purified Lin-28, the labelled pre-let-7a probe and 0.25 pmole of the unlabelled competitor RNA indicated above each lane. The non-overlapping let-7 and Loop oligoribonucleotides competed for binding as well as the full length precursor (**Lanes 3, 4 and 5**, respectively), but the let-7 star RNA (3'46-67, **Lane 6**) did not compete for binding. **Panel C.** Evidence for specific contacts with between Lin-28 and the conserved let-7 seed sequence. **Lanes 1 and 2** display free probe and probe plus affinity-purified Lin-28 in the absence of competitor RNA, respectively. Wildtype and point mutant let-7 RNA's were titrated as competitors in the EMSA (**Lanes 3-8**, competitor RNA added is indicated above each lane in fmole). The wildtype let-7 RNA efficiently competed for binding at 6.7 fmole (**Lane 7**), comparable inhibition with the mutant let-7 required 60 fmole (**Lane 4**). Additional contacts are made outside the seed, as overlapping 14 nt RNA's corresponding to nucleotides 1-14 and 9-22 of let-7a displayed similar effectiveness as competitors, (**Lanes 9-12**). The affinity of the shorter RNA's was reduced compared to 22 nt let-7a, as 0.2 pmole of the 14-mers was required for effective competition (**Lanes 9 and 10**).

### 3.4.6. *Lin-28* interferes with *Dicer* activity

The results of the RNA binding analysis suggested that *Lin-28* might interfere with access of *Dicer* to the pre-*let-7* stem and the cleavage site at the junction of the stem and the loop. In fact, addition of affinity-purified *Lin-28* to an EMSA reaction containing recombinant *Dicer* led to loss of *Dicer* binding to either pre-*let-7* (Figure 3.4.14) or pre-*mir-128*. Similar results were obtained upon addition of *Dicer* to EC cell extracts overexpressing *Lin-28*.

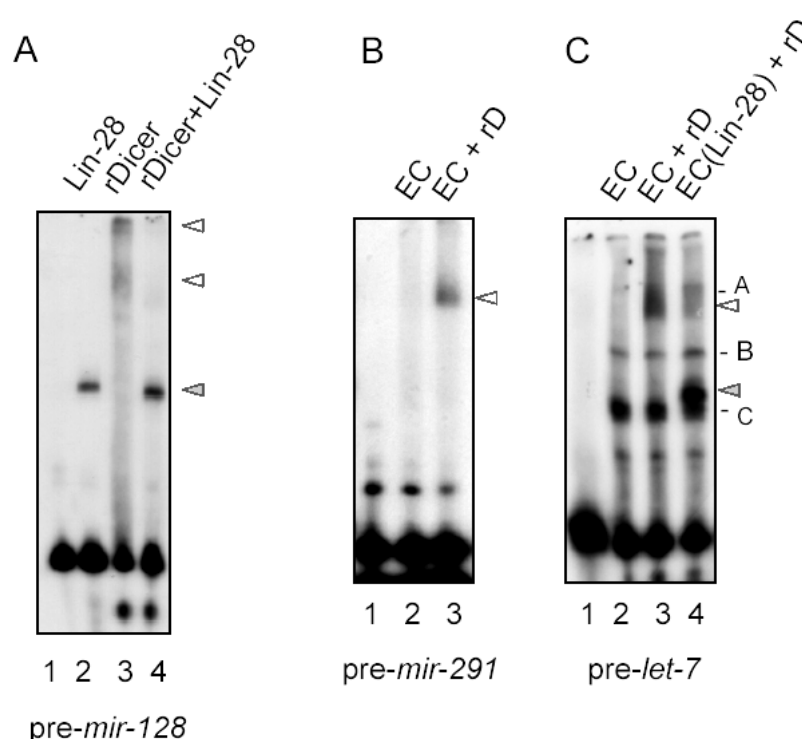


**Figure 3.4.14. *Lin-28* interferes with *Dicer* *let-7* precursor binding.** **Panel A.** *Lin-28* competes with *Dicer* for pre-*mir-128* occupancy. EMSA of *Dicer* binding to pre-*mir-128* in the presence or absence of affinity-purified *Lin-28*. **Lane 1** displays free probe, **Lane 2** the complex formed by *Lin-28* (gray arrowhead to the right), **Lane 3** the binding activity of recombinant *Dicer* protein (open arrowheads to the right), and **Lane 4** binding complexes formed after addition of both *Lin-28* and *Dicer*. **Panels B and C.** *Dicer* binding assay in the presence of crude cell extracts. In **Panel B**, binding of recombinant *Dicer* protein to the pre-*291* RNA is shown. Addition of *Dicer* protein to a binding reaction containing protein extract from undifferentiated EC cells led to formation of a low mobility complex with similar mobility to Complex A (open arrowhead, compare **Lane 2**, EC extract without *Dicer* to **Lane 3**, EC extract plus *Dicer*). Similarly, addition of *Dicer* to a binding reaction containing EC extract and the pre-*let-7* RNA as probe led to an additional band just below endogenous Complex A (**Panel C**, compare **Lanes 2 and 3**, open arrowhead). In **Lane 4**, *Dicer* was added to a binding reaction containing EC extract prepared from cells transfected with epitope-tagged *Lin-28* expression vector. Ectopic *Lin-28* formed a complex immediately above endogenous Complex C, in accordance with the triple epitope tag (gray arrowhead). The *Dicer* complex (open arrowhead) was clearly reduced in strength (compare **Lanes 3 and 4**).

To test the ability of *Lin-28* to interfere with *Dicer* activity, affinity-purified *Lin-28* was added to an *in vitro* processing reaction containing pre-*let-7* and recombinant *Dicer*. Addition of 10ng or

25ng Lin-28 led to a 2- to 2.5-fold reduction of processing activity, respectively. Dicer activity was not affected by addition of affinity-purified mLin-41 as control (Figure 3.4.15).

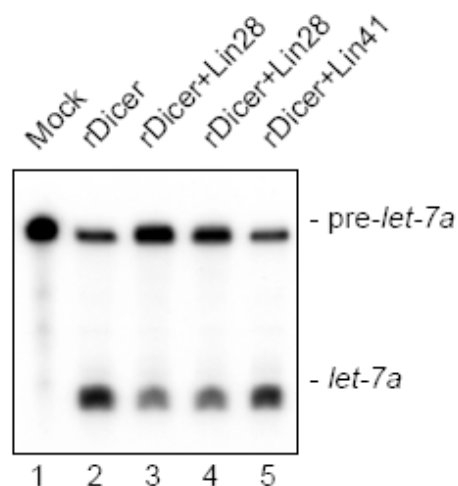


**Figure 3.4.15. Lin-28 inhibits Dicer activity.** Lane 1 is a mock reaction showing migration of radiolabelled pre-*let-7a*. Lane 2 shows cleavage of pre-*let-7a* by recombinant Dicer. In lanes 3–5, the cleavage reaction contained recombinant Dicer and 25 ng (lane 3) or 10 ng (lane 4) of affinity-purified Lin-28, or 25 ng affinity purified mLin-41 (lane 5).

### 3.4.7. Cytoplasmic action of Lin-28

Recently, evidence was *presented* for an alternative mechanism for Lin-28: interference with nuclear pri-*let-7* processing (Viswanathan et al., 2008). However, previous work from our laboratory demonstrated the presence of pre-*let-7* RNA in EC and ES cells (Wulczyn et al., 2007), implies that any block in nuclear pri-miRNA processing cannot be complete.

In support of cytoplasmic action of Lin-28, we examined its intracellular localization and verified that Lin-28 is primarily localized in the cytoplasm of the EC cells used in our assays (Figure 3.4.16).

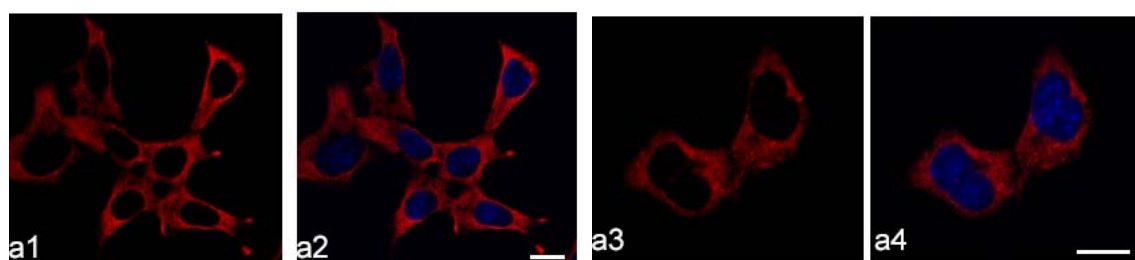


**Figure 3.4.16. Lin-28 is primarily localized to the cytoplasm in EC cells.** Images a1 and a3 show staining for endogenous Lin-28 protein at two magnifications obtained with polyclonal rabbit anti-Lin-28 antibody (Abcam). At the lower intensity used for a3, localization in cytoplasmic foci is evident, consistent with the previous report<sup>31</sup>. Plates a2 and a4 show merged confocal images of Lin-28 in red, and DAPI staining of nuclei in blue.

As evidence for cytoplasmic blockade *in vivo*, *in situ* hybridization was performed to determine the localization of *let-7* in EC cells. Staining was primarily observed in the cytoplasm, and was characterized by bright perinuclear foci. The results are similar to a previous report describing co-localization of *let-7* and miRNA pathway proteins in the chromatoid body of male germ cells. Cytoplasmic localization of *let-7* is consistent with a primary blockade of Dicer processing, and with our previous demonstration by northern blotting that pre-*let-7* is present in undifferentiated ES and EC cells (Wulczyn et al., 2007). The ability of Lin-28 to bind pre-*let-7* and influence the efficiency of cytoplasmic processing provides new insight into the role of this protein in the miRNA pathway, the heterochronic pathway, and the role of Lin-28 in the reestablishment of pluripotency after forced expression in somatic cells.

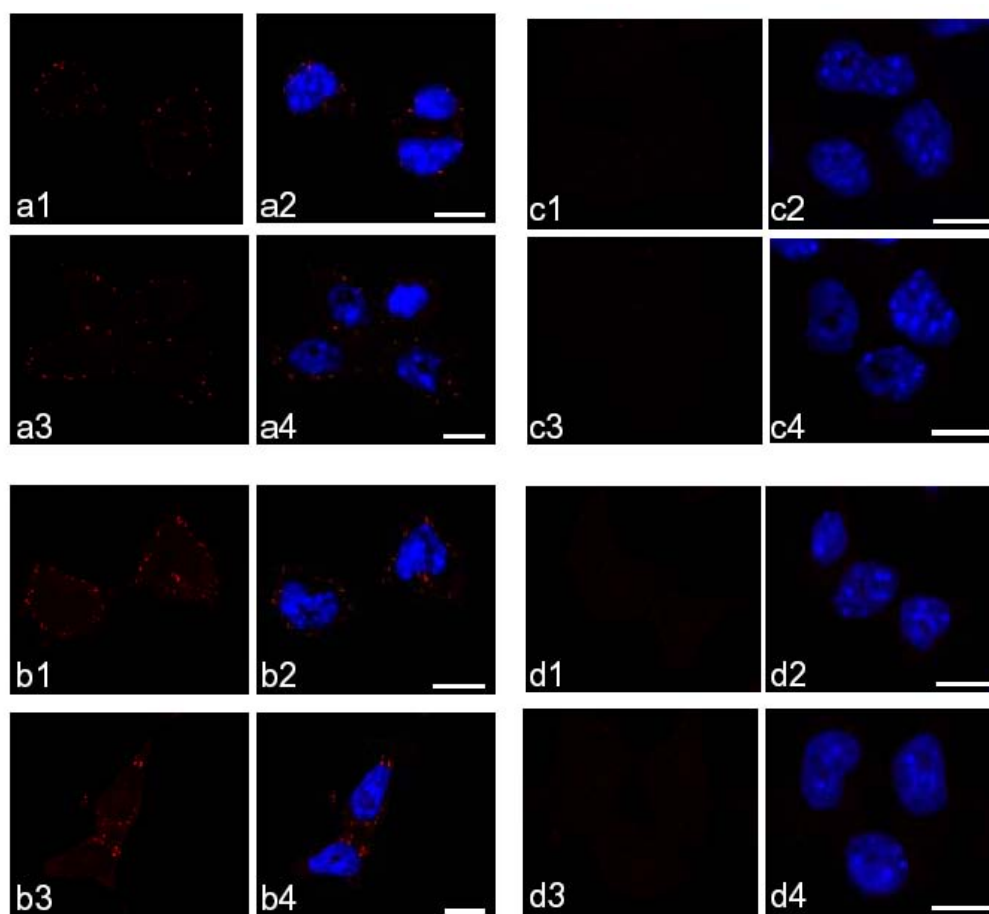


**Figure 3.4.17.A. Cell staining reveals cytoplasmic accumulation of pre-*let-7* in EC cells.** (a, b) EC cells were hybridized with LNA-probes complementary to 22-nucleotide *let-7a* (a) or pre-*let-7a* (b). Note that the *let-7a* probe recognizes pri-, pre- and mature *let-7a*, and the pre-*let-7a* probe recognizes pri- and pre-*let-7a*. (c, d) EC cells were hybridized with the corresponding point-mutant probes mutant *let-7a* (c) or mutant pre-*let-7a* (d). Two representative images are shown for each probe. Hybridization was visualized by confocal microscopy after fluorescent immunostaining with anti-digoxigenin monoclonal antibody followed by Alexa-568-coupled anti-mouse antibody.

## 4. Discussion

### 4.1. *let-7* miRNA expression

A prerequisite for understanding the function of miRNAs is to determine their expression during development. The original description of *let-7* expression in the mouse, by tissue-specific cloning, showed that the *let-7* miRNA family is not restricted to the nervous system but that it is one of the most highly represented miRNAs in the brain (Lagos-Quintana, 2002). With the advent of *in situ* hybridization techniques capable of detecting miRNAs, prominent expression in the zebrafish nervous system was demonstrated (Wienholds, 2005). We used this protocol, based on the use of locked nucleotide analogues (LNA) as hybridization probes to analyse the spatial and temporal expression of *let-7* in mouse development. LNA comprises a new class of high-affinity RNA analogues in which the furanose ring of the ribose sugar is chemically locked in an RNA-mimicking conformation by the introduction of an O2',C4'-methylene bridge. This modification results in enhanced affinity and a significant increase in the melting temperature of hybridization and thus allows sufficient stringency and signal strength with the short probes required for miRNA detection. Using LNA probes for *in situ* hybridization, we found that the distribution of three *let-7* family members closely resembled that of the paradigm brain-specific miRNA *mir-124* and the brain-enriched *mir-125* and *mir-128* (Thomson et al., 2004). In the E9.5 mouse embryo, *let-7* hybridization signal was obtained in the neuroepithelium of the brain and spinal cord, and in the first and second branchial arches. Similarly, widespread expression was observed at E12, but with the most prominent staining in the neuroepithelium of the brain, spinal cord and the cranial and dorsal root ganglia. In the postnatal brain overall expression was reduced in comparison to the embryo, with high levels of expression restricted to the neuron-rich layers of the hippocampus, cerebellum and cortex.

In *C.elegans*, the timing of *let-7* expression governs terminal cell differentiation (Reinhart, 2000), and it has been proposed that *let-7* may be involved in the regulation of either the timing or maintenance of cell fate decisions (Pasquinelli, 2002, 2004). To study *let-7* function in mammals we focused on identification of new aspects of *let-7* miRNA function in the timing of cell fate decisions in the mammalian CNS.

#### 4.2. *let-7* miRNA targets

To elucidate *let-7* function in mammalian stem cells, we performed mRNA profiling after ectopic overexpression of *let-7* miRNA. ES cells and EC cells are well suited to the functional study of miRNAs in general, and *let-7* in particular. In the pluripotent state very low levels of mature forms of most tissue specific miRNAs, including *let-7*, are present. The initiation of cellular differentiation is accompanied by the induction of miRNAs, similar to that observed in early development (Smirnova et al., 2005). Regulation of *let-7* induction operates at both the transcriptional and post-transcriptional levels and involves activation of both the nuclear and cytoplasmic processing events (Thomson et al., 2005; Wulczyn et al., 2007). Delivery of miRNA precursors into ES and EC cells by transfection, however, leads to efficient suppression of both artificial as well as endogenous target genes.

Lim et al were the first to show that ectopic overexpression of miRNAs had widespread effects on mRNA levels (Lim et al., 2005). Of the hundreds of genes they identified as miRNA responsive, they found an excellent correlation between downregulation and predicted miRNA binding sites. A similar effect on mRNA destabilization by miRNA overexpression was described by Baek et al. They described hundreds of genes directly repressed, albeit each to a modest degree, by individual miRNAs. Although some targets were repressed without detectable changes in mRNA levels, those translationally repressed by more than a third also displayed detectable mRNA destabilization, and, for the more highly repressed targets, mRNA destabilization usually comprised the major component of repression (Baek et al., 2008). In *C.elegans* *let-7* was recently shown to mediate mRNA destabilization of its target genes, including *Lin-41* (Bagga et al., 2005). Results from our lab suggest that the same mechanism operates in the mouse, as both the endogenous *mLin-41* mRNA and the *mlin-41* sensor mRNA are destabilized upon EC cell differentiation. Estimates of the number of *let-7* target genes run into the thousands. We detected far fewer candidates for direct regulation, perhaps because our assay was limited to those genes expressed in EC cells. Of the targets we identified there is a strong bias toward genes containing multiple *let-7* binding sites: *Hic-2* (16), *Nr6a1* (14), *Arid3b* (10), *Hmga2* (6), *mLin-41* (5), *Appb3* (2), *Tarbp2* (2) and *Tusc2* (2), suggesting that multiple *let-7* binding sites favor mRNA destabilization in our assay.

Neither the downregulated nor the upregulated genes can be easily fit into a simple model of their developmental function. In case of miRNAs broadly expressed in multiple tissues, such as *let-7*, simple patterns may be elusive and combinatorial interactions among microRNAs should be

taken into consideration. Nevertheless, certain patterns are apparent and it is therefore worthwhile to discuss the known functions of several of the putative target genes as they relate to stem cell biology, development and growth control.

Several of the genes are transcriptional regulators (Arid3b, Hic2, Nr6a1, Hmga2), so that many of the mRNAs detected in the microarray screen may be part of downstream transcriptional networks. Like mLin-41, many of the targets display early embryonic and germ line expression, and have been implicated in the regulation of pluripotency and cell growth. Arid3b has recently been shown to participate in a protein network centered on the pluripotency gene Nanog (Wang et al., 2006). Relatively little is known about the Hic2 protein, but its homolog, Hic1, is a tumor suppressor protein interacting with the p53 pathway (Wales et al., 1995; Carter et al., 2000). Nr6a1 is expressed in the embryonic primitive streak, and later in spermatocytes and oocytes (Zechel, 2005). Nr6a1 downregulates the pluripotency genes Oct-4 and Nanog during early development (Gu et al., 2004). Finally, Hmga2 is another tumor suppressor gene with a function in developmental growth control. Hmga2 is widely expressed in early embryogenesis (reviewed in Young et al., 2007) and expression is maintained in the male germ line. Although not exhaustive, this analysis of target gene function supports a role for *let-7* in the transition from rapidly proliferating, relatively undifferentiated cell states in early embryonic development.

#### **4.3. Characterization of the mouse *lin-41* homolog *mLin-41***

Previous work on mLin-41 in chicken and mouse development focused on a possible function in limb bud morphogenesis (Lancman et al., 2005; Schulman et al., 2005; Kanamoto et al., 2006) and as an effector of Sonic hedgehog (Lancman et al., 2005). Our studies extend these observations and describe mLin-41 expression in the embryonic ectoderm, in embryonic stem cells and in the postnatal stem cell niches of the testis, brain and skin. To briefly summarize, the mLin-41 staining pattern in the E7 embryonic ectoderm largely overlaps that of the pluripotency marker Oct-4. mLin-41 protein and mRNA are ubiquitously expressed throughout the neuroepithelia through E10. At E12 mLin-41 is expressed in the embryonic brain, neural tube and DRGs. In the neural tube a reciprocal expression of mLin-41 mRNA and *let-7* in the ventricular and mantle zone, respectively, was demonstrated. On the mRNA level, mLin-41 is close to undetectable in whole brain between E16 and P0, but levels begin to rise again at P5. The mRNA increase can largely be attributed to expression in the ependymal layers of the lateral and third ventricle, as revealed by immunohistochemistry.

Interestingly, in postnatal development mLin-41 was detected in several epithelia, including the olfactory neuroepithelium, the basal layer of the epidermis and the ependymal cells of the ventricles. All of these regions are proposed to contain a stem cell niche in the postnatal mouse, although in the case of ependymal cells this issue is still hotly debated. Ependymal cells are thought to be a terminal differentiation product of radial progenitors, arising primarily at E14-16 with functional maturation in the early post-natal period (Spassky et al., 2005). It is not known if an ependymal progenitor persists into adulthood, although there are many reports of ependymal proliferation in response to injury. In 1999, two groups reported apparently contradictory results: Johansson *et al.* provided evidence that ependymal cells, which constitute a ciliated, single-cell epithelial layer lining the lateral ventricle (LV), retain the characteristics of NSCs. In contrast, Doetsch *et al.* identified glial fibrillary acidic protein (GFAP)-positive astrocyte-like cells, which reside in a region beneath the ependymal layer called the subependymal layer or subventricular zone (SVZ), as NSCs. Although these two results were not necessarily mutually exclusive, they sparked a debate that has been ongoing ever since. Recently several groups have presented evidence supporting an ependymal stem cell identity (Gleason et al., 2008; Coskun et al., 2008). Gleason et al. showed that ependymal cells can be activated to divide by a combination of injury and growth factor stimulation (Gleason et al., 2008). Moreover, several markers of asymmetric cell division, characteristic for true stem cells, are expressed asymmetrically in the ependymal layer but not in the underlying subventricular zone. The authors suggested that the stem cells in the ependymal layer may have been missed in many previous studies because they are usually quiescent and divide only in response to strong stimuli (Gleason et al., 2008). Coskun et al. reported that in the adult mouse forebrain, immunoreactivity for a neural stem cell marker, prominin-1/CD133, is exclusively localized to the ependyma, although not all ependymal cells are CD133(+). Using transplantation and genetic lineage tracing approaches, they demonstrated that CD133(+) ependymal cells continuously produce new neurons destined for the olfactory bulb. Compared with GFAP expressing adult neural stem cells, CD133(+) ependymal cells can represent an additional-perhaps more quiescent-stem cell population in the mammalian forebrain (Coskun et al., 2008). That is why we would like to pursue the study of mLin-41 regulation in the ependymal lineage *in vitro*, using ependymal cell culture as a model.

mLin-41 has two close relatives in *Drosophila*, Brat and Dappled, with Dappled displaying the higher degree of homology to the *C.elegans* and mammalian Lin-41 proteins. In the early embryo Brat participates in the translational regulation of hunchback (Sonoda and Wharton, 2001) Later

in development, Brat is involved in the terminal differentiation of a set of post-embryonic neural progenitors (Bello et al., 2006). Dappled function has not been investigated in detail, however, it may also function as a growth suppressor because mutants develop fat body tumors (Rodriguez et al., 1996). There is evidence that Brat regulates cell growth by influencing RNA processing and metabolism (Betschinger et al., 2006). Lin-41 has been more directly linked to mRNA regulation, and more specifically the miRNA pathway, by the finding that it co-purifies with the *C. elegans* Dicer protein (Duchaine et al., 2006). This potential link to the miRNA pathway is strengthened by our observation that mLin-41 co-localizes with miRISC and P-body associated proteins.

First of all we found that endogenous mLin-41 protein in EC cells localizes to cytoplasmic foci with the appearance of P-bodies. This finding was confirmed in a transfection assay that revealed mLin-41 co-localization with the miRNA pathway proteins Mov10 and Tnrc6b to Hedls-positive P-bodies. Similarly, co-transfection assays in primary neurons revealed co-localization of mLin-41 and either Mov10 or Tnrc6b to cytoplasmic and dendritic foci.

mLin-41 (Trim71), together with Trim2 and Trim3 and Trim 32 is one of four related mammalian proteins containing an N-terminal Trim domain and a C-terminal NHL domain. The designation Trim refers to the Tripartite motif consisting of RING finger, two copies of the B-Box type zinc finger, and a coiled-coil domain. The Trim domain is widespread and frequently confers ubiquitin E3 ligase activity. E3 ubiquitin ligases are the final link in a chain of ubiquitin activation and transfer proteins that mediate recognition and ubiquitination of proteins targeted for degradation by the proteasome. The NHL domain is less well characterized but has been shown to mediate protein-protein interactions and RNA recognition. In several cases, mutations in a number of individual Trim proteins are associated with neurological phenotypes including glioblastoma, Alzheimer's, Opitz syndrome, and limb-girdle muscular dystrophy (Niikura et al., 2003; Berti et al., 2004). *Drosophila* has four Trim/NHL domain proteins, Abba, Brat, Dappled and Mei-p26. Brat (Brain tumor) is required for the terminal differentiation of a subset of neural progenitors, absence of Brat leads to lethal hyperproliferation of these progenitors (Bowman et al., 2008). Mei-P26 has been identified in a screen for suppressors of seizure genes, and was found to increase the threshold for seizure induction (Neumüller et al., 2008). Of the mammalian homologs, Trim2 has been identified as a specific marker of CA1-3 hippocampal neurons (Gray et al., 2004) and is upregulated in a kainate model of hippocampal seizure (Ohkawa et al., 2001).

Trim3 was identified as an outgrowth factor in PC12 cells, where it interacts with MyosinVa (El Husseini and Vincent, 1999). Functional studies of Trim71 have yet to be reported.

We have found that mLin-41 has E3 ubiquitin ligase activity, suggesting a previously unrecognized role for mLin-41 in the regulation of miRISC protein ubiquitination. Very recently, E3 ligase activity has also been demonstrated for Trim2 and Trim32. Mice deficient in Trim2 displayed an ataxic, neurodegenerative phenotype with axonopathy affecting several brain areas (Balastik et al., 2008).

Having shown that mLin-41 localizes to P-bodies, we next studied protein interaction partners for mLin-41 by immunoprecipitation. We confirmed that endogenous as well as Flag- or eGFP-tagged mLin-41 coprecipitates with the P-body proteins Ago-2 and Dicer. The presence of the E3 Ubiquitin ligase mLin-41 in Dicer/Ago-2 complexes raised the possibility that components of the miRNA pathway are post-translationally modified by ubiquitin. To date, there were just two indications for the role of posttranslational modifications in the context of the miRNA pathway. In one study, proteasomal degradation of TRBP was described in human cell lines growing at high cell density (Lee et al., 2006). More interestingly, it was demonstrated that the RNA helicase Armitage, the *Drosophila* homolog of Mov10, is subject to proteasomal degradation during synaptic stimulation in a learning paradigm using *Drosophila* olfactory neurons (Cook et al., 2004; Ashraf, 2006). Since mLin-41 directly interacts with Ago-2, we investigated Ago-2 ubiquitination status, after co-expression with mLin-41. Our data indicated that Ago-2 protein can be ubiquitinated *in vitro* as well as *in vivo* in the presence of mlin-41. However further study will be required to determine the functional consequence of the interaction with, and ubiquitination of, Ago-2. One can speculate about a possible role of ubiquitination in the assembly of P-bodies. To date the biochemical nature of P-bodies remains poorly understood. Recently, the small ubiquitin like modifier (SUMO) has been linked to PML (promyelotic leukemia) nuclear body-formation (PML-NBs). Sumoylation and noncovalent interactions with SUMO through SUMO binding motifs were found to mediate the assembly of PML-NBs and the dynamic distribution of proteins between PML-NBs and the nucleoplasm. Interestingly, a ubiquitin interaction domain (UBA) was predicted within one of the major P-body components, GW182, in *Drosophila* and mammals (Behm-Ansmant et al., 2006). However, if ubiquitination and ubiquitin-recognition indeed contribute to the integrity of P-bodies remain to be elucidated.

#### 4.4. Mechanism controlling *let-7* maturation during neural stem cell commitment

The findings presented above shed some light on *let-7* miRNA expression during developmental and its function as a regulator of diverse genes. However, to better understand its function, it was necessary to elucidate the mechanism regulating *let-7*.

Recent studies revealed that miRNA maturation events are highly regulated, and that the regulation can occur in the nucleus and the cytoplasm, reflecting the involvement of either the nuclear Microprocessor complex or the cytoplasmic Dicer/miRISC complex. Studying *let-7* miRNA expression in different cell lineages, we observed a disparity between accumulation of the precursor and mature forms (Wulczyn et al., 2007). Comparing *let-7* expression between undifferentiated and differentiated EC cells revealed strong induction of the mature ~22 nt *let-7* form after differentiation. In contrast, steady-state levels of the precursor were similar in undifferentiated and differentiated cells. This observation was the first evidence that the cytoplasmic precursor processing is an important if not essential step in the regulation of *let-7* expression. Employing *in vitro* processing assays as well as precursor RNA binding activity, we elucidated the mechanism controlling *let-7* miRNA maturation and proposed a new model for *let-7* regulation during stem cell differentiation (Figure 4.4.1)

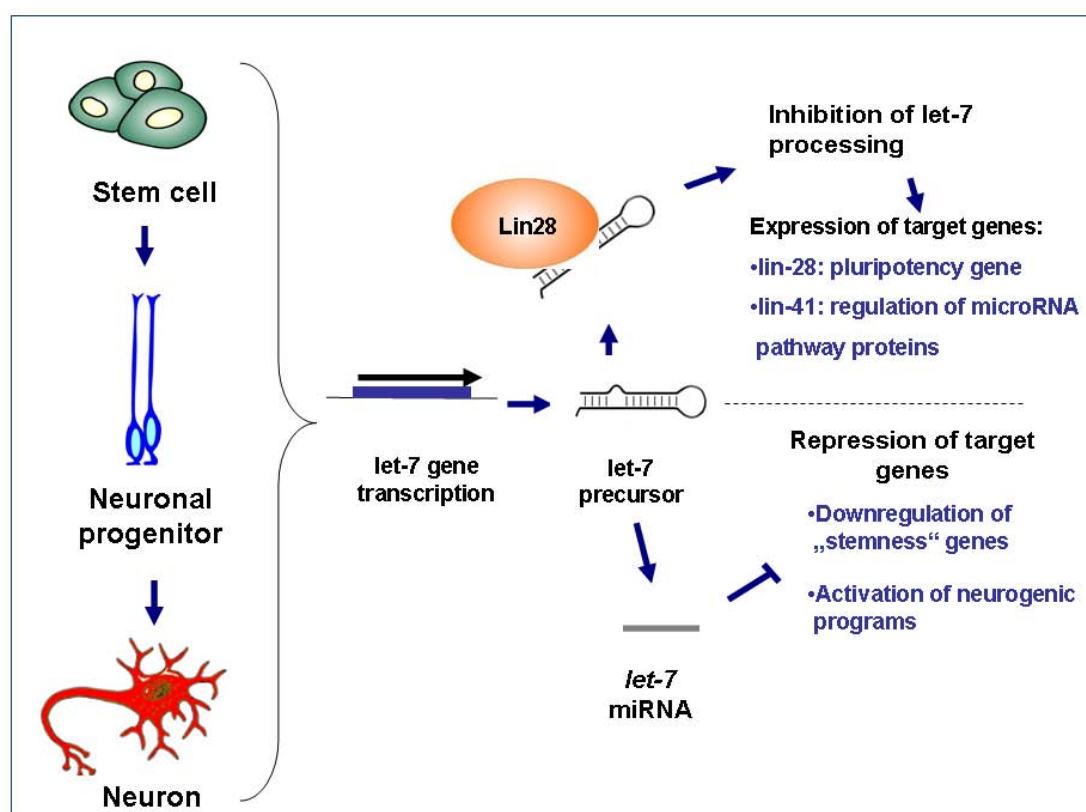


Figure 4.4.1. Model for *let-7* miRNA regulation during stem cell differentiation

In pluripotent cells, the inhibitory protein Lin-28 protects the cytoplasmic *let-7* precursor (pre-*let-7*) from the miRISC (the multi-protein cleavage complex responsible for miRNA maturation). Since Lin-28 is one of six genes that can contribute to the re-establishment of pluripotency in somatic cells (Yu et al., 2007), this regulatory circuit can be considered to be a central feature of “stemness”. The ability of Lin-28 to block biogenesis and accumulation of mature *let-7* involves repression of Dicer activity. This observation is consistent with the cytoplasmic localization of Lin-28 and pre-*let-7* in embryonic carcinoma cells. Using an *in vitro* processing assay and EMSA, we demonstrated that Lin-28 competes with Dicer for *let-7* precursor binding and cleavage. Our results suggest that Lin-28 prevents Dicer access through steric hindrance through its dual interaction with the 5' seed and loop sequences.

Recently, Viswanathan et al. and Newman et al. presented evidence for an alternative mechanism for Lin-28: interference with nuclear pri-*let-7* processing by the Microprocessor complex (Viswanathan et al., 2008; Newman et al., 2008). In terms of outcome, both proposed activities would delay production of mature *let-7*, but the site of Lin-28 action differs. Heo et al. presented evidence in support for our model, and at the same time added an extra piece to the story. They showed that Lin-28 not only inhibits Dicer activity but also induces pre-*let-7* degradation by promoting 3' terminal oligouridylation (Heo et al., 2008). The key role for Lin-28 in the regulation of *let-7* is reinforced by our finding that Lin-28 is a target gene for *let-7* (Rybak et al., 2008). This result establishes that the two molecules are engaged in a conserved double-negative feedback loop in that Lin28 suppresses *let-7*, while *let-7* downregulates Lin28. This type of regulatory circuit has two essential properties: the outcome of the interaction is self-reinforcing and it is exquisitely sensitive to outside regulatory influence. Therefore, Lin-28 and *let-7* are perfectly poised to act as gatekeepers for stem cell commitment.

## 5. Reference List

Ambros V, Lee RC, Lavanway A, Williams PT and Jewell D. MicroRNAs and other tiny endogenous RNAs in *C. elegans*, *Curr. Biol.* 13 (2003), 807–818.

Aravin AA, Lagos-Quintana M, Yalcin A, Zavolan M, Marks D, Snyder B, Gaasterland T, Meyer J, Tuschl T. The small RNA profile during *Drosophila melanogaster* development.. *Dev Cell.* 2003 Aug;5(2):337-50.

Ashraf SI, Kunes S. A trace of silence: memory and microRNA at the synapse. *Curr Opin Neurobiol.* 2006 Oct;16(5):535-9.

Ashraf SI, McLoon AL, Sclarsic SM, Kunes S. Synaptic protein synthesis associated with memory is regulated by the RISC pathway in *Drosophila*. *Cell.* 2006 Jan 13;124(1):191-205.

Baek D, Villén J, Shin C, Camargo FD, Gygi SP, Bartel DP. The impact of microRNAs on protein output. *Nature.* 2008 Sep 4;455(7209):64-71.

Babak T, Zhang W, Morris Q, Blencowe BJ, Hughes TR. Probing microRNAs with microarrays: tissue specificity and functional inference. *RNA.* 2004 Nov;10(11):1813-9

Bagga S, Pasquinelli AE. Identification and analysis of microRNAs. *Genet Eng (N Y).* 2006;27:1-20.

Balastik M, Ferraguti F, Pires-da Silva A, Lee TH, Alvarez-Bolado G, Lu KP, Gruss P. Deficiency in ubiquitin ligase TRIM2 causes accumulation of neurofilament light chain and neurodegeneration. *Proc Natl Acad Sci U S A.* 2008 Aug 19;105(33):12016-21.

Barad O, Meiri E, Avniel A, Aharonov R, Barzilai A, Bentwich I, Einav U, Gilad S, Hurban P, Karov Y, Lobenhofer EK, Sharon E, Shibolet Y, Shtutman M, Bentwich Z, Einat P. MicroRNA expression detected by oligonucleotide microarrays: system establishment and expression profiling in human tissues. *Genome Res.* 2004 Dec;14(12):2486-94

Barroso-del Jesus A, Romero-López C, Lucena-Aguilar G, Melen GJ, Sanchez L, Ligeró G, Berzal-Herranz A, Menendez P. Embryonic stem cell-specific miR302-367 cluster: human gene

structure and functional characterization of its core promoter. *Mol Cell Biol.* 2008 Nov;28(21):6609-19.

Baskerville S, Bartel DP. Microarray profiling of microRNAs reveals frequent coexpression with neighboring miRNAs and host genes. *RNA.* 2005 Mar;11(3):241-7.

Behm-Ansmant I, Rehwinkel J, Izaurralde E. MicroRNAs silence gene expression by repressing protein expression and/or by promoting mRNA decay. *Cold Spring Harb Symp Quant Biol.* 2006;71:523-30.

Behm-Ansmant I, Rehwinkel J, Izaurralde E. MicroRNAs silence gene expression by repressing protein expression and/or by promoting mRNA decay. *Cold Spring Harb Symp Quant Biol.* 2006;71:523-30.

Bello B, Reichert H, Hirth F. The brain tumor gene negatively regulates neural progenitor cell proliferation in the larval central brain of *Drosophila*. *Development.* 2006 Jul;133(14):2639-48.

Bentwich I. Prediction and validation of microRNAs and their targets. *FEBS Lett.* 2005 Oct 31;579(26):5904-10.

Bernstein E, Caudy AA, Hammond SM, Hannon GJ. Role for a bidentate ribonuclease in the initiation step of RNA interference. *Nature.* 2001 Jan 18;409(6818):363-6.

Bernstein E, Kim SY, Carmell MA, Murchison EP, Alcorn H, Li MZ, Mills AA, Elledge SJ, Anderson KV, Hannon GJ. Dicer is essential for mouse development. *Nat Genet.* 2003 Nov;35(3):215-7.

Berti C, Fontanella B, Ferrentino R, Meroni G. Mig12, a novel Opitz syndrome gene product partner, is expressed in the embryonic ventral midline and co-operates with Mid1 to bundle and stabilize microtubules. *BMC Cell Biol.* 2004 Feb 29;5:9.

Betschinger J, Mechtler K, Knoblich JA. Asymmetric segregation of the tumor suppressor brat regulates self-renewal in *Drosophila* neural stem cells. *Cell.* 2006 Mar 24;124(6):1241-53.

Borchert GM, Lanier W, Davidson BL. RNA polymerase III transcribes human microRNAs. *Nat Struct Mol Biol.* 2006 Dec;13(12):1097-101.

Brennecke J, Hipfner DR, Stark A, Russell RB, Cohen SM. bantam encodes a developmentally regulated microRNA that controls cell proliferation and regulates the proapoptotic gene hid in *Drosophila*. *Cell.* 2003 Apr 4;113(1):25-36.

Bruni JE. Ependymal development, proliferation, and functions: a review. *Microsc Res Tech.* 1998 Apr 1;41(1):2-13.

Cai X, Hagedorn CH, Cullen BR. Human microRNAs are processed from capped, polyadenylated transcripts that can also function as mRNAs. *RNA.* 2004 Dec;10(12):1957-66.

Calin GA, Dumitru CD, Shimizu M, Bichi R, Zupo S, Noch E, Aldler H, Rattan S, Keating M, Rai K, Rassenti L, Kipps T, Negrini M, Bullrich F, Croce CM. Frequent deletions and down-regulation of micro- RNA genes miR15 and miR16 at 13q14 in chronic lymphocytic leukemia. *Proc Natl Acad Sci U S A.* 2002 Nov 26;99(24):15524-9.

Caudy AA, Hannon GJ. Induction and biochemical purification of RNA-induced silencing complex from *Drosophila* S2 cells. *Methods Mol Biol.* 2004;265:59-72.

Chan NL, Hill CP. Defining polyubiquitin chain topology. *Nat Struct Biol.* 2001 Aug;8(8):650-2.

Chen CZ, Li L, Lodish HF, Bartel DP. MicroRNAs modulate hematopoietic lineage differentiation. *Science.* 2004 Jan 2;303(5654):83-6.

Chen PY, Manninga H, Slanchev K, Chien M, Russo JJ, Ju J, Sheridan R, John B, Marks DS, Gaidatzis D, Sander C, Zavolan M, Tuschl T. The developmental miRNA profiles of zebrafish as determined by small RNA cloning. *Genes Dev.* 2005 Jun 1;19(11):1288-93.

Chendrimada TP, Finn KJ, Ji X, Baillat D, Gregory RI, Liebhaber SA, Pasquinelli AE, Shiekhattar R. MicroRNA silencing through RISC recruitment of eIF6. *Nature.* 2007 Jun 14;447(7146):823-8.

Chendrimada TP, Gregory RI, Kumaraswamy E, Norman J, Cooch N, Nishikura K, Shiekhattar R. TRBP recruits the Dicer complex to Ago2 for microRNA processing and gene silencing. *Nature*. 2005 Aug 4;436(7051):740-4.

Chieffi P, Battista S, Barchi M, Di Agostino S, Pierantoni GM, Fedele M, Chiariotti L, Tramontano D, Fusco A. HMGA1 and HMGA2 protein expression in mouse spermatogenesis. *Oncogene*. 2002 May 16;21(22):3644-50.

Ciechanover A, Schwartz AL. The ubiquitin-proteasome pathway: the complexity and myriad functions of proteins death. *Proc Natl Acad Sci U S A*. 1998 Mar 17;95(6):2727-30.

Ciechanover A. The ubiquitin-proteasome pathway: on protein death and cell life. *EMBO J*. 1998 Dec 15;17(24):7151-60.

Coskun V, Wu H, Blanchi B, Tsao S, Kim K, Zhao J, Biancotti JC, Hutnick L, Krueger RC Jr, Fan G, de Vellis J, Sun YE. CD133+ neural stem cells in the ependyma of mammalian postnatal forebrain. *Proc Natl Acad Sci U S A*. 2008 Jan 22;105(3):1026-31

Croce CM, Calin GA. miRNAs, cancer, and stem cell division. *Cell*. 2005 Jul 15;122(1):6-7.

Diederichs S, Haber DA. Dual role for argonautes in microRNA processing and posttranscriptional regulation of microRNA expression. *Cell*. 2007 Dec 14;131(6):1097-108.

Dincbas-Renqvist V, Pépin G, Rakonjac M, Plante I, Ouellet DL, Hermansson A, Goulet I, Doucet J, Samuelsson B, Rådmark O, Provost P. Human Dicer C-terminus functions as a 5-lipoxygenase binding domain. *Biochim Biophys Acta*. 2008 Oct 28.

Ding L, Spencer A, Morita K, Han M. The developmental timing regulator AIN-1 interacts with miRISCs and may target the argonaute protein ALG-1 to cytoplasmic P bodies in *C. elegans*. *Mol Cell*. 2005 Aug 19;19(4):437-47.

Doench JG, Petersen CP, Sharp PA. siRNAs can function as miRNAs. *Genes Dev*. 2003 Feb 15;17(4):438-42

Dostie J, Mourelatos Z, Yang M, Sharma A and Dreyfuss G. Numerous microRNPs in neuronal cells containing novel microRNAs, *RNA* 2003 (9),631–632.

Dröge P, Davey CA. Do cells let-7 determine stemness? *Cell Stem Cell*. 2008 Jan 10;2(1):8-9.

Duchaine TF, Wohlschlegel JA, Kennedy S, Bei Y, Conte D Jr, Pang K, Brownell DR, Harding S, Mitani S, Ruvkun G, Yates JR 3rd, Mello CC. Functional proteomics reveals the biochemical niche of *C. elegans* DCR-1 in multiple small-RNA-mediated pathways. *Cell*. 2006 Jan 27;124(2):343-54.

El-Husseini AE, Vincent SR. Cloning and characterization of a novel RING finger protein that interacts with class V myosins. *J Biol Chem*. 1999 Jul 9;274(28):19771-7.

Enright AJ, John B, Gaul U, Tuschl T, Sander C, Marks DS. MicroRNA targets in *Drosophila*. *Genome Biol*. 2003;5(1):R1.

Esquela-Kerscher A, Trang P, Wiggins JF, Patrawala L, Cheng A, Ford L, Weidhaas JB, Brown D, Bader AG, Slack FJ. The let-7 microRNA reduces tumor growth in mouse models of lung cancer. *Cell Cycle*. 2008 Mar 15;7(6):759-64.

Eulalio A, Behm-Ansmant I, Izaurralde E. P bodies: at the crossroads of post-transcriptional pathways. *Nat Rev Mol Cell Biol*. 2007 Jan;8(1):9-22.

Eulalio A, Huntzinger E, Izaurralde E. Getting to the root of miRNA-mediated gene silencing. *Cell*. 2008 Jan 11;132(1):9-14.

Fischer MD, Budak MT, Bakay M, Gorospe JR, Kjellgren D, Pedrosa-Domellöf F, Hoffman EP, Khurana TS. Definition of the unique human extraocular muscle allotype by expression profiling. *Physiol Genomics*. 2005 Aug 11;22(3):283-91.

Friedländer MR, Chen W, Adamidi C, Maaskola J, Einspanier R, Knäuper S, Rajewsky N. Discovering microRNAs from deep sequencing data using miRDeep. *Nat Biotechnol*. 2008 Apr;26(4):407-15

Fuchs E, Raghavan S. Getting under the skin of epidermal morphogenesis. *Nat Rev Genet.* 2002 Mar;3(3):199-209.

Giraldez AJ, Mishima Y, Rihel J, Grocock RJ, Van Dongen S, Inoue K, Enright AJ, Schier AF. Zebrafish MiR-430 promotes deadenylation and clearance of maternal mRNAs. *Science.* 2006 Apr 7;312(5770):75-9.

Gleason D, Fallon JH, Guerra M, Liu JC, Bryant PJ. Ependymal stem cells divide asymmetrically and transfer progeny into the subventricular zone when activated by injury. *Neuroscience.* 2008 Sep 22;156(1):81-8.

Gregory RI, Chendrimada TP, Cooch N, Shiekhattar R. Human RISC couples microRNA biogenesis and posttranscriptional gene silencing. *Cell.* 2005 Nov 18;123(4):631-40.

Grimson A, Farh KK, Johnston WK, Garrett-Engele P, Lim LP, Bartel DP. MicroRNA targeting specificity in mammals: determinants beyond seed pairing. *Mol Cell.* 2007 Jul 6;27(1):91-105.

Grishok A, Pasquinelli AE, Conte D, Li N, Parrish S, Ha I, Baillie DL, Fire A, Ruvkun G, Mello CC. Genes and mechanisms related to RNA interference regulate expression of the small temporal RNAs that control *C. elegans* developmental timing. *Cell.* 2001 Jul 13;106.

Grosshans H, Johnson T, Reinert KL, Gerstein M, Slack FJ. The temporal patterning microRNA let-7 regulates several transcription factors at the larval to adult transition in *C. elegans*. *Dev Cell.* 2005 Mar;8(3):321-30.

Grosshans H, Filipowicz W. Proteomics joins the search for microRNA targets. *Cell.* 2008 Aug 22;134(4):560-2.

Gu P, LeMenuet D, Chung AC, Mancini M, Wheeler DA, Cooney AJ. Orphan nuclear receptor GCNF is required for the repression of pluripotency genes during retinoic acid-induced embryonic stem cell differentiation. *Mol Cell Biol.* 2005 Oct;25(19):8507-19.

Haglund K, Di Fiore PP, Dikic I. Distinct monoubiquitin signals in receptor endocytosis. *Trends Biochem Sci.* 2003 Nov;28(11):598-603.

Han J, Lee Y, Yeom KH, Kim YK, Jin H, Kim VN. The Drosha-DGCR8 complex in primary microRNA processing. *Genes Dev.* 2004 Dec 15;18(24):3016-27.

Han J, Lee Y, Yeom KH, Nam JW, Heo I, Rhee JK, Sohn SY, Cho Y, Zhang BT, Kim VN. Molecular basis for the recognition of primary microRNAs by the Drosha-DGCR8 complex. *Cell.* 2006 Jun 2;125(5):887-901.

Hatfield S, Ruohola-Baker H. microRNA and stem cell function. *Cell Tissue Res.* 2008 Jan;331(1):57-66.

Heo I, Joo C, Cho J, Ha M, Han J, Kim VN. Lin28 mediates the terminal uridylation of let-7 precursor MicroRNA. *Mol Cell.* 2008 Oct 24;32(2):276-84.

Hershko A, Ciechanover A. The ubiquitin system. *Annu Rev Biochem.* 1998;67:425-79.

Hillebrand J, Barbee SA, Ramaswami M. P-body components, microRNA regulation, and synaptic plasticity. *ScientificWorldJournal.* 2007 Nov 2;7:178-90.

Houbaviy HB, Murray MF and Sharp PA. Embryonic stem cell-specific MicroRNAs, *Dev. Cell* 2003 (5), 351–358.

Humphreys DT, Westman BJ, Martin DI, Preiss T. MicroRNAs control translation initiation by inhibiting eukaryotic initiation factor 4E/cap and poly(A) tail function. *Proc Natl Acad Sci U S A.* 2005 Nov 22;102(47):16961-6.

Iorio MV, Visone R, Di Leva G, Donati V, Petrocca F, Casalini P, Taccioli C, Volinia S, Liu CG, Alder H, Calin GA, Ménard S, Croce CM. MicroRNA signatures in human ovarian cancer. *Cancer Res.* 2007 Sep 15;67(18):8699-707.

Jang W, Kim KP, Schwob JE. Nonintegrin laminin receptor precursor protein is expressed on olfactory stem and progenitor cells. *J Comp Neurol.* 2007 May 20;502(3):367-81.

Jin P, Alisch RS, Warren ST. RNA and microRNAs in fragile X mental retardation. *Nat Cell Biol.* 2004 Nov;6(11):1048-53.

Johansson CB, Svensson M, Wallstedt L, Janson AM, Frisén J. Neural stem cells in the adult human brain. *Exp Cell Res*. 1999 Dec 15;253(2):733-6.

John B, Enright AJ, Aravin A, Tuschl T, Sander C, Marks DS. Human MicroRNA targets. *PLoS Biol*. 2004 Nov;2(11):363.

John B, Sander C, Marks DS. Prediction of human microRNA targets. *Methods Mol Biol*. 2006;342:101-13.

Johnson SM, Grosshans H, Shingara J, Byrom M, Jarvis R, Cheng A, Labourier E, Reinert KL, Brown D, Slack FJ. RAS is regulated by the let-7 microRNA family. *Cell*. 2005 Mar 11;120(5):635-47.

Kanamoto T, Terada K, Yoshikawa H, Furukawa T. Cloning and regulation of the vertebrate homologue of lin-41 that functions as a heterochronic gene in *Caenorhabditis elegans*. *Dev Dyn*. 2006 Apr;235(4):1142-9.

Kanellopoulou C, Muljo SA, Kung AL, Ganesan S, Drapkin R, Jenuwein T, Livingston DM, Rajewsky K. Dicer-deficient mouse embryonic stem cells are defective in differentiation and centromeric silencing. *Genes Dev*. 2005 Feb 15;19(4):489-501.

Kent OA, Mendell JT. A small piece in the cancer puzzle: microRNAs as tumor suppressors and oncogenes. *Oncogene*. 2006 Oct 9;25(46):6188-96.

Kim VN, Nam JW. Genomics of microRNA. *Trends Genet*. 2006 Mar;22(3):165-73.

Kiriakidou M, Tan GS, Lamprinaki S, De Planell-Saguer M, Nelson PT, Mourelatos Z. An mRNA m7G cap binding-like motif within human Ago2 represses translation. *Cell*. 2007 Jun 15;129(6):1141-51.

Kloosterman WP, Wienholds E, de Bruijn E, Kauppinen S, Plasterk RH. In situ detection of miRNAs in animal embryos using LNA-modified oligonucleotide probes. *Nat Methods*. 2006 Jan;3(1):27-9.

Kok KH, Ng MH, Ching YP, Jin DY. Human TRBP and PACT directly interact with each other and associate with dicer to facilitate the production of small interfering RNA. *J Biol Chem*. 2007 Jun 15;282(24):17649-57

Kosik KS. The neuronal microRNA system. *Nat Rev Neurosci*. 2006 Dec;7(12):911-20.

Kotaja N, Sassone-Corsi P. The chromatoid body: a germ-cell-specific RNA-processing centre. *Nat Rev Mol Cell Biol*. 2007 Jan;8(1):85-90.

Krek A, Grün D, Poy MN, Wolf R, Rosenberg L, Epstein EJ, MacMenamin P, da Piedade I, Gunsalus KC, Stoffel M, Rajewsky N. Combinatorial microRNA target predictions. *Nat Genet*. 2005 May;37(5):495-500.

Krichevsky AM, King KS, Donahue CP, Khrapko K, Kosik KS. A microRNA array reveals extensive regulation of microRNAs during brain development. *RNA*. 2003 Oct;9(10):1274-81. Erratum in: *RNA*. 2004 Mar;10(3):551

Krichevsky AM, Sonntag KC, Isacson O, Kosik KS. Specific microRNAs modulate embryonic stem cell-derived neurogenesis. *Stem Cells*. 2006 Apr;24(4):857-64.

Krichevsky AM. MicroRNA profiling: from dark matter to white matter, or identifying new players in neurobiology. *ScientificWorldJournal*. 2007 Nov 2;7:155-66.

Lagos-Quintana M, Rauhut R, Lendeckel W and Tuschl T. Identification of novel genes coding for small expressed RNAs, *Science* 2001 (294), 853–858.

Lagos-Quintana M, Rauhut R, Meyer J, Borkhardt A, Tuschl T. New microRNAs from mouse and human. *RNA*. 2003 Feb;9(2):175-9.

Lagos-Quintana M, Rauhut R, Yalcin A, Meyer J, Lendeckel W, Tuschl T. Identification of tissue-specific microRNAs from mouse. *Curr Biol*. 2002 Apr 30;12(9):735-9.

Lancman JJ, Caruccio NC, Harfe BD, Pasquinelli AE, Schageman JJ, Pertsemlidis A, Fallon JF. Analysis of the regulation of lin-41 during chick and mouse limb development. *Dev Dyn*. 2005 Dec;234(4):948-60.

Laskowski A, Howell OW, Sosunov AA, McKhann G, Gray WP. NPY mediates basal and seizure-induced proliferation in the subcallosal zone. *Neuroreport*. 2007 Jul 2;18(10):1005-8.

Lau NC, Lim LP, Weinstein EG and Bartel DP. An abundant class of tiny RNAs with probable regulatory roles in *Caenorhabditis elegans*, *Science* 294 (2001), 858–862.

Lee Y, Kim M, Han J, Yeom KH, Lee S, Baek SH, Kim VN. MicroRNA genes are transcribed by RNA polymerase II. *EMBO J*. 2004 Oct 13;23(20):4051-60.

Lee YS, Dutta A. The tumor suppressor microRNA let-7 represses the HMGA2 oncogene. *Genes Dev*. 2007 May 1;21(9):1025-30.

Lee RC, Feinbaum RL and Ambros V. The *C. elegans* heterochronic gene *lin-4* encodes small RNAs with antisense complementarity to *lin-14*. *Cell* 1993 (75): 843–854.

Lewis BP, Shih IH, Jones-Rhoades MW, Bartel DP, Burge CB. Prediction of mammalian microRNA targets. *Cell*. 2003 Dec 26;115(7):787-98.

Lim LP, Glasner ME, Yekta S, Burge CB and Bartel DP. Vertebrate microRNA genes, *Science* 299 (2003), 1540

Lim LP, Lau NC, Garrett-Engele P, Grimson A, Schelter JM, Castle J, Bartel DP, Linsley PS, Johnson JM. Microarray analysis shows that some microRNAs downregulate large numbers of target mRNAs. *Nature*. 2005 Feb 17;433(7027):769-73.

Liu CG, Calin GA, Volinia S, Croce CM. MicroRNA expression profiling using microarrays. *Nat Protoc*. 2008;3(4):563-78.

Liu CG, Spizzo R, Calin GA, Croce CM. Expression profiling of microRNA using oligo DNA arrays. *Methods*. 2008 Jan;44(1):22-30.

Liu J, Rivas FV, Wohlschlegel J, Yates JR 3rd, Parker R, Hannon GJ. A role for the P-body component GW182 in microRNA function. *Nat Cell Biol*. 2005 Dec;7(12):1261-6.

Maniatakis E, Mourelatos Z. A human, ATP-independent, RISC assembly machine fueled by pre-miRNA. *Genes Dev*. 2005 Dec 15;19(24):2979-90.

Mathonnet G, Fabian MR, Svitkin YV, Parsyan A, Huck L, Murata T, Biffo S, Merrick WC, Darzynkiewicz E, Pillai RS, Filipowicz W, Duchaine TF, Sonenberg N. MicroRNA inhibition of translation initiation in vitro by targeting the cap-binding complex eIF4F. *Science*. 2007 Sep 21;317(5845):1764-7.

Meister G, Landthaler M, Patkaniowska A, Dorsett Y, Teng G, Tuschl T. Human Argonaute2 mediates RNA cleavage targeted by miRNAs and siRNAs. *Mol Cell*. 2004 Jul 23;15(2):185-97.

Meister G, Landthaler M, Peters L, Chen PY, Urlaub H, Lührmann R, Tuschl T. Identification of novel argonaute-associated proteins. *Curr Biol*. 2005 Dec 6;15(23):2149-55.

Merkle FT, Mirzadeh Z, Alvarez-Buylla A. Mosaic organization of neural stem cells in the adult brain. *Science*. 2007 Jul 20;317(5836):381-4.

Meroni G, Diez-Roux G. TRIM/RBCC, a novel class of 'single protein RING finger' E3 ubiquitin ligases. *Bioessays*. 2005 Nov;27(11):1147-57.

Michel CI, Kraft R, Restifo LL. Defective neuronal development in the mushroom bodies of *Drosophila* fragile X mental retardation 1 mutants. *J Neurosci*. 2004 Jun 23;24(25):5798-809.

Miska EA, Alvarez-Saavedra E, Townsend M, Yoshii A, Sestan N, Rakic P, Constantine-Paton M, Horvitz HR. Microarray analysis of microRNA expression in the developing mammalian brain. *Genome Biol*. 2004;5(9):R68

Moss EG, Lee RC and Ambros V. The cold shock domain protein LIN-28 controls developmental timing in *C. elegans* and is regulated by the lin-4 RNA, *Cell* 88 (1997), 637–646.

Mourelatos Z, Dostie J, Paushkin S, Sharma A, Charroux B, Abel L, Rappsilber J, Mann M and Dreyfuss G, miRNPs: a novel class of ribonucleoproteins containing numerous microRNAs, *Genes Dev*. 2002 Nov (16), 720–728.

Murchison EP, Partridge JF, Tam OH, Cheloufi S, Hannon GJ. Characterization of Dicer-deficient murine embryonic stem cells. *Proc Natl Acad Sci U S A*. 2005 Aug 23;102(34):12135-40.

Naguibneva I, Ameyar-Zazoua M, Polesskaya A, Ait-Si-Ali S, Groisman R, Souidi M, Cuvellier S, Harel-Bellan A. The microRNA miR-181 targets the homeobox protein Hox-A11 during mammalian myoblast differentiation. *Nat Cell Biol.* 2006 Mar;8(3):278-84.

Newman MA, Thomson JM, Hammond SM. Lin-28 interaction with the Let-7 precursor loop mediates regulated microRNA processing. *RNA.* 2008 Aug;14(8):1539-49.

Neumüller RA, Betschinger J, Fischer A, Bushati N, Poernbacher I, Mechtler K, Cohen SM, Knoblich JA. Mei-P26 regulates microRNAs and cell growth in the Drosophila ovarian stem cell lineage. *Nature.* 2008 Jul 10;454(7201):241-5

Niikura T, Hashimoto Y, Tajima H, Ishizaka M, Yamagishi Y, Kawasumi M, Nawa M, Terashita K, Aiso S, Nishimoto I. A tripartite motif protein TRIM11 binds and destabilizes Humanin, a neuroprotective peptide against Alzheimer's disease-relevant insults. *Eur J Neurosci.* 2003 Mar;17(6):1150-8.

Nottrott S, Simard MJ, Richter JD. Human let-7a miRNA blocks protein production on actively translating polyribosomes. *Nat Struct Mol Biol.* 2006 Dec;13(12):1108-14.

Obernosterer G, Leuschner PJ, Alenius M, Martinez J. Post-transcriptional regulation of microRNA expression. *RNA.* 2006 Jul;12(7):1161-7.

O'Donnell KA, Wentzel EA, Zeller KI, Dang CV, Mendell JT. c-Myc-regulated microRNAs modulate E2F1 expression. *Nature.* 2005 Jun 9;435(7043):839-43.

Ohkawa N, Kokura K, Matsu-Ura T, Obinata T, Konishi Y, Tamura TA. Molecular cloning and characterization of neural activity-related RING finger protein (NARF): a new member of the RBCC family is a candidate for the partner of myosin V. *J Neurochem.* 2001 Jul;78(1):75-87

Olsen PH, Ambros V. The lin-4 regulatory RNA controls developmental timing in *Caenorhabditis elegans* by blocking LIN-14 protein synthesis after the initiation of translation. *Dev Biol.* 1999 Dec 15;216(2):671-80

Ozen M, Creighton CJ, Ozdemir M, Ittmann M. Widespread deregulation of microRNA expression in human prostate cancer. *Oncogene.* 2008 Mar 13;27(12):1788-93.

Pan L, Zhang YQ, Woodruff E, Broadie K. The *Drosophila* fragile X gene negatively regulates neuronal elaboration and synaptic differentiation. *Curr Biol*. 2004 Oct 26;14(20):1863-70.

Pasquinelli AE, Reinhart BJ, Slack F, Martindale MQ, Kuroda M, Maller B, Srinivasan A, Fishman M, Hayward D and Ball E. Conservation across animal phylogeny of the sequence and temporal regulation of the 21 nucleotide *let-7* heterochronic regulatory RNA, *Nature* 2000 (408), 86–89.

Pauley KM, Eystathioy T, Jakymiw A, Hamel JC, Fritzler MJ, Chan EK.. Formation of GW bodies is a consequence of microRNA genesis. *EMBO Rep*. 2006 Sep;7(9):904-10.

Perron MP, Provost P. Protein interactions and complexes in human microRNA biogenesis and function. *Front Biosci*. 2008 Jan 1;13:2537-47.

Petersen CP, Bordeleau ME, Pelletier J, Sharp PA. Short RNAs repress translation after initiation in mammalian cells. *Mol Cell*. 2006 Feb 17;21(4):533-42.

Pillai RS. MicroRNA function: multiple mechanisms for a tiny RNA? *RNA*. 2005 Dec;11(12):1753-61.

Plante I, Provost P. Hypothesis: A Role for Fragile X Mental Retardation Protein in Mediating and Relieving MicroRNA-Guided Translational Repression? *J Biomed Biotechnol*. 2006;2006(4):16806.

Reymond A, Meroni G, Fantozzi A, Merla G, Cairo S, Luzi L, Riganelli D, Zanaria E, Messali S, Cainarca S, Guffanti A, Minucci S, Pelicci PG, Ballabio A. The tripartite motif family identifies cell compartments. *EMBO J*. 2001 May 1;20(9):2140-51.

Robb GB, Rana TM. RNA helicase A interacts with RISC in human cells and functions in RISC loading. *Mol Cell*. 2007 May 25;26(4):523-37.

Rodriguez A, Vigorito E, Clare S, Warren MV, Couttet P, Soond DR, van Dongen S, Grocock RJ, Das PP, Miska EA, Vetrie D, Okkenhaug K, Enright AJ, Dougan G, Turner M, Bradley A. Requirement of *bic/microRNA-155* for normal immune function. *Science*. 2007 Apr 27;316(5824):608-11.

Rybak A, Fuchs H, Smirnova L, Brandt C, Pohl EE, Nitsch R, Wulczyn FG. A feedback loop comprising lin-28 and let-7 controls pre-let-7 maturation during neural stem-cell commitment. *Nat Cell Biol.* 2008 Aug;10(8):987-93.

Sampson VB, Rong NH, Han J, Yang Q, Aris V, Soteropoulos P, Petrelli NJ, Dunn SP, Krueger LJ. MicroRNA let-7a down-regulates MYC and reverts MYC-induced growth in Burkitt lymphoma cells. *Cancer Res.* 2007 Oct 15;67(20):9762-70.

Sarnat HB. Regional differentiation of the human fetal ependyma: immunocytochemical markers. *J Neuropathol Exp Neurol.* 1992 Jan;51(1):58-75.

Sasaki T, Shiohama A, Minoshima S, Shimizu N. Identification of eight members of the Argonaute family in the human genome small star, filled. *Genomics.* 2003 Sep;82(3):323-30.

Schratt GM, Tuebing F, Nigh EA, Kane CG, Sabatini ME, Kiebler M, Greenberg ME. A brain-specific microRNA regulates dendritic spine development. *Nature.* 2006 Jan 19;439(7074):283-9.

Schulman BR, Esquela-Kerscher A, Slack FJ. Reciprocal expression of lin-41 and the microRNAs let-7 and mir-125 during mouse embryogenesis. *Dev Dyn.* 2005 Dec;234(4):1046-54.

Schultz J, Lorenz P, Gross G, Ibrahim S, Kunz M. MicroRNA let-7b targets important cell cycle molecules in malignant melanoma cells and interferes with anchorage-independent growth. *Cell Res.* 2008 May;18(5):549-57.

Scott GK, Goga A, Bhaumik D, Berger CE, Sullivan CS, Benz CC. Coordinate suppression of ERBB2 and ERBB3 by enforced expression of micro-RNA miR-125a or miR-125b. *J Biol Chem.* 2007 Jan 12;282(2):1479-86.

Sempere LF, Freemantle S, Pitha-Rowe I, Moss E, Dmitrovsky E, Ambros V. Expression profiling of mammalian microRNAs uncovers a subset of brain-expressed microRNAs with possible roles in murine and human neuronal differentiation. *Genome Biol.* 2004;5(3):R13

Sharp PA. RNA interference--2001. *Genes Dev.* 2001 Mar 1;15(5):485-90.

Sheth U, Parker R. Decapping and decay of messenger RNA occur in cytoplasmic processing bodies. *Science*. 2003 May 2;300(5620):805-8.

Siomi H, Ishizuka A, Siomi MC. RNA interference: a new mechanism by which FMRP acts in the normal brain? What can *Drosophila* teach us? *Ment Retard Dev Disabil Res Rev*. 2004;10(1):68-74.

Slack FJ, Basson M, Liu Z, Ambros V, Horvitz HR, Ruvkun G. The *lin-41* RBCC gene acts in the *C. elegans* heterochronic pathway between the *let-7* regulatory RNA and the *LIN-29* transcription factor. *Mol Cell*. 2000 Apr;5(4):659-69.

Smirnova L, Gräfe A, Seiler A, Schumacher S, Nitsch R, Wulczyn FG. Regulation of miRNA expression during neural cell specification. *Eur J Neurosci*. 2005 Mar;21(6):1469-77.

Sokol NS, Xu P, Jan YN, Ambros V. *Drosophila let-7* microRNA is required for remodeling of the neuromusculature during metamorphosis. *Genes Dev*. 2008 Jun 15;22(12):1591-6.

Song JJ, Smith SK, Hannon GJ, Joshua-Tor L. Crystal structure of Argonaute and its implications for RISC slicer activity. *Science*. 2004 Sep 3;305(5689):1434-7.

Sonoda J, Wharton RP. *Drosophila* Brain Tumor is a translational repressor. *Genes Dev*. 2001 Mar 15;15(6):762-73.

Spassky N, Merkle FT, Flames N, Tramontin AD, García-Verdugo JM, Alvarez-Buylla A. Adult ependymal cells are postmitotic and are derived from radial glial cells during embryogenesis. *J Neurosci*. 2005 Jan 5;25(1):10-8.

Stark KL, Xu B, Bagchi A, Lai WS, Liu H, Hsu R, Wan X, Pavlidis P, Mills AA, Karayiorgou M, Gogos JA. Altered brain microRNA biogenesis contributes to phenotypic deficits in a 22q11-deletion mouse model. *Nat Genet*. 2008 Jun;40(6):751-60.

Suh MR, Lee Y, Kim JY, Kim SK, Moon SH, Lee JY, Cha KY, Chung HM, Yoon HS, Moon SY, Kim VN, Kim KS. Human embryonic stem cells express a unique set of microRNAs. *Dev Biol*. 2004 Jun 15;270(2):488-98.

Takamizawa J, Konishi H, Yanagisawa K, Tomida S, Osada H, Endoh H, Harano T, Yatabe Y, Nagino M, Nimura Y, Mitsudomi T, Takahashi T. Reduced expression of the let-7 microRNAs in human lung cancers in association with shortened postoperative survival. *Cancer Res.* 2004 Jun 1;64(11):3753-6.

Tang X, Gal J, Zhuang X, Wang W, Zhu H, Tang G. A simple array platform for microRNA analysis and its application in mouse tissues. *RNA.* 2007 Oct;13(10):1803-22.

Thomson JM, Parker J, Perou CM, Hammond SM. A custom microarray platform for analysis of microRNA gene expression. *Nat Methods.* 2004 Oct;1(1):47-53.

Ule J, Darnell RB. RNA binding proteins and the regulation of neuronal synaptic plasticity. *Curr Opin Neurobiol.* 2006 Feb;16(1):102-10.

van Rooij E, Olson EN. microRNAs put their signatures on the heart. *Physiol Genomics.* 2007 Nov 14;31(3):365-6.

Vella MC, Choi EY, Lin SY, Reinert K, Slack FJ. The *C. elegans* microRNA let-7 binds to imperfect let-7 complementary sites from the lin-41 3'UTR. *Genes Dev.* 2004 Jan 15;18(2):132-7

Viswanathan SR, Daley GQ, Gregory RI. Selective blockade of microRNA processing by Lin28. *Science.* 2008 Apr 4;320(5872):97-100.

Volinia S, Calin GA, Liu CG, Ambs S, Cimmino A, Petrocca F, Visone R, Iorio M, Roldo C, Ferracin M, Prueitt RL, Yanaihara N, Lanza G, Scarpa A, Vecchione A, Negrini M, Harris CC, Croce CM. A microRNA expression signature of human solid tumors defines cancer gene targets. *Proc Natl Acad Sci U S A.* 2006 Feb 14;103(7):2257-61.

Voorhoeve PM, le Sage C, Schrier M, Gillis AJ, Stoop H, Nagel R, Liu YP, van Duijse J, Drost J, Griekspoor A, Zlotorynski E, Yabuta N, De Vita G, Nojima H, Looijenga LH, Agami R. A genetic screen implicates miRNA-372 and miRNA-373 as oncogenes in testicular germ cell tumors. *Cell.* 2006 Mar 24;124(6):1169-81.

Wakiyama M, Takimoto K, Ohara O, Yokoyama S. Let-7 microRNA-mediated mRNA deadenylation and translational repression in a mammalian cell-free system. *Genes Dev.* 2007 Aug 1;21(15):1857-62.

Wales MM, Biel MA, el Deiry W, Nelkin BD, Issa JP, Cavenee WK, Kuerbitz SJ, Baylin SB. p53 activates expression of HIC-1, a new candidate tumour suppressor gene on 17p13.3. *Nat Med.* 1995 Jun;1(6):570-7.

Watanabe T, Takeda A, Mise K, Okuno T, Suzuki T, Minami N, Imai H. Stage-specific expression of microRNAs during *Xenopus* development. *FEBS Lett.* 2005 Jan 17;579(2):318-24.

White-Grindley E, Si K. RISC-y Memories. *Cell.* 2006 Jan 13;124(1):23-6.

Wu L, Fan J, Belasco JG. MicroRNAs direct rapid deadenylation of mRNA. *Proc Natl Acad Sci U S A.* 2006 Mar 14;103(11):4034-9.

Woods K, Thomson JM, Hammond SM. Direct regulation of an oncogenic micro-RNA cluster by E2F transcription factors. *J Biol Chem.* 2007 Jan 26;282(4):2130-4

Wulczyn FG, Smirnova L, Rybak A, Brandt C, Kwidzinski E, Ninnemann O, Strehle M, Seiler A, Schumacher S, Nitsch R. Post-transcriptional regulation of the let-7 microRNA during neural cell specification. *FASEB J.* 2007 Feb;21(2):415-26.

Yanaihara N, Caplen N, Bowman E, Seike M, Kumamoto K, Yi M, Stephens RM, Okamoto A, Yokota J, Tanaka T, Calin GA, Liu CG, Croce CM, Harris CC. Unique microRNA molecular profiles in lung cancer diagnosis and prognosis. *Cancer Cell.* 2006 Mar;9(3):189-98.

Yoshinaga K, Nishikawa S, Ogawa M, Hayashi S, Kunisada T, Fujimoto T, Nishikawa S. Role of c-kit in mouse spermatogenesis: identification of spermatogonia as a specific site of c-kit expression and function. *Development.* 1991 Oct;113(2):689-99.

Yu F, Yao H, Zhu P, Zhang X, Pan Q, Gong C, Huang Y, Hu X, Su F, Lieberman J, Song E. let-7 regulates self renewal and tumorigenicity of breast cancer cells. *Cell.* 2007 Dec 14;131(6):1109-23.

Yu J, Vodyanik MA, Smuga-Otto K, Antosiewicz-Bourget J, Frane JL, Tian S, Nie J, Jonsdottir GA, Ruotti V, Stewart R, Slukvin II, Thomson JA. Induced pluripotent stem cell lines derived from human somatic cells. *Science*. 2007 Dec 21;318(5858):1917-20. Epub 2007 Nov 20.

Zechel C. The germ cell nuclear factor (GCNF). *Mol Reprod Dev*. 2005 Dec;72(4):550-6.

Zhang B, Pan X, Cobb GP, Anderson TA. microRNAs as oncogenes and tumor suppressors. *Dev Biol*. 2007 Feb 1;302(1):1-12.

Zhang H, Kolb FA, Jaskiewicz L, Westhof E, Filipowicz W. Single processing center models for human Dicer and bacterial RNase III. *Cell*. 2004 Jul 9;118(1):57-68.

## **6. Appendix**

### **6.1. Statement**

Hiermit erkläre ich dass ich die vorliegende Dissertation selbstständig durchgeführt habe. Ich habe keine Hilfsmitteln und Hilfern als der in der Arbeit angegebenen verfasst. Des weiteren versichere ich, dass die vorliegende Arbeit an keiner anderen Universität angereicht wurde.

## 6.2. Publications:

Wulczyn FG, Smirnova L, **Rybak A**, Brandt C, Kwidzinski E, Ninnemann O, Strehle M, Seiler A, Schumacher S, and Nitsch R. *Post-transcriptional regulation of the let-7 microRNA during neural cell specification*. **FASEB J**, 2007

**Rybak A** and Fuchs H, Smirnova L, Brandt Ch, Pohl E, Nitsch R & Wulczyn F. G, *A feedback loop comprising lin-28 and let-7 controls pre-let-7 maturation during neural stem-cell commitment*. **Nature Cell Biology**, 2008

Smirnova L, **Rybak A**, Fuchs H, Pekarik V, Wulczyn FG (2008) *miRNAs in Neurobiology*. In Encyclopedia of Neuroscience Binder, M.D.; Hirokawa, N.; Windhorst, U.; Hirsch, M.C. (Eds.) Springer Verlag ISBN: 978-3-540-29678-2

**Rybak A**, Fuchs H, Smirnova L, Michel G, Nitsch R, Krappmann D and Wulczyn FG, *Mouse Lin-41 is a stem cell specific E3 ubiquitin ligase for the miRNA pathway protein Ago2*, *Nature Cell Biology*, in review.

## 6.3. Oral Presentations:

**Rybak A**, Wulczyn FG. *Expression and function of the let-7 microRNA during the CNS development*. Berlin Brain Days, Berlin 2007

**Rybak A**, Fuchs H, Wulczyn FG. *let-7 and Lin-28: a stem loop controlling neural stem cell commitment*. DFG Berichtskolloquium des Graduiertenkollegs 1123.

## 6.4. Poster presentations

**Rybak A**, Smirnowa L, Fuchs H, Nitsch R and Wulczyn GF. *microRNA expression and function during mouse CNS development*. **BNF 2006**. Liebenwalde (Germany), June 2006.

Smirnowa L, **Rybak A**, Fuchs H, Nitsch R and Wulczyn G. *Regulation and function of let-microRNA during neural differentiation*. **BNF 2006**. Liebenwalde (Germany), June 2006.

**Rybak A**, Smirnowa L, Fuchs H, Nitsch R and Wulczyn GF. *microRNA expression and function during mouse CNS development*. **5<sup>th</sup> FENS Forum**. Vienna (Austria), July 2006.

Smirnowa L, **Rybak A**, Fuchs H, Nitsch R and Wulczyn G. *Regulation and function of let-microRNA during neural differentiation*. **5<sup>th</sup> FENS Forum**. Vienna (Austria), July 2006.

**Rybak A**, Fuchs H, Smirnova L, Nitsch R and Wulczyn G. *microRNAs expression and functions during CNS development*. Society for Neuroscience annual meeting, San Diego (USA) November 2007.

**Rybak A**, Fuchs H, Smirnova L, Nitsch R and Wulczyn G. SFB 650, *Expression and function of the let-7 microRNA during the CNS development*. Potsdam, November 2007

**Rybak A**, Fuchs H, Smirnova L, Nitsch R and Wulczyn FG. *Expression and function of the let-7 microRNA during development of the CNS*. Keystone Symposium, Whistler (Canada), March 2008.

**Rybak A**, Fuchs H, Smirnova L, Nitsch R and Wulczyn FG. *microRNA Europe Expression and function of the let-7 microRNA during the CNS development*. Cambridge (UK), November 2008.

Fuchs H, **Rybak A**, Smirnova L, Nitsch R and Wulczyn FG. *A feedback loop comprising lin-28 and let-7 controls pre-let-7 maturation during neural stem-cell commitment*. microRNA Europe Cambridge (UK), November 2008.

**Rybak A**, Fuchs H, Smirnova L, Nitsch R and Wulczyn FG. *Expression and function of the let-7 microRNA and its target gene – mLin-41 during the CNS development*. Brain Tumor Meeting, Berlin December 2008

Fuchs H, **Rybak A**, Smirnova L, Nitsch R and Wulczyn FG. *A feedback loop comprising lin-28 and let-7 controls pre-let-7 maturation during neural stem-cell commitment*. Brain Tumor Meeting, Berlin, December 2008.

**Rybak A**, Fuchs H, Wulczyn FG. *let-7 and Lin-28: a stem loop controlling neural stem cell commitment*. DFG Berichtskolloquium des Graduiertenkollegs 1123.

### **6.5. Workshops attended:**

Workshop 3 DFG-Graduiertenkollegs, Hegne, 2008

Short course: small RNAs in Neuroscience, San Diego 2007

Poster Preparation and Presentation Workshop in English, 1.5 day, Berlin 2007, Bioscript

Getting Founded Workshop in English, 2.5 day, Berlin 2007, Bioscript

Workshop ‘Molecular Interactions’, Berlin 2007

Presentation technique workshop in English, 2.5 day Berlin 2005, Bioscript

Effective Scientific Writing Workshop in English, 2.5 day Berlin 2006, Bioscript

Annual Meeting 2006 – Grant writing

# Curriculum Vitae

For reasons of data protection, the curriculum vitae is not included in the online version